
Theses and Dissertations

Spring 2011

Synthesis of new biodegradable polysulfenamides for applications in medicine

Jun Yoo

University of Iowa

Copyright 2011 Jun Yoo

This dissertation is available at Iowa Research Online: <http://ir.uiowa.edu/etd/1114>

Recommended Citation

Yoo, Jun. "Synthesis of new biodegradable polysulfenamides for applications in medicine." PhD (Doctor of Philosophy) thesis, University of Iowa, 2011.
<http://ir.uiowa.edu/etd/1114>.

Follow this and additional works at: <http://ir.uiowa.edu/etd>

 Part of the [Chemistry Commons](#)

SYNTHESIS OF NEW BIODEGRADABLE POLYSULFENAMIDES FOR
APPLICATIONS IN MEDICINE

by
Jun Yoo

An Abstract

Of a thesis submitted in partial fulfillment
of the requirements for the Doctor of
Philosophy degree in Chemistry
in the Graduate College of
The University of Iowa

May 2011

Thesis Supervisor: Associate Professor Ned B. Bowden

ABSTRACT

The first polysulfenamides were synthesized with S-N and N-S-N bonds along the backbone. We demonstrated that sulfenamides were stable in polar protic and aprotic solvents, but degraded rapidly when exposed to acidic conditions. Microparticles were fabricated from polysulfenamides with S-N bonds, their surfaces were readily functionalized, and they were internalized by cells allowing for intracellular delivery of their cargo. These microparticles were also stable at physiological pH, degraded under acidic conditions, and possessed minimal toxicity towards cells. This work demonstrated that polysulfenamides form the basis for a new set of polymers for drug delivery that greatly differ from prior work in this field.

New biodegradable polymers with N-S-N bonds along the backbone were synthesized. These were the first polymers with these bonds and possessed many of the same characteristics as polymers synthesized with S-N bonds.

The synthesis and characterization of comb block copolymers with arms composed of poly(lactic acid), poly(butyl acrylate), and poly(styrene-*b*-vinylpyridine) were described. The self-assembled morphologies in the solid state of comb tri- and tetrablock copolymers with poly(styrene) were also described. These assemblies demonstrated that well-ordered and complex morphologies were assembled from these polymers.

The steric effect of substitutions on oxanorbornenes in ring-opening metathesis polymerization (ROMP) was investigated. Oxanorbornenes substituted with methyls at the bridgehead positions showed limited reactivity with the Grubbs first and second generation catalysts and the Grubbs first generation methylenide catalyst.

Abstract Approved: _____
Thesis Supervisor

Title and Department

Date

SYNTHESIS OF NEW BIODEGRADABLE POLYSULFENAMIDES FOR
APPLICATIONS IN MEDICINE

by
Jun Yoo

A thesis submitted in partial fulfillment
of the requirements for the Doctor of
Philosophy degree in Chemistry
in the Graduate College of
The University of Iowa

May 2011

Thesis Supervisor: Associate Professor Ned B. Bowden

Graduate College
The University of Iowa
Iowa City, Iowa

CERTIFICATE OF APPROVAL

PH.D. THESIS

This is to certify that the Ph.D. thesis of

Jun Yoo

has been approved by the Examining Committee
for the thesis requirement for the Doctor of Philosophy
degree in Chemistry at the May 2011 graduation.

Thesis Committee: _____
Ned B. Bowden, Thesis Supervisor

James B. Gloer

Sarah C. Larsen

Jan-Uwe Rohde

Aliasger K. Salem

To my God

ACKNOWLEDGMENTS

I would first of all like to thank God for being with me all the time and strengthening me to overcome many challenges by faith during my PhD study. Without Him all things would be meaningless. He is the reason and purpose of my being. I dedicate this dissertation to Him. I confess that I will serve Him by dedicating myself to Him all my life.

Thanks to my advisor Ned B. Bowden for his perfect guidance, support, and patience throughout the past five years. He has been a great mentor, tutor, boss, and friend. It was a great honor and joy for me to personally talk with a great scholar like him about research every week. When I was in a personal trial, he was very generous to wait for me until I rose again. I will never forget what he has done for me. I would also like to thank my committee members for their advice and guidance. Thanks also to the fellow Bowdenites past and present for promoting a good research environment.

I would also like to thank God's servants, Dr. John Jun, P. Abraham Kim, Mother Sarah Barry, Grace A. Lee, Dr. David Lee, and Shp. Philip Lee who prayed for me and served me with the love of God. I wish to thank my coworkers, M. Samuel Kim, Natalie, George, Fabian, and Kurt for their faithfulness.

Last but not least, I want to thank my family. Thanks to my mother for her unconditional love for me. Because of her devoted love, I could quickly overcome my trial. I also want to thank my two brothers, sister, sisters-in-law, and brother-in-law for always being there for me. Thanks to John and Hannah who have truly been a blessing and have allowed me to be pleasantly distracted from my studies at times. I wish to thank my wife, Jiil Hwang, who willingly married me and loved my kids. Because of her dedication and love for me, I could focus on my research without any worries and overcome deep grief. I will repay her love all my life.

TABLE OF CONTENTS

LIST OF TABLES	viii
LIST OF FIGURES	ix
CHAPTER 1 INTRODUCTION	1
Biomedical Polymers	1
Biomedical Polymers from Nature	1
Synthetic Biomedical Polymers	3
Scaffolds for Tissue Engineering and Organ Replacement	6
Hydrogels	7
Polymeric Scaffolds for Regeneration of Cells	10
Synthetic Biomedical Polymers for Drug Delivery Systems	12
Polyanhydrides	14
Polyesters	17
Requirements of New Biodegradable Polymers for Drug Delivery Systems	21
Objectives	23
Polysulfenamides	23
Polymers with N-S-N Bonds	23
Comb Block Copolymers	24
Steric Effects on Grubbs Catalysts	24
CHAPTER 2 SYNTHESIS OF POLYSULFENAMIDES FOR DRUG DELIVERY APPLICATIONS	25
Abstract	25
Introduction	25
Results and Discussion	27
Synthesis of Polysulfenamides	27
Degradation of Sulfenamides in Aprotic and Protic Solvents	31
Fabrication and Degradation of Microparticles of Polysulfenamides	34
Uptake of Microparticles into Cells and Cytotoxicity	37
Conclusions	39
Experimental Section	40
Materials and Methods	40
Materials	40
Cell culture	40
Characterization of small molecules and polysulfenamides	41
Synthesis of Small Molecules and Polymers	41
Hexanesulfonyl chloride	41
2,2'-Oxydiethanesulfonyl dichloride	42
<i>N</i> -Ethylmethyl-hexanesulfenamide (Molecule A)	42
<i>N,N'</i> -Ethylmethyl-bis(2-mercaptoethyl)disulfenamide	42
<i>N</i> -(Hexanethio)succinimide (Molecule B) ⁹⁸	43
(2,2'-Oxydiethenthio)disuccinimide	43
<i>N,N'</i> -(Hexanethio)disuccinimide	43
<i>N</i> -Benzylmethyl-hexanesulfenamide (Molecule C)	44
Polymer A	44

Polymer B.....	45
Polymer C.....	45
Polymer D.....	46
Polymer E.....	46
Polymer C from a disulfenamide.....	47
Kinetic Reactions with Sulfenamides and Thiosuccinimides.....	47
Kinetics of molecule A and <i>N</i> -benzylmethylamine (Figure 2.1c).....	47
Kinetics of molecule B and <i>N</i> -benzylmethylamine (Figure 2.1d).....	47
Kinetics of reaction between <i>N,N'</i> -(hexanethio)disuccinimide and piperazine (Figure 2.1e).....	48
Degradation of Sulfenamides.....	48
Kinetics of the degradation of molecule C under neutral conditions (Figure 2.2a).....	48
Kinetics of the degradation of molecule C with benzoic acid in CD ₃ OD.....	48
Degradation of molecule C with acetic acid in water (Figure 2.2b).....	49
Degradation of molecule C with <i>p</i> -toluenesulfonic acid in water.....	50
Characterization of Microparticles.....	50
Preparation of microparticles.....	50
Surface morphology.....	51
Particle size and zeta potential.....	51
Crosslinking with polyethylene imine (PEI).....	51
<i>In vitro</i> analysis of microparticle degradation.....	52
Particle uptake.....	52
Cytotoxicity evaluation of microparticles.....	52
Statistical analysis.....	53
CHAPTER 3 SYNTHESIS OF POLYMERS WITH BIODEGRADABLE N-S-N BONDS.....	54
Introduction.....	54
Results and Discussion.....	55
Synthesis and Reactions of Sulfur Transfer Reagents.....	55
Kinetics of Transamination Reactions.....	57
Synthesis of Polymers with NSN Bonds.....	60
Degradation of the N-S-N Bond.....	62
Conclusions.....	62
Experimental Section.....	63
Materials and Methods.....	63
Materials.....	63
Characterization.....	63
Synthesis of Small Molecules and Polymers.....	64
Bis(tributyltin) sulfide (Molecule A).....	64
Bis(succinimide) sulfide (Molecule B) ¹⁰²	64
<i>N,N'</i> -Dithiobis-ethylmethylamine (Molecule C) ¹⁰³	65
<i>N</i> -Ethylmethylsulfonyl chloride (Molecule D) ¹⁰⁴	65
Bis(<i>N</i> -ethylmethyl)sulfide (Molecule E) ¹⁰⁴	65
<i>N,N'</i> -Dithiobis-dimethylamine ¹⁰³	66
<i>N</i> -Dimethylsulfonyl chloride ¹⁰⁴	66
Bis(<i>N,N'</i> -dimethyl) sulfide (Molecule F) ¹⁰⁴	66

Polymer A	67
Polymer B.....	67
Polymer C.....	67
Calculation of Degree of Polymerization Based on ¹ H NMR Spectroscopy.....	68
Kinetic Reactions with Molecule E and <i>N</i> -Benzylmethylamine.....	68
Transamination Reaction of Molecule F and <i>N</i> -Benzylmethylamine	69
Degradation of N-S-N Bonds	69
CHAPTER 4 SYNTHESIS OF COMPLEX ARCHITECTURES OF COMB BLOCK COPOLYMERS AND THEIR ASSEMBLY IN THE SOLID STATE.....	71
Abstract.....	71
Introduction.....	71
Experimental Section.....	74
Materials and Methods	74
Materials.....	74
Characterization	74
Synthesis of Comb Block Copolymers.....	75
Synthesis of comb block copolymers with poly(butyl acrylate) arms	75
Synthesis of comb block copolymers with poly(lactic acid) arms	76
Synthesis of comb block copolymers with poly(styrene- <i>block</i> -4-vinylpyridine) arms.....	76
Results and Discussion	77
Synthesis of Comb Block Copolymers with Arms Composed of Poly(butyl acrylate)	77
Synthesis of Comb Block Copolymers with Arms Composed of Poly(lactic acid).....	81
Synthesis of Comb Block Copolymers with Block Copolymer Arms	84
Assembly of Comb Triblock Copolymers with Polystyrene Arms.....	86
Conclusions.....	87
Supporting Information	88
Series of Comb Tri- and Tetra-Block Copolymers with Polystyrene Arms	88
Structure and Characterization	88
Self-assembly and characterization of multi-block copolymer films.....	89
SEM Micrographs for the Polymers in Table 4.3.....	90
CHAPTER 5 FACILE SYNTHESIS OF THE GRUBBS FIRST GENERATION METHYLIDENE CATALYST AND ITS REACTIVITY TOWARDS STERICALLY HINDERED OXANORBORNES.....	112
Abstract.....	112
Introduction.....	112
Results and Discussion	113
Conclusions.....	116
Experimental Section.....	116
Synthesis and NMR Data	116
RuCl ₂ (=CH ₂)(PCy ₃) ₂ (1).....	116

1,4-Dimethyl-7-oxabicyclo[2.2.1]heptene-2,3-dicarboxylic anhydride (A)	118
1-Methyl-7-oxabicyclo[2.2.1]heptene-2,3-dicarboxylic anhydride (B).....	118
1,4-Dimethyl-7-oxabicyclo[2.2.1]heptene-2,3-dimethanol (C)	119
1-Methyl-7-oxabicyclo[2.2.1]heptene-2,3-dimethanol (D)	119
 CHAPTER 6 CONCLUSIONS AND RECOMMENDATIONS FOR FUTURE WORK.....	 122
Conclusions.....	122
Recommendations for Future Work	124
 APPENDIX SYNTHESIS OF COMB TRI- AND TETRABLOCK COPOLYMERS CATALYZED BY THE GRUBBS FIRST GENERATION CATALYST.....	 127
Abstract.....	127
Introduction.....	127
Experimental Section.....	129
Materials	129
Kinetic Experiments	130
Size Exclusion Chromatography (SEC).....	130
Synthesis of ABA Triblock Copolymer by ROMP	131
Synthesis of CACA Tetra-block Copolymer by ROMP	131
Synthesis of Comb Polymers and Cleavage of Their Arms from the Backbone	132
Self-assembly of Comb Block Copolymer Films.....	132
Results and Discussion	132
Conclusions.....	141
 REFERENCES	 142

LIST OF TABLES

Table 2.1 Synthesis of polysulfenamides.....	30
Table 3.1 Transamination reactions of molecule F and benzylmethylamine.	60
Table 3.2 Synthesis of N-S-N bond polymers.	61
Table 4.1 Synthesis of comb block copolymers with poly(butyl acrylate) arms.....	79
Table 4.2 Synthesis of comb block copolymers with poly(lactic acid) arms.	83
Table 4.3 Characterization of multi-block comb polymers.	89
Table A.1 Characterization of multi-block backbones.	136
Table A.2 Characterization of multi-block comb polymers.	139

LIST OF FIGURES

Figure 1.1 Natural biopolymers derived from polysaccharides. a) Alginate. b) Hyaluronic acid. c) Chondroitin sulfate. d) Chitosan. ¹	2
Figure 1.2 Synthetic biomedical polymers and their chemical structures. a) Nonbiodegradable polymers. b) Biodegradable polymers.	4
Figure 1.3 Schematic illustration of how to form a hydrogel through a cross-linked network of hydrophilic polymers. The cross-links between polymers can be generated through physical connections, covalent bonds, or ionic bonds. ¹	8
Figure 1.4 Schematic diagram of how to encapsulate cells within hydrogels and create bilayer hydrogels using photopolymerization. ¹	9
Figure 1.5 Photopolymerization of poly(ethylene glycol) diacrylate to yield a hydrogel for the treatment of arthrosis. a) Procedure of photopolymerization to form a hydrogel on the defect of human cadaveric knee. b) The defects filled with the hydrogel after 5 min of photopolymerization. ¹	9
Figure 1.6 Confocal microscopy images showing the application of PLGA scaffolds for growing neural stem cells (NSCs) and Schwann cells (SCs) <i>in vitro</i> . a) The shape of the PLGA scaffolds. b) and d) NSCs and SCs stained blue distributed in the scaffold channels after 2 hour in culture c) and e) The channels were filled with the proliferated NSC and SCs after 65 hours in culture. f) NSCs maintained the ability to proliferate after 24 hours in culture. ³⁵	11
Figure 1.7 Application of biodegradable polymers for regeneration of nerves. a) A fabricated conduit made from photo-crosslinked poly(ϵ -caprolactone fumerate) (PCLF). b) Overview of a crosslinked PCLF conduit implanted between sciatic nerve stumps (shown by the arrow) after 17 weeks. Reprinted from Wang et al. ³⁶	12
Figure 1.8 Synthetic methods to yield polyanhydrides. a) Melt condensation. b) and c) Dehydrochlorination. d) Dehydrative coupling. e) Ring-opening polymerization.	15
Figure 1.9 Treatment for malignant brain tumors using Griadel®, polyanhydride drug delivery matrix of polyanhydride in the surgical resection cavity. a) - c) Magnetic resonance imaging of the brain in axial, coronal, and sagittal views, respectively, after implanting Griadel wafers to the resection bed (arrows pointed). d) – f) Magnetic resonance imaging of the brain demonstrating no enhanced lesion with tumor activity after four months. ⁴⁵	16
Figure 1.10 Methods to yield poly(ϵ -caprolactone). a) Anionic ring-opening polymerization. b) Cationic ring-opening polymerization. c) Coordination-insertion ring-opening polymerization. d) Free radical ring-opening polymerization.	18

Figure 1.11 Synthesis of a) poly(lactic acid), b) poly(glycolic acid), and c) poly(lactic- <i>co</i> -glycolic acid) through coordination-insertion ring-opening polymerization.	19
Figure 1.12 Scanning electron microscopy micrographs of microparticles from PLGA. a) Gross view of microparticles fabricated by a water-in-oil-in-oil double emulsion technique. b) Inside view of one microparticle to show its interior morphology. ⁴⁶	20
Figure 1.13 Effects of chemical modifications of PEI on the efficacy of gene delivery. a) Dodecylation of primary amines along the backbone of branched PEI with dodecyl iodide, resulting in increased gene delivery efficacy and a nontoxic polymer. b) Acylation of primary and secondary amines along the backbone of branched PEI with an amino acid, resulting in 2 times increased gene delivery efficacy and reduced cytotoxicity. ⁵⁸	22
Figure 2.1 Synthesis of polysulfenamides and the kinetics of transamination reactions. a) In one method dithiols were reacted to form S-Cl bonds which were readily transformed <i>in situ</i> into sulfenamides. The polymerization proceeded by displacement of <i>N</i> -ethylmethylamine with a different amine. b) In a second method dithiols were activated by reaction with <i>N</i> -chlorosuccinimide to yield stable products which were purified and then exposed to secondary diamines to yield polymer. c) The kinetics of reaction of a sulfenamide with a secondary amine in CD ₃ OD. The reaction yielded a 50/50 mixture of the two sulfenamides. d) The kinetics of reaction of a thiosuccinimide with a secondary amine in CD ₂ Cl ₂ . The reaction yielded >97% sulfenamide after extended reaction times. e) The kinetics of a typical polymerization to demonstrate that the polymerizations were rapid and went to quantitative conversions at reasonable concentrations. f) A polymerization that was completed. g) The structure of allicin.	28
Figure 2.2 Degradation of sulfenamides and characterization of their products. a) Molecule C was added to C ₆ D ₆ and CD ₃ OD to study how rapidly it degraded. b) Molecule C was added to D ₂ O with seven molar equivalents of acetic acid. Products D, E, and F were characterized. c) Sulfenic acids were the first product of degradation of molecule C, but they were known to rapidly react to yield thiosulfinates as shown. d) Sulfenamides were protonated by benzoic acid in CD ₃ OD.	32

Figure 2.3	Microparticles with the structure of entry 2 in Table 2.1 were studied for their degradation and surface reactions. a) Time dependent weight loss of the polymer incubated at acidic pH (4.0) and physiological pH (7.4). Data represents the percentage weight loss as mean of three samples. The weight loss was significant at all the time points as indicated (***) $P < 0.001$, ** $P < 0.01$, two-tailed unpaired t test). b) Scanning electron microscopy (SEM) image of microparticles as prepared. c) SEM image of microparticles after incubation in acetate buffer (pH 4.0) for 14 days. Microparticles at various stages of degradation can be observed. d) A small fraction of the microparticles that were degraded at different pHs were removed at the indicated times, dissolved in CHCl_3 , and studied by size exclusion chromatography. The molecular weight of the polymers as a function of time the microparticles were degraded is shown. e) Microparticles were exposed to PEI that coated their surfaces. We believe that the amines in PEI reacted with the sulfenamides on the surface to covalently bond the PEI to the surface of the microparticle according to the reaction shown in Figure 1c and reproduced here.	35
Figure 2.4	Uptake of microparticles fabricated from entry 2 in Table 1 and loaded with rhodamine and studied using confocal microscopy. a) – e) The cells are JAWSII immature dendritic cells and in f)-j) they are HEK293 cells. The nucleus of the cell was stained with DAPI to appear blue and the rhodamine appeared red. In d) and i) the transmitted light images indicate the periphery of the cells and the location of the microparticles. In e) and j) merged images clearly outline the periphery of the cell, the location of the nucleus, and the microparticles to clearly demonstrate that the microparticles were found on the interior of the cells. The images were taken at different sections to ensure that the microparticles were in the same focal plane as the planes taken through the cells. The microparticle in the far left of images g)-j) was not found in a cell and was used to show a free microparticle.	37
Figure 2.5	Cytotoxicity of microparticles fabricated with the structure shown in entry 2 of Table 1 towards HEK293 cells. Microparticles were suspended in media immediately before addition into cells. Cells were incubated with the microparticles for 24 hours at 37 °C in a humidified 5% CO_2 -containing atmosphere. Cell viability was determined by MTS assay and the expressed as percentage of control (without microparticles).	39
Figure 3.1	The synthesis of polysulfenamides and polymers with NSN bonds.	54
Figure 3.2	Two approaches to synthesize SN bonds that were successful in our prior work.	55
Figure 3.3	The synthesis of two sets of sulfur transfer reagents. a) The synthesis of a dithiosuccinimide. b) and c) The synthesis of two examples of bis-aminosulfides.	56

Figure 3.4 Kinetics of transamination reactions. a) The reaction that was studied in a sealed NMR tube. b) The conversion of the transamination reactions as a function of time. The conversion was defined as the sum of the S-N(CH ₃)Bn bonds divided by the sum of all of the S-N bonds for molecules E, H, and I. c) The plot of the initial data points to find the rate constants for each solvent.....	58
Figure 3.5 Transamination reactions with dimethylamine as the leaving group.	59
Figure 3.6 Degradation of N-S-N bond: Molecule D was added to C ₆ D ₆ , CDCl ₃ , DMSO-d ₆ , and DMSO-d ₆ /D ₂ O (10/1 v/v) to study how rapidly it degraded.	62
Figure 4.1 Architectures of comb polymers. a) A chemical structure and schematic of a comb polymer with poly(styrene) arms is shown. b) A comb block copolymer is shown with a schematic of its structure.....	72
Figure 4.2 Synthesis of a comb block copolymer with poly(butyl acrylate) arms. a) How the backbone polymer was synthesized in one pot. b) How poly(butyl acrylate) arms were grown from the backbone polymer.	78
Figure 4.3 SEC micrographs of comb polymers with a) poly(butyl acrylate) arms and b) poly(lactic acid) arms.	79
Figure 4.4 Synthesis of a comb block copolymer with poly(lactic acid) arms. a) The monomers that were used to synthesize the backbone polymer for comb polymers with poly(lactic acid) arms. b) The polymerization to yield comb block copolymers is shown.	81
Figure 4.5 Cross-links between the comb polymers will only occur when transesterification occurs with the ester group in the backbone polymer.	82
Figure 4.6 Vinylpyridine was polymerized from comb block copolymers with poly(styrene) arms.....	84
Figure 4.7 Comb block copolymers and their morphologies. a) Two examples of comb polymers with poly(styrene) arms that were assembled in the solid state. The capitalized letters refers to the monomer units along the backbone and the subscript letters refer to the degree of polymerization along the backbone and polystyrene arms as shown. b) An SEM micrograph of an assembled array of a comb polymer with composition of B ₅₀₀ A _{100:3950} B ₅₀₀ is shown. c) and d) SEM micrographs of an assembled array of a comb polymer with a composition of A _{50:5190} B ₁₀₀₀ A _{50:5190} is shown. e) A SEM micrograph of an assembled array of a comb polymer with composition of B ₅₀₀ A _{100:4710} B ₅₀₀ is shown.....	86
Figure 4.8 Structure of multi-block comb polymers.....	88
Figure 4.9 SEM micrographs of entry 1.	90
Figure 4.10 SEM micrographs of entry 2.	91
Figure 4.11 SEM micrographs of entry 3.	92

Figure 4.12 SEM micrographs of entry 4.	93
Figure 4.13 SEM micrographs of entry 5.	94
Figure 4.14 SEM micrographs of entry 6.	95
Figure 4.15 SEM micrographs of entry 7.	96
Figure 4.16 SEM micrographs of entry 8.	97
Figure 4.17 SEM micrographs of entry 9.	98
Figure 4.18 SEM micrographs of entry 10.	99
Figure 4.19 The SEM micrograph of entry 11.	100
Figure 4.20 SEM micrographs of entry 12.	101
Figure 4.21 SEM micrographs of entry 13.	102
Figure 4.22 SEM micrographs of entry 14.	103
Figure 4.23 SEM micrographs of entry 15.	104
Figure 4.24 SEM micrographs of entry 16.	105
Figure 4.25 SEM micrographs of entry 17.	106
Figure 4.26 SEM micrographs of entry 18.	107
Figure 4.27 SEM micrographs of entry 19.	108
Figure 4.28 SEM micrographs of entry 20.	109
Figure 4.29 SEM micrographs of entry 21.	110
Figure 4.30 SEM micrographs of entry 22.	111
Figure 5.1 How the ruthenium methylidenes were synthesized.	113
Figure 5.2 All of these molecules were isolated as the pure exo isomers.	114
Figure 5.3 Steric effects of the methyl at the bridgehead position of oxanorbornes. a) Significant steric crowding exists between the Grubbs second generation catalyst and monomer 6 when it undergoes a metathesis reaction. b) and c) The reaction of monomer 7 and the Grubbs first generation methylidene catalyst has significant steric interactions in the transition state regardless of the orientation of molecule 7.	115
Figure 5.4 ^1H NMR spectrum of $\text{RuCl}_2(=\text{CH}_2)(\text{PCy}_3)_2$	117
Figure 5.5 ^{13}C NMR spectrum of $\text{RuCl}_2(=\text{CH}_2)(\text{PCy}_3)_2$	117
Figure 5.6 ^{13}C NMR spectrum of $\text{RuCl}_2(=\text{CH}_2)(\text{PCy}_3)_2$	118

Figure 5.7 ^1H NMR spectrum of 1,4-Dimethyl-7-oxabicyclo[2.2.1]heptene-2,3-dimethanol.....	120
Figure 5.8 ^{13}C NMR spectrum of 1,4-Dimethyl-7-oxabicyclo[2.2.1]heptene-2,3-dimethanol.....	120
Figure 5.9 ^1H NMR spectrum of 1-Methyl-7-oxabicyclo[2.2.1]heptene-2,3-dimethanol.....	121
Figure 5.10 ^{13}C NMR spectrum of 1-Methyl-7-oxabicyclo[2.2.1]heptene-2,3-dimethanol.....	121
Figure 6.1 Polymerization of disulfenamide with dimethylamine as a leaving group. ...	125
Figure 6.2 Functionalization of polysulfenamides. a) Synthesis of a polysulfenamide with an alcohol group along the backbone. b) Functionalization of a polysulfenamide with a cyclooctyne derivative using Cu-free click chemistry with azide-modified biomolecules.....	126
Figure A.1 Synthesis of comb tri- and tetra block copolymers. a) The simple, two-step synthesis of an oxanorbornene and the resulting monomers used in this study. b) The synthesis of comb block copolymers by ROMP and ATRP. In the final step, the arms were cleaved from the backbone polymer and characterized by SEC.	133
Figure A.2 Kinetics of ring opening metathesis polymerizations of monomer A and B. a) Plots of conversion versus time were measured by ^1H NMR spectroscopy for monomer B with a monomer to catalyst ratio of 50:1, and monomer A with monomer to catalyst ratios of 500:1 and 1000:1. The initial concentration of monomer was 0.058 M for the monomer to catalyst ratio of 50:1, and it was 0.33 M for monomer to catalyst ratios of 500:1 and 1000:1. b) The kinetics of the polymerizations were measured for the monomer to catalyst ratios of 50:1, 500:1, and 1000:1.	134
Figure A.3 Changes of SEC traces, M_n , and PDI of block polymers. a) SECs of three polymers to show the progression from a homopolymer to diblock polymer to triblock polymer. b) Monomer A (500 units) was initially polymerized to completion. Next, 100 equivalents of 4-octene were added to study the effect of cross metathesis on the polymer. The molecular weight and PDI of the polymer were consistent over four hours after the addition of 4-octene.....	136
Figure A.4 SEM micrographs of morphologies of a) $\text{A}_{200}\text{C}_{10:3280}\text{A}_{750}\text{C}_{100:3280}$ and b) $\text{A}_{500}\text{B}_{100:1430}\text{A}_{500}$ that were assembled in the solid state.....	140

CHAPTER 1

INTRODUCTION

Biomedical Polymers

In this chapter I will briefly review some of the key polymers used in medicine and their properties. This field is too large to be reviewed in its entirety; rather, I will focus on the most important polymers in this field and give a few key examples of their applications to illustrate the applied aspects of polymers in medicine. For instance, these polymers are used to deliver drugs and DNA; as scaffolds to grow organs, bone, or nerve cells; and as replacements for heart valves. The applications of these polymers require an understanding of their chemical properties and I will discuss how their chemical structures are chosen to achieve the right mechanical or physical properties.

Biomedical Polymers from Nature

Biomedical polymers can be defined as polymers which are used for medical treatments and therapies such as the regeneration of damaged tissues and organs, cell therapies, materials for artificial organs and prostheses, and drug delivery systems. Because of their applications in the body, biomedical polymers must be biocompatible or biodegradable such that they promote no toxic or harmful effects. Naturally occurring polymers such as collagen, fibrin, and derivatives of polysaccharides (Figure 1.1) are widely used for biomedical purposes.¹ These polymers show little to no cytotoxicity and readily mimic cellular environments because they are derived from biological sources such as animal tissues, body-fluids, and plants. In the subsequent paragraphs I will discuss some of these polymers, their origins, and key applications.

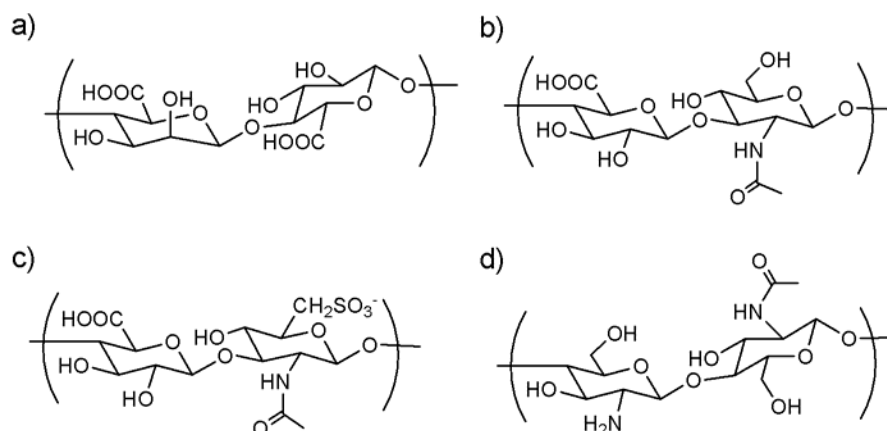


Figure 1.1 Natural biopolymers derived from polysaccharides. a) Alginate. b) Hyaluronic acid. c) Chondroitin sulfate. d) Chitosan.¹

Collagen is a group of proteins which are found in the tissue of all vertebrates.² It is extracted from animal skin and can be processed into various forms such as gels, sponges, and films.³ Collagen has been mainly used for wound dressing and scaffolds on which artificial liver, bone, cartilage, and skin are grown.³

Fibrin is another kind of natural polypeptide which originates in the process of blood coagulation and plays a pivotal role in wound treatment.^{4,5} Because of its adhesiveness, fibrin has been used as surgical glue for plastic and reconstructive surgery, as a surgical sealant for skin repair, and to grow bone graft. It is also known to form heparin-containing hydrogels which can deliver growth factor to cells.⁵

Alginate is extracted from seaweed and possesses an abundant number of carboxylic acid groups along its backbone compared to other polysaccharide-derivatives as shown in Figure 1.1a. Because of the carboxylic acid groups, alginate is negatively charged and cross-links well in the presence of the divalent cation Ca^{2+} through the ionic

interactions with two acids. Alginate has been used for wound dressing and as a hydrogel scaffolding for tissue engineering.⁶

Hyaluronic acid (HA), one of a group of polysaccharides, exists in all tissues and body fluids of vertebrates.⁷ Hyaluronic acid plays a pivotal role in biological process such as tissue repair, tissue hydration, and cell differentiation.⁴ Hyaluronic acid has been widely utilized for ocular surgery, alleviating osteoarthritis, and wound healing applications.⁸⁻¹⁰

Chitosan, another polysaccharide-derivative, is biosynthetically produced by deacylating chitin, which is found in the shell of clams.^{11, 12} Chitosan is a semi-crystalline polymer and its degree of crystallinity is determined by the degree of deacylation.¹ It is degraded in cells by various chitinases and the rate of its biodegradation varies with the number of acetyl group remaining in the backbone.¹³ Because chitosan is positively charged due to amine groups along its backbone, it is one of most promising nonviral vectors for gene delivery.¹⁴ Chitosan also has been widely investigated for space-filling prostheses, wound dressings, and a scaffold for tissue engineering because of its biodegradability and biocompatibility.^{15, 16}

Although these naturally derived polymers possess numerous positive attributes as biomedical polymers, there are some limitations to their use due to their rapid degradation *in vivo* and lack of long term physical stability.¹ The physical weakness of natural polymers and their rapid degradation profiles make it challenging to control their physicochemical properties and limit their applications. Consequently, synthetic biomedical polymers have attracted the attention of scientists as a way to tailor the chemical and physical properties of polymers used in medicine.

Synthetic Biomedical Polymers

Numerous synthetic biomedical polymers have been used for more than four decades because of their ease of synthesis, the ability to control their physical properties

through molecular weights and chemical composition, and the ease of molding devices with tailored properties. Synthetic biomedical polymers can be categorized into two basic types: nonbiodegradable and biodegradable polymers. In Figure 1.2 the structures of common synthetic polymers used in biomedical applications are shown.

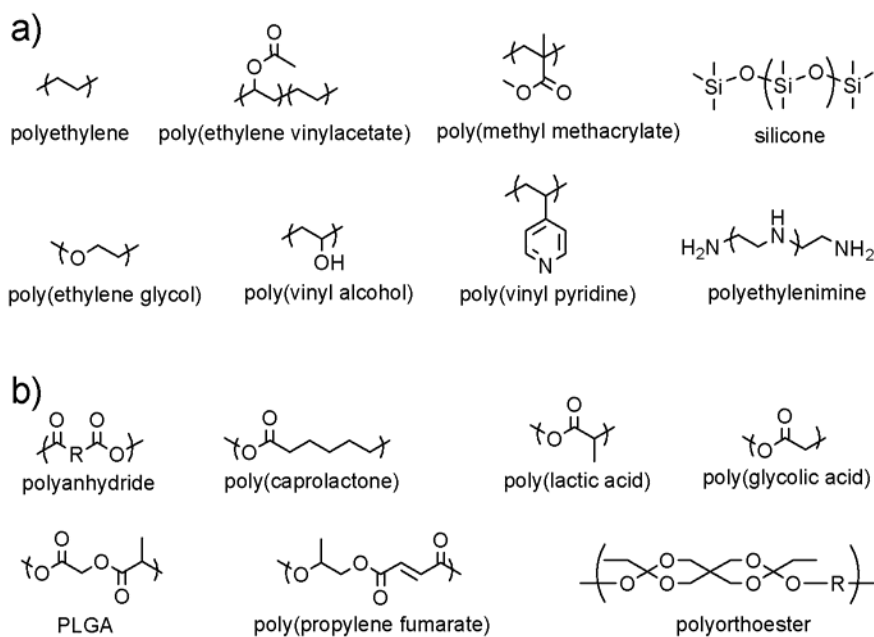


Figure 1.2 Synthetic biomedical polymers and their chemical structures. a) Nonbiodegradable polymers. b) Biodegradable polymers.

As can be seen in Figure 1.2a, nonbiodegradable polymers lack functional groups along their backbones that can be cleaved to degrade the polymer *in vivo*. Therefore, these polymers are mostly inert and persist in the human body. These polymers are typically used in applications where they must persist for long periods of time such as for

hip replacements or to increase the molecular weight of proteins to increase their lifetime in blood.

These polymers include ultrahigh-molecular-weight polyethylene (UHMWPE) which has a molecular weight in excess of a million g mol^{-1} .¹⁷ Although UHMWPE is nondegradable in the body, it is considered biocompatible because it has no solubility in blood. Because UHMWPE is a hard material and relatively safe *in vivo*, it is used as a major material for joint replacements such as artificial hips and knees.^{18, 19}

Silicones are also important polymers for biomedical application because of their biocompatibility, ease of fabrication, and high permeability to various steroids.²⁰⁻²² As a result, silicones have been exploited for cosmetics, shampoos, contraceptives, lubricating oils, and transdermal delivery of drugs.²³

Among the nonbiodegradable polymers used in medicine, poly(ethylene glycol), poly(vinyl alcohol), poly(vinyl pyridine), and polyethyleneimine are all water-soluble. These polymers possess amine, carboxylic acid, ethyleneoxy, or amine groups along their backbone, and can be easily hydrated, ionized, or protonated to dissolve in physiological fluids. Water-soluble polymers have a number of applications such as matrices for drug delivery applications, hydrogels for tissue engineering,²⁴ and nonviral vectors for DNA delivery.²⁵ Many of these polymers are commonly used for preparing capsules and tablets of drugs which are orally administered. When these capsules and tablets are taken into the body, the drugs are slowly released as the polymers dissolve. The size and shape of the tablet as well as the molecular weight and identity of polymers influence the rate of release of drug.²²

Biodegradable polymers possess a backbone that can be fragmented *in vivo* to shorter chains through a chemical reaction. As a result of the fragmentation, the segmented chains are water-soluble or small enough to be excreted from the body by physiological metabolic pathways. These biodegradable polymers mainly contain hydrolyzable functional groups such as ester and anhydride groups along their backbone

as shown in Figure 1.2b and readily degrade through a hydrolysis reaction in physiological fluids. Commercially available and widely used biodegradable polymers are poly(ϵ -caprolactone), poly(lactic acid), poly(glycolic acid) and numerous polyanhydrides. Their synthesis, properties, and applications as a drug delivery matrix will be discussed in more detail later in this chapter.

Scaffolds for Tissue Engineering and Organ Replacement

One of the remarkable applications of biomedical polymers is that they can be utilized for tissue engineering and as scaffolds to grow replacement organs. In tissue engineering applications, damaged tissues and organs are healed by the growth of new cells on a defective site. Tissue engineering typically requires three components: a group of reparative cells which have ability to migrate, proliferate, and differentiate; biodegradable scaffolds on or in which cells can grow; and growth factors which provide nutrients to the cells.^{1, 26} The scaffold plays a key role because it influences the growth, differentiation, and organization of the cells as well as the size and shape of the revived tissue. In order to provide the optimal environment for the growth of cells, the scaffold should ideally meet the following requirements.²⁷

1. The scaffold material should be biocompatible and biodegradable with controlled kinetics of degradation.
2. The scaffold should possess an appropriate surface chemistry which facilitates the attachment of cell, proliferation, and differentiation.
3. The mechanical properties of the scaffold should match the properties of the site where the scaffold is implanted.
4. The architecture of the scaffold should expedite the formation of the ingenuous structure of tissue and be manufactured reproducibly to medically proper sizes and shapes.

5. The scaffold should be three-dimensional and extremely porous. The pores should be interconnected to allow cellular migration, production of the extracellular matrix, and the exchange of nutrients and metabolic waste.

Poly(lactic acid), poly(glycolic acid), poly(lactic-*co*-glycolic acid), and poly(ϵ -caprolactone) are the main polymers used to prepare scaffolds because they fulfill the five requirements.²⁶ Among those five requirements, the preparation of a highly porous and interconnected pore structure is the most challenging. Consequently, efforts to produce a highly porous scaffold with interconnected pores have been investigated by many groups. Techniques such as gas-foaming, salt-leaching, thermally induced phase separation, and freeze drying have been used to fabricate such scaffolds.²⁸

The main problems with these methods are that resulting scaffolds do not have a high concentration of interconnected pores. As a result, scaffolds derived from these methods are ineffective at cultivating cells inside them because of the lack of internal channels to effectively facilitate transport of oxygen, nutrients, and metabolic wastes.²⁸ Therefore, alternative techniques to produce fully interconnected channels within a porous scaffold are still needed.

Hydrogels

Hydrogels are a distinct type of three-dimensional polymeric scaffold that consist of hydrophilic, water-soluble cross-linked polymers in contrast to the scaffolds mentioned previously which were prepared from hydrophobic polymers.²⁹ The cross-linked scaffold is constructed through physical connections, covalent bonds, or ionic bonds as shown in Figure 1.3.¹ Hydrogels have an important advantage in that they are prepared in water without organic solvents so the risks of toxicity from organic solvents, which may cause serious inflammation to cells, are eliminated.

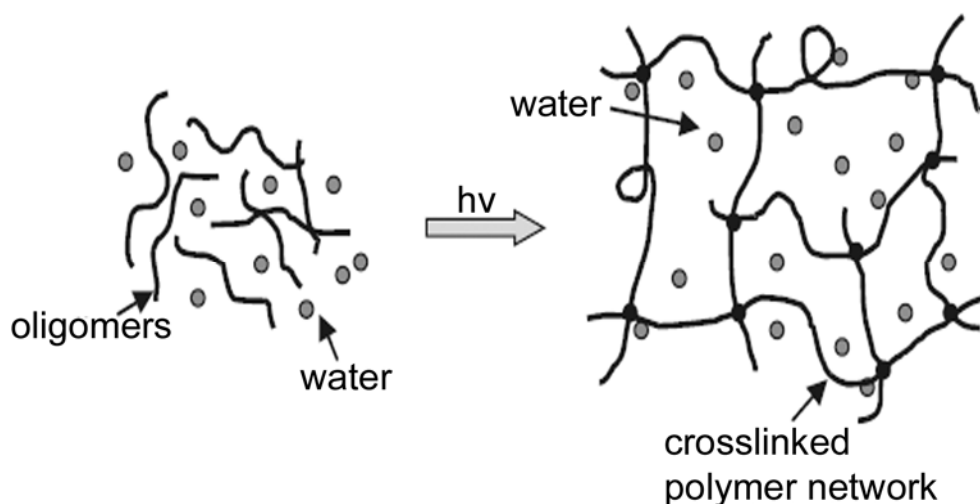


Figure 1.3 Schematic illustration of how to form a hydrogel through a cross-linked network of hydrophilic polymers. The cross-links between polymers can be generated through physical connections, covalent bonds, or ionic bonds.¹

The physical properties of hydrogels such as swelling, elasticity, and permeability are determined by the molecular weight and chemical structure of the polymers. Because hydrogels are quite analogous to biological aqueous gels in the human body,²⁹ they may provide an optimal biological environment for cells. Covalent cross-linked hydrogels are generally prepared by radical polymerization using water-soluble polymers which have a vinyl group at the end of the polymer chain.³⁰ The radical polymerization of the vinyl group can be initiated by heat, redox catalysts, or UV light.^{31, 32} The use of photopolymerization for cross-linking polymers is favored because it is simple, fast, and controllable, thus enabling the formation of gels *in situ*.³³ Direct photoencapsulation of cells in a hydrogel can be performed by reacting photo-reactive oligomers in solution with cells in one batch as shown in Figure 1.4.^{1, 33}

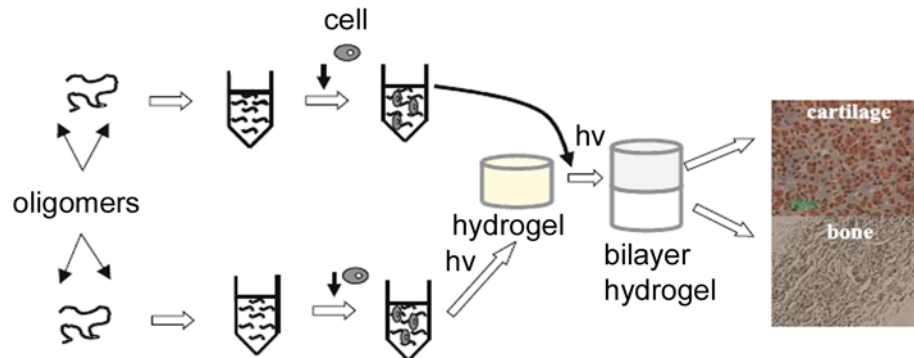


Figure 1.4 Schematic diagram of how to encapsulate cells within hydrogels and create bilayer hydrogels using photopolymerization.¹

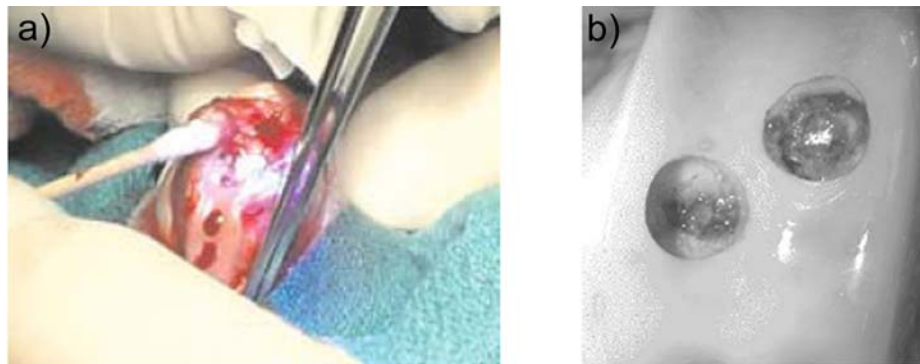


Figure 1.5 Photopolymerization of poly(ethylene glycol) diacrylate to yield a hydrogel for the treatment of arthrosis. a) Procedure of photopolymerization to form a hydrogel on the defect of human cadaveric knee. b) The defects filled with the hydrogel after 5 min of photopolymerization.¹

One of the best advantages of using photo-hydrogelation is the ability to directly prepare a hydrogel with viable cells *in situ* at the defective site. Consequently, it is possible to implant a hydrogel-cell material into a body with a minimally invasive procedure,³⁴ whereas, the scaffold made from hydrophobic polymers requires invasive surgical operations because the scaffolds are implanted in the body after growing the encapsulated cells in the scaffolds *in vitro* for several weeks.²⁸ Varghese et al. showed that spatial, controllable, and fast photo-hydrogelation is possible by injecting poly(ethylene glycol) diacrylate with a photoinitiator into the defective site on a human cadaver knee using a syringe and polymerizing it with UV light for 5 min (Figure 1.5).¹

Polymeric Scaffolds for Regeneration of Cells

The applications of the scaffolds composed of either hydrophobic or hydrophilic polymers discussed in this chapter will focus on musculoskeletal tissue such as cartilage, bone, muscle, and tendon. One advantage of synthetic biodegradable polymers is that they can be cast into molds due to their ease of fabrication and durability, whereas, biomedical polymers from nature are not readily cast into molds. For instance, if three-dimensional scaffolds with multichannels possessing specific sizes, shapes, and durability are required for implantation, only synthetic biodegradable polymers can provide the appropriate mechanical and physical properties for these scaffolds.

Olson et al. prepared a scaffold 2 mm in length and 3 mm in diameter with seven internal channels using poly(lactic-*co*-glycolic acid) for regeneration of neural stem cells (NSCs) and Schwann cells (SCs) to support axonal regeneration to heal spinal cord injuries.³⁵ They demonstrated that the NSCs and SCs in the multichannel scaffolds successfully proliferated *in vitro* for 65 h (Figure 1.6) and *in vivo* for 1 month after transplantation of the scaffolds into rats. When the axonal regeneration was quantitatively analyzed 1 month post-transplantation, the number of axons in the scaffolds seeded with NSCs and SCs significantly increased compared to the controls with no NSCs and SCs.

This results show that the scaffolds made from poly(lactic-*co*-glycolic acid) are potentially effective at guiding axonal regeneration in the spinal cord.

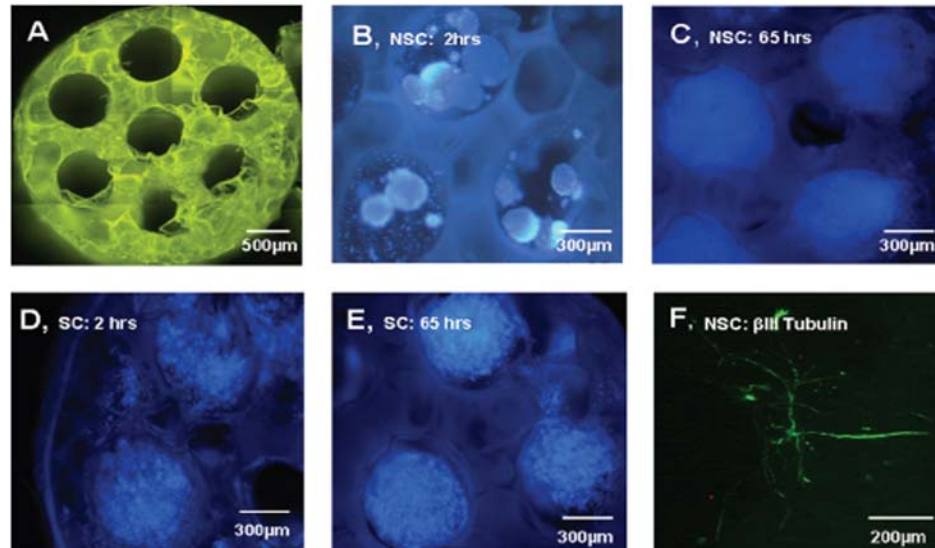


Figure 1.6 Confocal microscopy images showing the application of PLGA scaffolds for growing neural stem cells (NSCs) and Schwann cells (SCs) *in vitro*. a) The shape of the PLGA scaffolds. b) and d) NSCs and SCs stained blue distributed in the scaffold channels after 2 hour in culture c) and e) The channels were filled with the proliferated NSC and SCs after 65 hours in culture. f) NSCs maintained the ability to proliferate after 24 hours in culture.³⁵

Wang et al. fabricated a single-channel scaffold 1.92 mm in outer diameter and 10.22 mm in length by photo-crosslinking poly(ϵ -caprolactone-*co*-fumerate) in a glass mold for regeneration of peripheral nerve as shown in Figure 1.7a.³⁶ The conduit fabricated from cross-linked poly(ϵ -caprolactone-*co*-fumerate) was able to hold sutures that connected it to the surrounding tissue, flexible such that it remained connected to tissues for long periods of time, biocompatible, and biodegradable such that 70 ~ 80 % of the original weight was lost after 71 weeks. The surface properties of the conduit were

also favorable to support the attachment and proliferation of cells. When the conduit was sutured between the proximal and distal sciatic nerve stumps of a rat as shown in Figure 1.7b, a nerve cable with myelinated axons was observed after 17 weeks. This result demonstrated that poly(ϵ -caprolactone-*co*-fumerate) was an excellent candidate for preparing a scaffold for the regeneration of nerve cells.

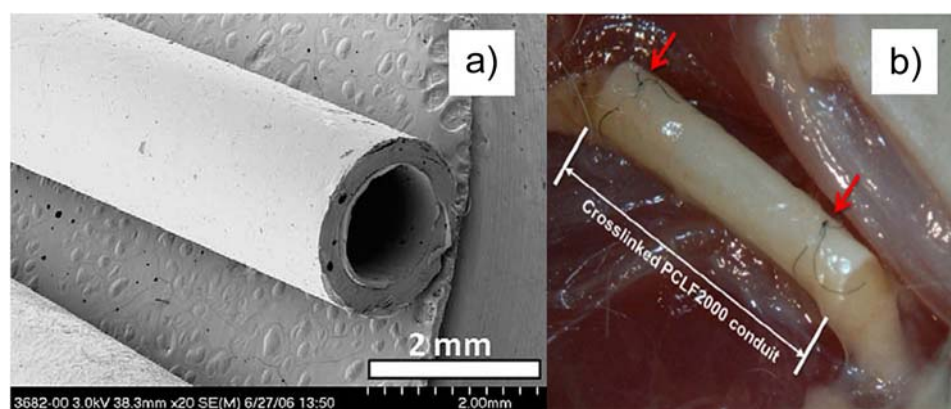


Figure 1.7 Application of biodegradable polymers for regeneration of nerves. a) A fabricated conduit made from photo-crosslinked poly(ϵ -caprolactone fumerate) (PCLF). b) Overview of a crosslinked PCLF conduit implanted between sciatic nerve stumps (shown by the arrow) after 17 weeks. Reprinted from Wang et al.³⁶

Synthetic Biomedical Polymers for Drug Delivery Systems

Medications given orally consist of active pharmaceutical ingredients, which are often reactive in the human body and are readily damaged by gastric enzymes and acidic fluids of the stomach before they reach the site of action. Also, drugs are commonly toxic or have adverse reaction in the body when their total dosage is released at once.

Therefore, direct administration of drugs to the body without any delivery vector is limited. To safely deliver drugs to a target in the body, the drugs need to be coated or encapsulated and released at a controlled rate over an extended period of time.

Synthetic biomedical polymers have been used as vectors for the delivery of drugs because they do not immediately dissolve in the body, form polymeric membranes to coat or encapsulate drugs, and enable the controlled release of drugs through the mechanisms of diffusion, osmotic effects, and erosion of the polymer.^{20, 37}

The polymers used for drug delivery matrices need to be biodegradable for optimal safety and controlled-release profiles. If the polymers are nonbiodegradable, they will be accumulated in organs such as the liver, heart, and spleen and may result in toxic effects in the body. Accordingly, polymers in drug delivery systems need to be degraded and their degradation products should be biocompatible or effectively excreted by kidneys.

The degradation of polymers also needs to be controlled by physiological stimuli such as pH, temperature, cations, or enzymes. For instance, if drugs are targeted to the lysosomal compartments of cells, the polymer matrix which surrounds the drugs should be stable in the bloodstream at pH 7.4 but readily degrade in the lysosome at pH 4.5 to 5 to release the drugs.

Another significant factor in designing synthetic biomedical polymers for the application of drug delivery is that the polymeric matrix should be readily functionalized with receptors to directly bind to the surface of specific cells. However, most developed synthetic biomedical polymers lack reactive functional groups on their backbone or the surface of their polymeric matrix, thereby limiting their use in various applications.

The most extensively studied and commonly used synthetic biomedical polymers for drug delivery systems are polyanhydrides and polyesters as shown in Figure 1.2b because they are simple to design and synthesize, readily biodegrade through hydrolysis,

and are biocompatible such that some are approved for use by the Food and Drug Administration (FDA).^{23, 38}

Polyanhydrides

Polyanhydrides are among the most intensively investigated biodegradable polymers for use in drug delivery systems. Polyanhydrides composed of aliphatic, aromatic, and heterocyclic dicarboxylic acid monomers have been synthesized because the polymers and their syntheses possess the following advantages.³⁹

1. These polymers are synthesized through a one-step reaction without the need for further purification.
2. Commercially available, inexpensive dicarboxylic acid monomers are used for the preparation of these polymers.
3. The structure and molecular weight of the polymers are well characterized and they degrade via hydrolysis reactions with controllable kinetics of degradation. Thus, the controlled release of drugs is possible by varying the composition of the polymers.
4. Polymeric matrices are easily fabricated through melting or compression at low temperature, and the physical properties of the resulting materials can be varied by manipulating the composition of polymers, additives, and surface area.
5. The products of degradation are typically nontoxic in the body and are readily removed from the body within a reasonable period of time.
6. These polymers can be disinfected via terminal γ -irradiation.

Polyanhydrides are synthesized by melt condensation, dehydrochlorination, dehydrative coupling, and ring-opening polymerization as shown in Figure 1.8.³⁹ In melt condensation, dicarboxylic monomers are first reacted in refluxing acetic anhydride to

yield low molecular weight prepolymers with degrees of polymerization between 1 and 20, followed by further polymerization at high temperature under vacuum to produce polymers with degrees of polymerization from 100 to over 1,000.⁴⁰ Melt condensation enabled chemists to synthesize the first high molecular weight polyanhydrides with no further purification.⁴¹ Although successful, this method is unsuitable for heat sensitive monomers.

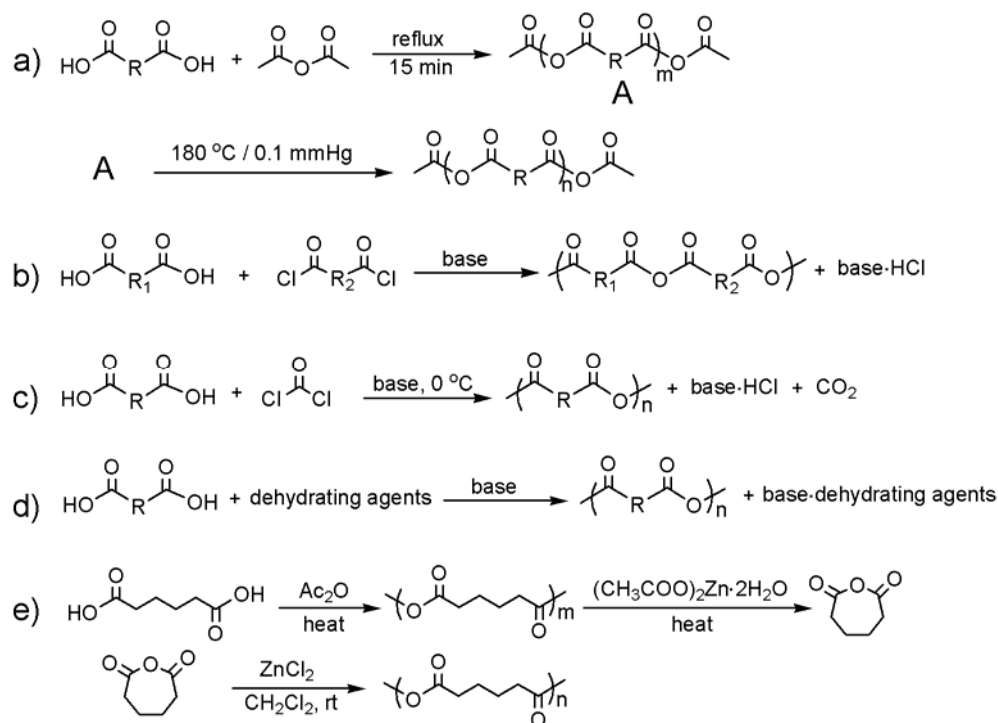


Figure 1.8 Synthetic methods to yield polyanhydrides. a) Melt condensation. b) and c) Dehydrochlorination. d) Dehydrative coupling. e) Ring-opening polymerization.

For heat-sensitive monomers, polymerization under mild conditions can be achieved by reacting dicarboxylic acid monomers with diacyl chloride or phosgene in the presence of a base to neutralize the hydrochloric acid produced during the reaction.^{42, 43} A

second option is to react dicarboxylic acid monomers with a dehydrating agent in the presence of base. The both methods yield reasonable molecular weight polymers with degrees of polymerization of 15 to 30.⁴³

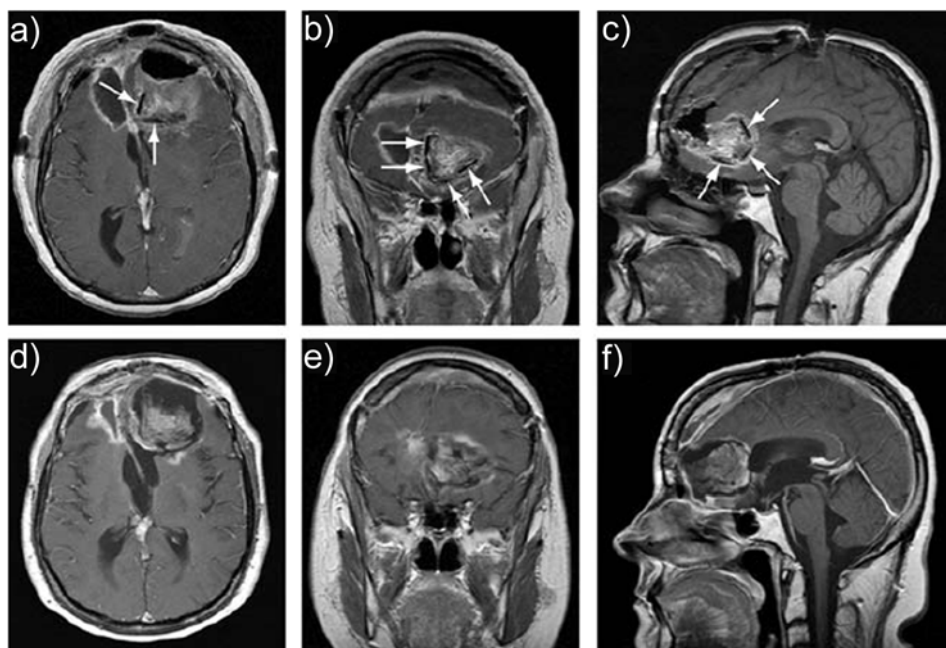


Figure 1.9 Treatment for malignant brain tumors using Griadel®, polyanhydride drug delivery matrix of polyanhydride in the surgical resection cavity. a) - c) Magnetic resonance imaging of the brain in axial, coronal, and sagittal views, respectively, after implanting Griadel wafers to the resection bed (arrows pointed). d) – f) Magnetic resonance imaging of the brain demonstrating no enhanced lesion with tumor activity after four months.⁴⁵

An important property of polyanhydrides is that their anhydride bonds are susceptible to hydrolysis with water and their degradation products are non-toxic diacids. Because of their rapid hydrolysis, the surface of a polymeric matrix of polyanhydrides is readily eroded in water and the rate of surface erosion is faster than the rate of permeation of water into the polymeric matrix.²² Because of these features, polyanhydrides are

mostly used to fabricate drug delivery matrices in the form of wafers, slabs, beads, or rods to deliver drugs locally in the body.^{39, 44} For instance, Gliadel® made from poly[(carboxyphenoyl)propane-sebacic anhydride] is commercially used to deliver the brain cancer drug carmustine through surgery as shown in Figure 1.9.⁴⁵

Polyesters

Polyesters are a representative group of biodegradable polymers which have ester bonds along their backbone. The most commonly used polyesters are poly(ϵ -caprolactone), poly(lactic acid), poly(glycolic acid), and poly(lactic-*co*-glycolic acid) shown in Figure 1.2b. Unlike polyanhydrides, water can readily permeate into a polyester matrix which results in bulk erosion.^{46, 47} The rate of hydrolytic degradation is determined by the chemical composition, hydrophobicity, and crystallinity of the matrix.⁴⁸ In the preparation of polyesters, ring-opening polymerization (ROP) of cyclic esters is favored over polycondensation of hydroxycarboxylic acid because the ROP results in higher molecular weight polymers, well-defined end groups, and the copolymerization of multiple esters.⁴⁹

Poly(ϵ -caprolactone) is prepared from ϵ -caprolactone through several different ROPs such as anionic polymerization, cationic polymerization, coordination-insertion polymerization, and free-radical polymerization as shown Figure 1.10.^{49, 50} The anionic ROP of ϵ -caprolactone is initiated when a carbonyl carbon is attacked by a nucleophile forming a negatively charged propagating species. Although the synthesis of high molecular weight polymers is possible using anionic ROP, extensive intermolecular transesterification can occur. In cationic ROP, cationic initiators such as protic acids and Lewis acids associate with the carbonyl oxygen to form a positively charged ϵ -caprolactone which reacts with a second monomer. A drawback of cationic ROP is that this method does not result in high molecular weight polymers. In the proposed mechanism of coordination-insertion ROP, the catalyst coordinates to the monomer with

the co-initiating alcohol to form a metal-alkoxide complex and the monomer inserts into the metal-oxygen bond to yield the propagating species. Various metal alkoxides or metal carboxylates such as tin(II) 2-ethylhexanoate ($\text{Sn}(\text{Oct})_2$), zinc butoxide, and aluminum tri-isopropoxide can be used as catalysts.^{49, 51} Free-radical ROP utilizes 2-methylene-1,3-dioxepane and a radical initiator as shown in Figure 1.10d.⁵²

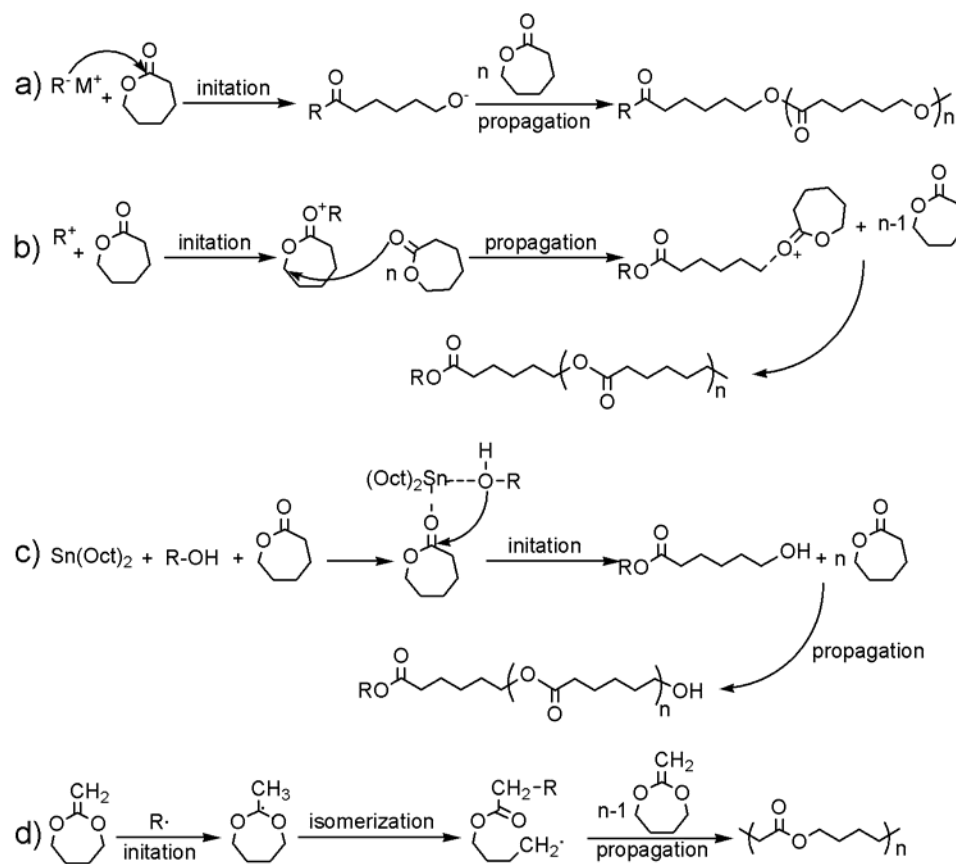


Figure 1.10 Methods to yield poly(ϵ -caprolactone). a) Anionic ring-opening polymerization. b) Cationic ring-opening polymerization. c) Coordination-insertion ring-opening polymerization. d) Free radical ring-opening polymerization.

Poly(ϵ -caprolactone) degrades at a significantly slower rate than poly(lactic acid) and poly(glycolic acid) because it has a longer hydrophobic alkyl group. Therefore, poly(ϵ -caprolactone)s are used for long-term drug delivery within a implantable matrix.⁴⁸ In addition, poly(ϵ -caprolactone) is readily copolymerized with other polymers such as poly(ethylene glycol), poly(lactic acid), and poly(glycolic acid). The use of copolymers allows the degradation profile to be tuned for each application.⁴⁸

Poly(lactic acid), poly(glycolic acid), and their copolymer [poly(lactic-*co*-glycolic acid)] are preferentially prepared from the ROP of cyclic diesters using coordination catalysts as shown in Figure 1.11. The direct condensation of lactic acid and glycolic acid yields low molecular weight polymers.⁵¹ Tin(II) 2-ethylhexanoate is commonly used as the catalyst for the ROP of these monomers because it has a reasonable solubility in various solvents, a low toxicity, and a high catalytic activity.⁵³

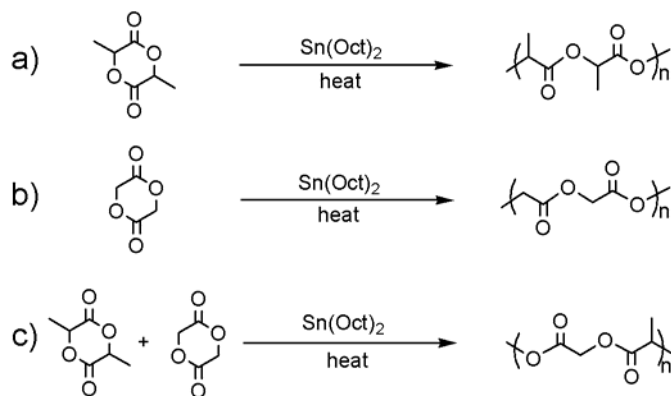


Figure 1.11 Synthesis of a) poly(lactic acid), b) poly(glycolic acid), and c) poly(lactic-*co*-glycolic acid) through coordination-insertion ring-opening polymerization.

Poly(lactic acid) (PLA), poly(glycolic acid) (PGA), and poly(lactic-*co*-glycolic acid) (PLGA) are widely accepted biodegradable and biocompatible polymers and have

been approved by the FDA.^{23, 54-56} PLA degrades more slowly than PGA because PLA possesses an additional hydrophobic methyl group.⁴⁷ The degradation of PLA and PGA yields carboxylic acids which accelerate further degradation.²⁸ Their degradation products, lactic acid and glycolic acid, are eventually converted to water and carbon dioxide and are eliminated through the citric acid cycle.⁴⁷ Because lactic acid (LA) exists as three stereoisomers, L-lactide, D-lactide, and *meso*-lactide, PLA also exists in three forms of L-PLA, D-PLA, and D,L-PLA, with varying physical properties.^{23, 53} L-PLA, and D-PLA are semicrystalline, whereas D,L-PLA is an amorphous polymer.^{48, 51} By adjusting the ratio of PLA and PGA, the physical properties and degradation profiles of PLGAs can be controlled. Microspheres fabricated from PLGAs (Figure 1.12) have been widely used in drug delivery systems.⁵⁵

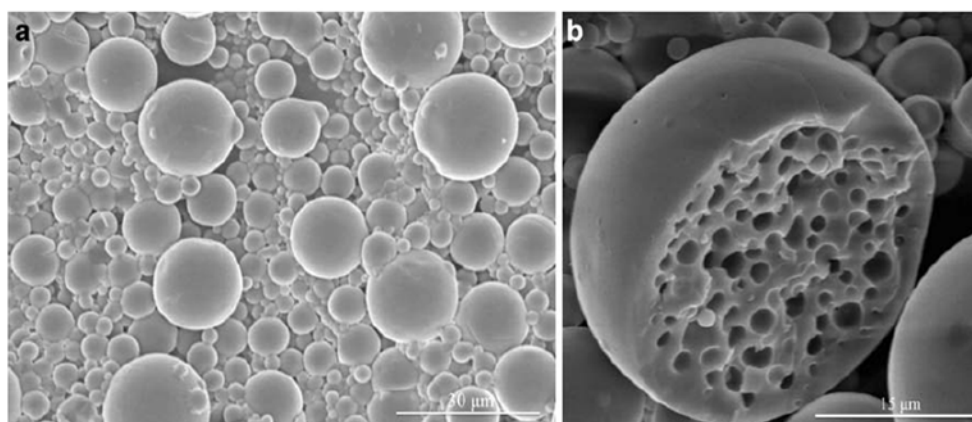


Figure 1.12 Scanning electron microscopy micrographs of microspheres from PLGA. a) Gross view of microspheres fabricated by a water-in-oil-in-oil double emulsion technique. b) Inside view of one microsphere to show its interior morphology.⁴⁶

Requirements of New Biodegradable Polymers for Drug Delivery Systems

Although a number of biodegradable polymers have been synthesized and used for drug delivery systems, the development of new biodegradable polymers is still required for the following reasons.

First, current biodegradable systems of polymers mostly depend on the hydrolysis of ester or anhydride groups along polymer backbones. Although acidic conditions promote the hydrolytic degradation of these polymers, the controlling factor is not strictly a change in pH. Microparticles composed of these polymers release some of their drug cargo in the blood stream before they are taken into cells. The nonspecific release of drugs is an important issue that requires further study.

Second, it is challenging to functionalize a polymeric matrix of polyesters or polyanhydrides to express ligands on their surfaces. In order to target the delivery of drugs to specific cells, the surface of the polymeric matrix must be functionalized with ligands. However, the functionalization of microparticles composed of polyesters or polyanhydrides is limited due to the lack of reactive moieties on their backbones and typically uses the end groups of the polymers which are present in dilute amounts on the surface of microparticles. Therefore, although polyesters and polyanhydrides are biodegradable and biocompatible, their applications in direct drug delivery are limited.

Third, the optimal delivery vehicle for each drug may require a unique release profile and ability to direct to targeted cells. It is well known that changes in polymer structures affect the efficacy of drug delivery.⁵⁷ For instance, dodecylation of primary amines on polyethylenimine (PEI) results in an increase of five times of gene delivery. If the primary and secondary amines are acylated, the gene delivery efficacy doubles and its cytotoxicity is also reduced (Figure 1.13).⁵⁸ These results demonstrate how changes in polymer structures yield dramatic and unexpected effects on the function of a polymeric

matrix. Accordingly, if new polymers with new structures are synthesized, they may provide superb drug delivery systems.

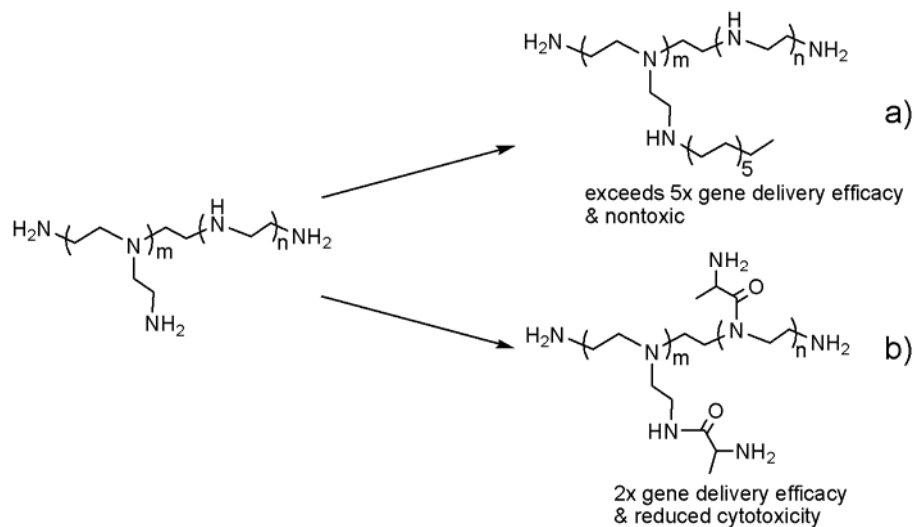


Figure 1.13 Effects of chemical modifications of PEI on the efficacy of gene delivery. a) Dodecylation of primary amines along the backbone of branched PEI with dodecyl iodide, resulting in increased gene delivery efficacy and a nontoxic polymer. b) Acylation of primary and secondary amines along the backbone of branched PEI with an amino acid, resulting in 2 times increased gene delivery efficacy and reduced cytotoxicity.⁵⁸

In conclusion, the drugs, target organs, and routes of administration may require unique chemical and physical properties that spur the development of new biodegradable polymers. Furthermore, new drugs are being continually developed may require specifically devised drug delivery systems based on new biodegradable and biocompatible polymers which are readily functionalized with specific ligands or are positive charged. Therefore, the development of new polymers with new mechanisms of degradation and new structures is required.

Objectives

Polysulfenamides

- Synthesize sulfenamide molecules
- Develop the synthesis of disulfenamide molecules
- Study the kinetics of sulfenamides with secondary amine in organic solvents
- Perform the transamination reactions of sulfenamides and secondary amine
- Synthesize thiosuccinimide molecule
- Develop the synthesis of thiodisuccinimide molecules
- Study the kinetics of thiosuccinimides with secondary amine in several organic solvents.
- Perform the transamination reactions of thiosuccinimide and secondary amine
- Polymerize thiodisuccinimides with various secondary diamines
- Study the stability of sulfenamides in organic solvents
- Study the stability of S-N bond in the presence of acid
- Isolate the degradation-products of sulfenamide in acidic water
- Produce microparticles from polysulfenamide
- Show the uptake of microparticles of polysulfenamides into cells
- Study the toxicity of microparticles of polysulfenamides toward cells
- Functionalize the surface of microparticles of polysulfenamides

Polymers with N-S-N Bonds

- Synthesize dithiobis-secondary amines
- Develop the synthesis of bis(secondary amine)sulfides
- Study the kinetics of bis(*N*-ethylmethyl)sulfide with secondary amine in several organic solvents
- Perform the transamination reactions of bis(*N*-ethylmethyl)sulfide and bis(*N,N'*-dimethyl)sulfide with secondary amine in several organic solvents

- Polymerize bis(*N,N'*-dimethyl)sulfide and various secondary diamines
- Study the stability of bis(*N*-ethylmethyl)sulfide in organic solvents
- Synthesize water-soluble N-S-N molecule and study its kinetics under various acidic conditions (pH 3 ~ 10)

Comb Block Copolymers

- Synthesize three types of comb block copolymers with poly(butyl acrylate), poly(lactic acid), and poly(styrene-*b*-vinylpyridine) arms.
- Develop how to graft poly(4-vinylpyridine) arms from comb block copolymers with poly(styrene) arms
- Self-assemble comb block copolymers in the solid state
- Image the morphologies of assembled polymer films by SEM

Steric Effects on Grubbs Catalysts

- Synthesis of Grubbs first and second generation methylidene catalysts.
- Study the reactivity of sterically hindered oxanorbornenes on their bridgehead carbon with Grubbs catalysts.

CHAPTER 2
SYNTHESIS OF POLYSULFENAMIDES FOR DRUG DELIVERY
APPLICATIONS

Abstract

Most synthetic polymers used to deliver pharmaceutical drugs in the body are polyesters, polyanhydrides, or polyamides because of the need to degrade these polymers into small, excretable molecules before any toxic effects are observed. We introduce a major advance in this field by using a new functional group to synthesize biodegradable, nontoxic polymers and show, for the first time, that polysulfenamides possess many of the desired characteristics for drug delivery. The sulfenamide (RSNR_2) is a new functional group in polymer chemistry – no reports of polysulfenamides are known – so we synthesized the first polymers with this functional group along their backbones. We demonstrated that sulfenamides were stable in polar protic and aprotic solvents, but degraded rapidly when exposed to acidic conditions. These properties are important because polysulfenamides were formulated into microparticles loaded with drugs. These microparticles must be stable in blood where the pH is 7.4 but rapidly degrade when endocytosed into lysosomes in the cells where the pH is approximately 4-5. The drug should be released from the microparticles only under acidic conditions where polysulfenamides are rapidly degraded. Microparticles were fabricated from polysulfenamides, their surfaces were readily functionalized, and they were internalized by cells allowing for intracellular delivery of their cargo. This work demonstrates that polysulfenamides form the basis for a new set of polymers for drug delivery that greatly differ from the prior work in this field.

Introduction

Biodegradable polymers have shown wide utility in a variety of biomedical applications ranging from sutures, scaffolds for the growth of cells, and polymeric depots

that provided sustained release of therapeutic agents.⁵⁹⁻⁶⁴ Optimal use of these materials requires their molecular and macromolecular properties be tailored to the specific application for which the material is to be used.^{60, 65-67} For instance, polymeric particles loaded with drugs that are targeted to the endosomal compartments of cells should ideally be stable at physiological pH in the bloodstream, but readily break down at a lower pH to release its drug cargo in the endosome where the pH is approximately 4 to 5.⁶⁸⁻

⁷¹Biodegradable polymers are attractive in drug delivery applications because polymeric particles injected *in vivo* can accumulate in several organs including the liver, spleen, lungs and heart and often result in toxic side effects if they do not break apart into smaller, easily excretable side products.^{72, 73} The degradation of these polymers is also the mechanism by which controlled release of drugs and other therapeutics is achieved. Most synthetic polymers in biomedical research are polyesters, polyamides, polyanhydrides, or some combination of these three functional groups. These polymers degrade to short polymers or small molecules at reasonable times without the use of enzymes.⁷⁴⁻⁷⁶ Thus, these polymers can be excreted from the body before toxic side-effects occur.

It is very challenging to design a polymer with a new functional group along its backbone that renders it stable at physiological pH but also allows it to be degraded at reasonable time scales in the body without toxic side effects. The introduction of a new functional group that can be used to synthesize biopolymers has the potential to open up new applications in this field and will allow more complex, potentially “smart” drug delivery vehicles to be synthesized.^{65, 69, 75} In this paper, we report the first synthesis of polymers with the sulfenamide functional group within the backbone, how these polymers degrade under different conditions, and how they can be fabricated into micron-sized particles loaded with fluorescent dye that are internalized into cells with minimal toxicity. Polysulfenamides are a new class of polymers that we believe will have real applications in medicine.

Sulfenamides are an understudied functional group with the general formula of $RS-NR'R''$ that are used as protecting groups for amines [typically as $(CPh_3)S-NR_2$] and vulcanizing agents in the rubber industry.⁷⁷⁻⁸² Although a variety of different functional groups are identified as sulfenamides or sulfenamines (e.g. $RSSNR_2$, $RSN(R)SR$, and R_2NSNR_2), this paper focuses on sulfenamides formed from secondary amines and thiols having the general formula $RS-NR'R''$.⁷⁸

Results and Discussion

Synthesis of Polysulfenamides

Because polysulfenamides were unknown prior to this work, the first step in this project was to develop their synthesis. Two different methods to synthesize polysulfenamides were attempted based on transamination reactions. In one method, dithiols were reacted with SO_2Cl_2 to yield molecules with S-Cl bonds that were too unstable to be isolated (Figure 2.1a). Rather, these molecules were reacted with *N*-ethylmethylamine to yield sulfenamides in high yields. These sulfenamides were reacted with diamines to yield a polymer; the leaving group in this polymerization was *N*-ethylmethylamine (boiling point of 36-37 °C) which was removed with heat to drive the reaction to completion. In the second method, dithiols were reacted with *N*-chlorosuccinimide to yield dithiosuccinimides (Figure 2.1b). These molecules were then reacted with diamines to yield polysulfenamides. The second approach was developed due to the better leaving group on the sulfur that would be expected to accelerate the polymerization reaction.

Simple bimolecular reactions were studied to determine the kinetics of each transamination reaction shown in Figure 2.1 to determine the best conditions for the polymerization. Molecule A was synthesized and reacted with *N*-benzylmethylamine in C_6D_6 , $DMSO-d_6$, and CD_3OD at different temperatures (Figure 2.1c). This reaction was very slow in C_6D_6 with no conversion after 24 h at room temperature and only 11%

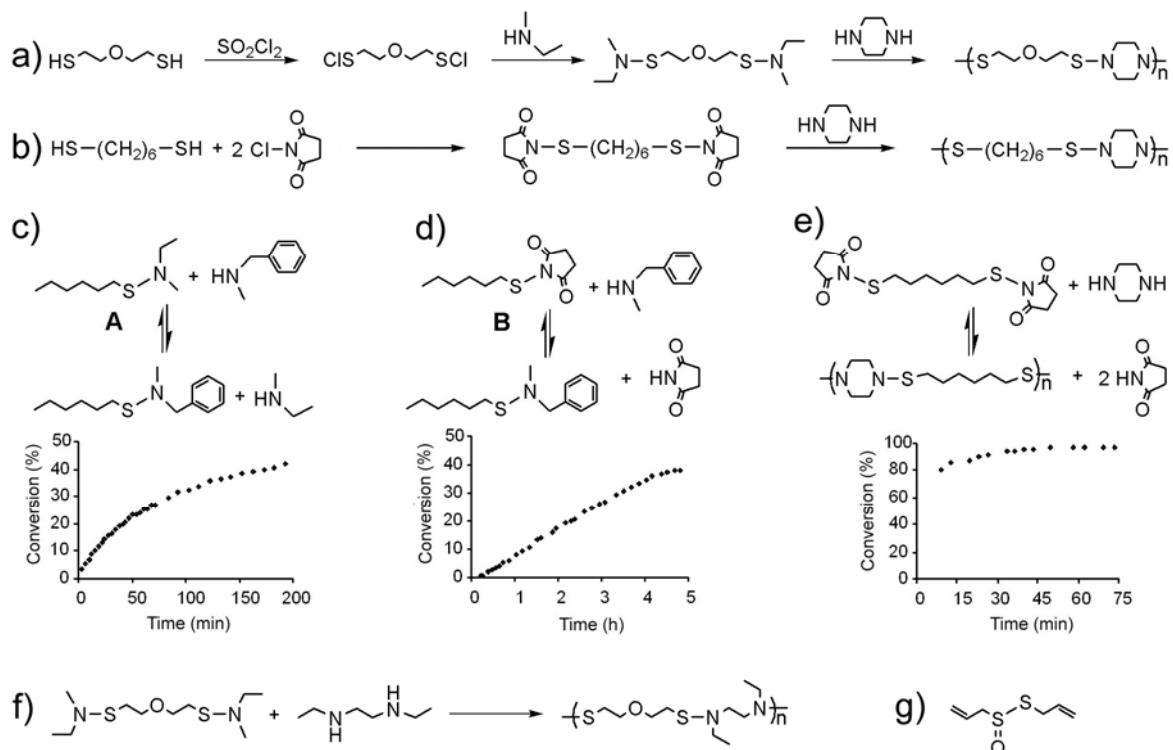


Figure 2.1 Synthesis of polysulfenamides and the kinetics of transamination reactions. a) In one method dithiols were reacted to form S-Cl bonds which were readily transformed *in situ* into sulfenamides. The polymerization proceeded by displacement of *N*-ethylmethylamine with a different amine. b) In a second method dithiols were activated by reaction with *N*-chlorosuccinimide to yield stable products which were purified and then exposed to secondary diamines to yield polymer. c) The kinetics of reaction of a sulfenamide with a secondary amine in CD₃OD. The reaction yielded a 50/50 mixture of the two sulfenamides. d) The kinetics of reaction of a thiosuccinimide with a secondary amine in CD₂Cl₂. The reaction yielded >97% sulfenamide after extended reaction times. e) The kinetics of a typical polymerization to demonstrate that the polymerizations were rapid and went to quantitative conversions at reasonable concentrations. f) A polymerization that was completed. g) The structure of alliin.

conversion after 24 h at 60 °C. When DMSO-*d*₆ was used as the solvent, the conversion reached 7% after 24 h at room temperature and 32% after 24 h at 50 °C. Clearly aprotic solvents were poor choices for this reaction, so the solvent was switched to CD₃OD.

Here, the kinetics were much faster at room temperature with a rate constant of $5.04 \times 10^{-4} \text{ M}^{-1} \text{ s}^{-1}$ (Figure 2.1c). This reaction was run in a sealed NMR tube and reached a

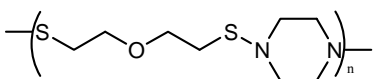
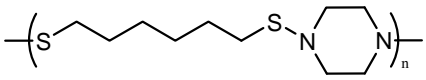
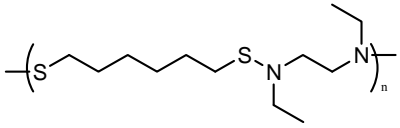
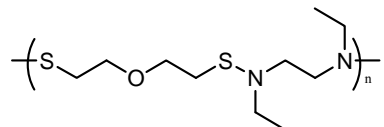
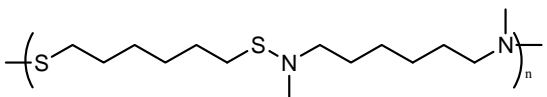
conversion of 40% after 3 h, and at longer periods of time it reached an equilibrium mixture of 50% of each sulfenamide.

When the polymerization of a disulfenamide with a diamine was attempted as shown below, the results were not promising (Figure 2.1f). Although the kinetics of reaction were rapid in methanol, the resulting polymer was insoluble in methanol which made this solvent a poor choice to conduct polymerizations. Polymerizations at high concentrations of monomers in solvent mixtures of (1/1 v/v) CD₃OD/CDCl₃ or (1.2/1 v/v) CD₃OD/DMSO-*d*₆ at 40 °C yielded soluble oligomers even after 3 days. This polymerization was attempted in refluxing benzene for 24 h with the reaction vented to allow *N*-ethylmethylanine to boil off resulting in a low yield of a modest molecular weight polymer (M_w = 2,840 g mol⁻¹). This method of polymerization was hindered by lack of solubility of the polymer in methanol and the slow kinetics for polymerization in aprotic solvents.

The reaction of a thiosuccinimide (molecule B in Figure 2.1d) with *N*-benzylmethylanine was much faster in aprotic solvents than the same reaction between molecule A and *N*-benzylmethylanine. In CD₂Cl₂ at room temperature the reaction between molecule B and *N*-benzylmethylanine had a rate constant of 8.18 x 10⁻⁴ M⁻¹ s⁻¹ and reached 35% conversion after 4 h. Not only was this transamination reaction approximately 1.6x faster than the reaction between molecule A and *N*-benzylmethylanine in CD₃OD, but the difference in solvent was also critically important. Methylene chloride and chloroform were excellent solvents for both monomers and polymers, and the reaction of thiosuccinimides with secondary amines went to >97% conversion at reasonable concentrations at room temperature. For instance, the polymerization reaction shown in Figure 2.1e went to >95% conversion within 50 min in CDCl₃ at room temperature. This polymerization method was used in all subsequent polymerizations.

A series of polymers were synthesized from dithiosuccinimides and secondary diamines (Table 2.1). The polymerizations were completed in methylene chloride or chloroform at room temperature for 24 h. The polymers had molecular weights up to $6,300 \text{ g mol}^{-1}$ and degrees of polymerization that ranged from 90% to 97%. Secondary diamines were chosen for this work because the synthesis of polymers using primary diamines (such as $\text{NH}_2\text{CH}_2\text{CH}_2\text{NH}_2$) resulted in cross-linked polymers possibly due to the reaction of an amine with two equivalents of a thiosuccinimide to yield cross-links of the form $\text{RN}(\text{SR}')_2$.

Table 2.1 Synthesis of polysulfenamides.

Entry	Composition	M_w (g mol^{-1}) ^a	PDI
1		3,700	1.42
2 ^b		6,300	1.22
3 ^b		3,700	1.06
4		2,300	1.60
5 ^b		2,900	1.13

^aThe absolute M_w and PDI were measured with multi-angle laser light scattering and refractive index detectors unless otherwise noted. ^bThe M_w and PDI were measured versus polystyrene standards using a calibration curve and the reflective index peaks of the polymer.

Polysulfenamides were synthesized to probe whether they could act as new drug delivery vehicles through the formation of μm -sized particles. No polymers have been reported with S-N bonds along the backbone despite their apparent ease of synthesis and that this bond is stable at neutral pH but can be hydrolyzed in water under acidic conditions.^{79, 80, 83-85} Polysulfenamides represent a new class of polymers that may have real applications in the delivery of pharmaceuticals. Some of the minimal requirements for a polymer to be useful as a drug delivery vehicle are that it should be biocompatible, biodegradable, able to be loaded with a drug, taken into cells, and able to be functionalized on its surface to express molecules that can be used as ligands to target certain cell lines. Here, we have demonstrated that polysulfenamides meet all of these requirements.^{60, 62, 86-89}

Degradation of Sulfenamides in Aprotic and Protic

Solvents

Because most synthetic polymers in the body cause toxic effects if they do not degrade at a reasonable rate, it is important to use a polymer that degrades by reaction with water without the need for enzymes. Prior evidence by others indicated that the S-N bond would degrade under acidic conditions with protic solvents. In fact, one challenge of working with small molecules containing sulfenamides is that they tend to degrade on acidic silica gel and poor yields are obtained after column chromatography.^{84, 85} We observed poor yields for sulfenamides cleaned on silica gel, but when they were cleaned by chromatography on basic aluminum oxide the isolated yields were high. Furthermore, when a small molecule with a sulfenamide bond was added to a NMR tube in CDCl_3 with 30 mg of silica gel, approximately 50% of it decomposed after 16 h at room temperature but no decomposition was seen in an identical experiment in the absence of silica gel. These results indicated that polymers with sulfenamides along the backbone would

decompose under acidic conditions – a result that is desirable for many applications in drug delivery.

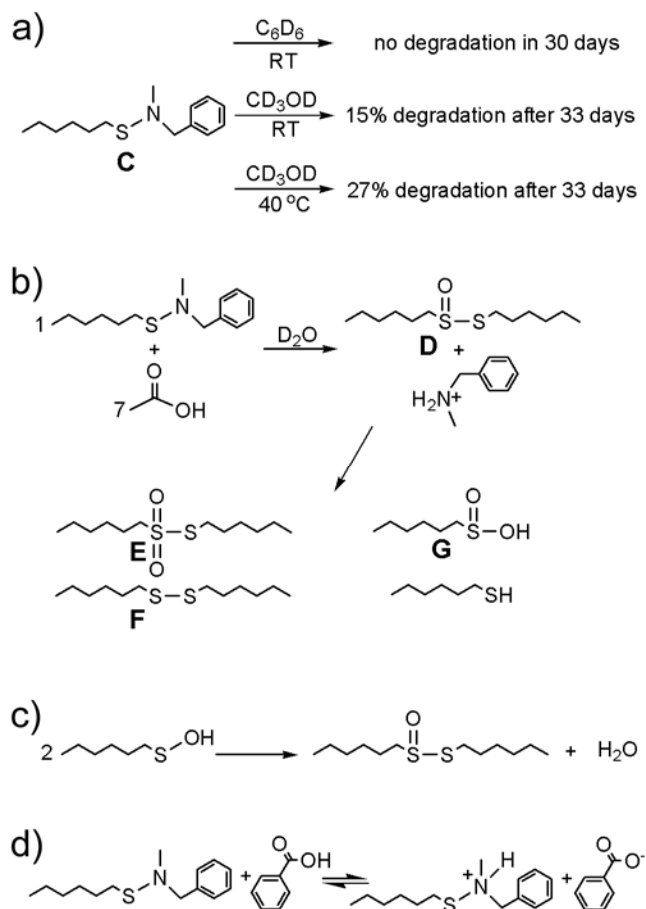


Figure 2.2 Degradation of sulfenamides and characterization of their products. a) Molecule C was added to C_6D_6 and CD_3OD to study how rapidly it degraded. b) Molecule C was added to D_2O with seven molar equivalents of acetic acid. Products D, E, and F were characterized. c) Sulfenic acids were the first product of degradation of molecule C, but they were known to rapidly react to yield thiosulfonates as shown. d) Sulfenamides were protonated by benzoic acid in CD_3OD .

To further study the degradation of the S-N functional group, molecule C from Figure 2.2a was synthesized and studied under a variety of reaction conditions. To probe the stability of this molecule under neutral conditions, it was added to CD₃OD and C₆D₆. After 30 days, the ¹H NMR spectrum of molecule C in C₆D₆ was unchanged which demonstrated its stability in aprotic solvents. This molecule slowly degraded in CD₃OD; after 33 days 15% of it degraded at room temperature and only 27% degraded when heated to 40 °C for the same period of time. These conditions were attempted to provide an understanding of the stability of polysulfenamides in water under neutral conditions and indicate that these polymers will slowly degrade at neutral pH, but possess reasonable stabilities under neutral conditions in a polar, protic solvent.

The degradation of molecule C was studied under acidic conditions in CD₃OD and D₂O to understand how polysulfenamides would break down in the endosome of cells where the pH is approximately 4 to 5. Molecule C was not soluble in D₂O so the kinetics of degradation were not studied in this solvent, but the products were isolated and characterized. Molecule C was added to D₂O with seven molar equivalents of acetic acid. After 41 h the organics were extracted and initially studied by ¹H NMR spectroscopy prior to isolation by column chromatography. The ¹H NMR spectrum of the extract before chromatography indicated that approximately 75% of the product was the thiosulphinate (molecule D in Figure 2.2b) with the remainder mostly composed of molecules E and F. The initial reaction of molecule C with water yielded a sulfenic acid, but sulfenic acids are transient intermediates that rapidly condense as shown in Figure 2.2c.^{77, 90, 91} Based on literature precedent, molecule D further decomposed via multiple pathways to yield molecule E, molecule F, and a sulfinic acid (molecule G).⁹¹⁻⁹⁴ Thiosulfinate esters such as molecule D are known oxidation states for cysteine residues and found in nature products such as allicin (a component of garlic; Figure 2.1g). As such, thiosulfates are already present in the body and are known to decompose at

reasonable rates – the half-life of the decomposition of allicin at pH = 7.5 at 37 °C is approximately 2 days.^{66, 92}

When the kinetics of degradation of molecule C were studied in CD₃OD with benzoic acid, it decomposed at a much faster rate than in the identical reaction without benzoic acid. With five equivalents of benzoic acid the molecule reached 51% degradation within 4 min compared to only 15% degradation after 33 days in the absence of benzoic acid. When molecule C was exposed to two molar equivalents of *p*-toluenesulfonic acid (pKa < -2) or trifluoroacetic acid (pKa = 0.3) in CD₃OD it degraded to >90% within four minutes. Clearly, the decomposition of sulfenamides is catalyzed by acid as observed by others in prior work.^{84, 85} During the course of these experiments, we also noticed that benzoic acid only partially protonated the sulfenamide (Figure 2.2d). This result indicated that the protonated sulfenamide had approximately the same pKa as benzoic acid (pKa of 4.2 in water) despite the typical pKa of approximately ten for protonated amines. The reason for the low pKa of sulfenamides was due to the α -lone pair effect which typically lowers a pKa by orders of magnitude and has been observed in other molecules such as hydrogen peroxide.^{95, 96}

Fabrication and Degradation of Microparticles of Polysulfenamides

Microparticles were fabricated from the polymer in entry 2 in Table 2.1 to study whether these polymers could form the basis of drug delivery vehicles. The microparticles were prepared using an oil in water single emulsion solvent evaporation methodology. In this approach, the polymer was dissolved in chloroform and then emulsified in surfactant containing water phase. The emulsion was stirred overnight until the chloroform evaporated. Drugs and fluorescent molecules such as rhodamine could be incorporated into the microparticles by mixing them in the polymer/chloroform mixture prior to emulsification. The average size of the microparticle was 2.6 microns with a PDI

of 0.62. They were spherical in shape, had a smooth surface, and had a negative charge of -41 mV in PBS buffer at pH = 7.4 (Figure 2.3b). The reason for the negative charge was

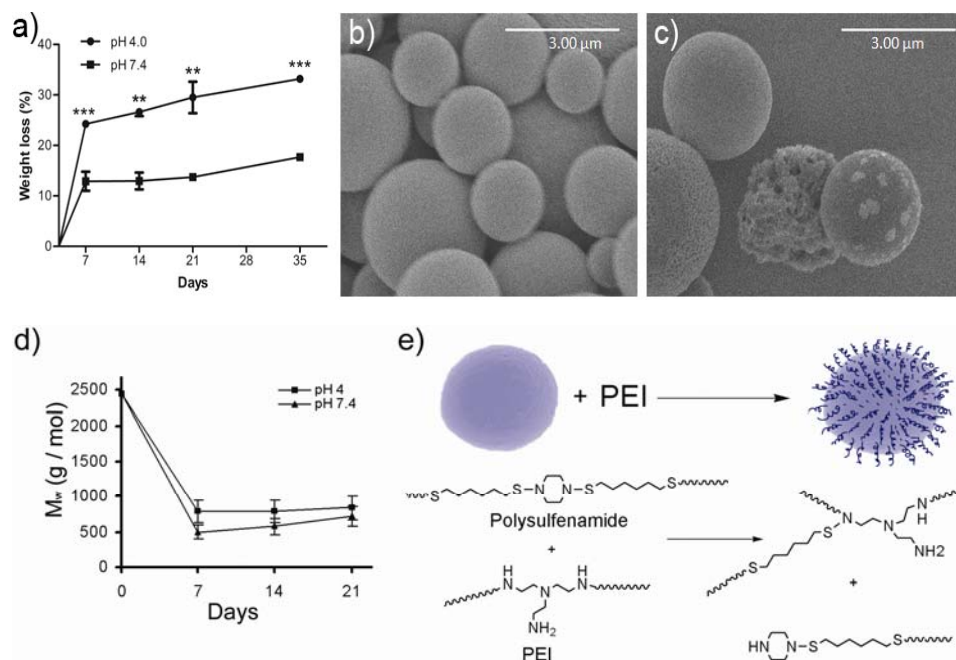


Figure 2.3 Microparticles with the structure of entry 2 in Table 2.1 were studied for their degradation and surface reactions. a) Time dependent weight loss of the polymer incubated at acidic pH (4.0) and physiological pH (7.4). Data represents the percentage weight loss as mean of three samples. The weight loss was significant at all the time points as indicated (***) $P < 0.001$, ** $P < 0.01$, two-tailed unpaired t test). b) Scanning electron microscopy (SEM) image of microparticles as prepared. c) SEM image of microparticles after incubation in acetate buffer (pH 4.0) for 14 days. Microparticles at various stages of degradation can be observed. d) A small fraction of the microparticles that were degraded at different pHs were removed at the indicated times, dissolved in CHCl_3 , and studied by size exclusion chromatography. The molecular weight of the polymers as a function of time the microparticles were degraded is shown. e) Microparticles were exposed to PEI that coated their surfaces. We believe that the amines in PEI reacted with the sulfenamides on the surface to covalently bond the PEI to the surface of the microparticle according to the reaction shown in Figure 1c and reproduced here.

understood in terms of prior experiments that demonstrated that sulfenamides did not appreciably protonate at pH = 7.4, but they slowly degraded to yield sulfinic acids that deprotonated and led to a negatively charged surface.

The most common biodegradable polymer used in drug delivery applications is poly(lactic-*co*-glycolic acid) but this polymer lacks reactive surface functional groups that can be functionalized to expose ligands to direct attachment to cells. An important property of microparticles used in drug delivery is that their surfaces should be readily functionalized to bind therapeutics or to conjugate ligands that can target and bind cell surface specific receptors. To study whether these microparticles could be functionalized by the transamination reaction shown in Figure 2.1c, they were reacted with polyethylene imine in water at 4 °C for 5 h (Figure 2.3). After washing with copious amounts of deionized water, they were collected by centrifugation and their surface charge was measured. These particles had surface charges from 8 to 25 mV in PBS buffer at pH = 7.4 which indicated that they were coated with positively charged amines. This work demonstrated the ability to functionalize the surface of these particles using simple transamination reactions with free amines.

Microparticle degradation was studied at both physiological pH (7.4) and acidic pH (4.0) to learn whether these particles would decompose over time. Figure 2.3a shows the percentage weight loss of the samples at different points in time. After one week, a weight loss of 24% was observed for microparticles in acetate buffer as compared to a weight loss of 13% for particles in PBS. On day 35, the weight loss in acidic buffer was ~33% as compared to ~17% at physiological pH. Weight loss was significantly higher for particles in acetate buffer as compared to particles in PBS, indicating faster degradation of the microparticles in acidic environments. The differences in the rates of degradation at pH 7.4 and 4.0 were expected based on the rapid degradation of molecule C under acidic conditions in methanol and its slow degradation in methanol in the absence of acid. SEM images of the acidic pH-degraded particles revealed a rough morphology of the

polymer surface that was consistent with polymer degradation (Figure 2.3c). Some microparticles were dissolved in chloroform at each time period and size exclusion chromatography spectra were obtained. These spectra showed that the polymer had a lower molecular weight after being degraded in water as expected (Figure 2.3d).

This difference in rate of degradation at different pHs is often desired. Microparticles of this polymer containing a drug should be stable in the bloodstream where the pH is 7.4; however, when they are endocytosed into a cell they should break down rapidly in the endosome where the pH is approximately 4 to 5.

Uptake of Microparticles into Cells and Cytotoxicity

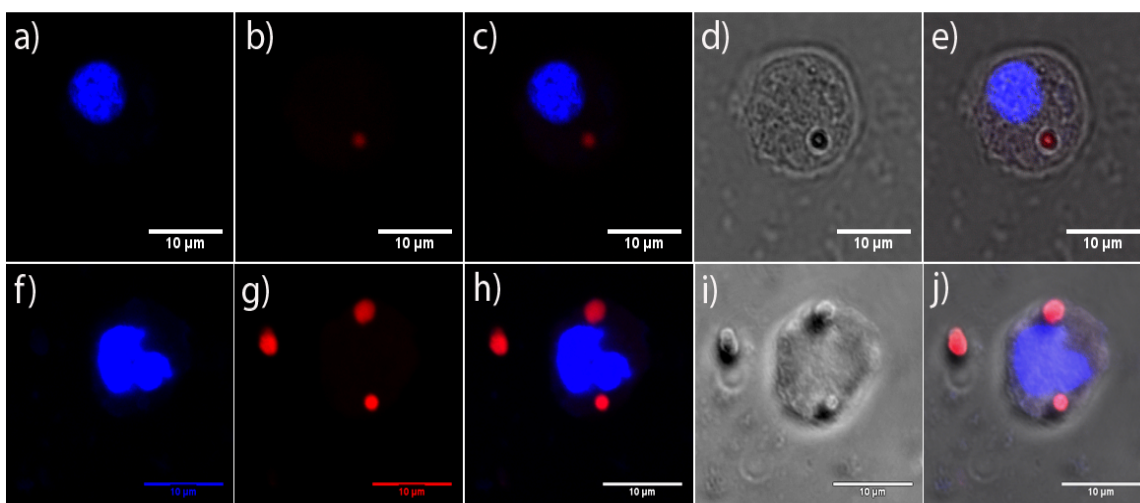


Figure 2.4 Uptake of microparticles fabricated from entry 2 in Table 1 and loaded with rhodamine and studied using confocal microscopy. a) – e) The cells are JAWSII immature dendritic cells and in f)-j) they are HEK293 cells. The nucleus of the cell was stained with DAPI to appear blue and the rhodamine appeared red. In d) and i) the transmitted light images indicate the periphery of the cells and the location of the microparticles. In e) and j) merged images clearly outline the periphery of the cell, the location of the nucleus, and the microparticles to clearly demonstrate that the microparticles were found on the interior of the cells. The images were taken at different sections to ensure that the microparticles were in the same focal plane as the planes taken through the cells. The microparticle in the far left of images g)-j) was not found in a cell and was used to show a free microparticle.

The uptake of these microparticles was studied in JAWSII and human embryonic kidney (HEK293) cells using confocal microscopy. JAWSII cells are immature dendritic cells derived from mouse bone marrow and are commonly targeted by particle based vaccines for generation of therapeutic immune responses. HEK293 cells are one of the most common cell lines used to evaluate novel gene therapies. Microparticles were loaded with rhodamine B during fabrication and were then exposed to the JAWSII and HEK293 cells. The microparticles were found to be located near the cytoplasm of the cell, indicating the phagocytosis of the microparticles by cells (Figure 2.4). The uptake of microparticles by both cell lines suggests that this system has potential in immunological applications, especially in vaccine delivery and potential for gene therapy applications.

The *in vitro* toxicity of these microparticles was evaluated with HEK293 cells. In initial work, these cells were incubated with the microparticles at a range of concentrations of 1 to 1,000 μg per mL of growth medium for 4 h. The cell viability was measured by standard techniques of measuring the metabolic activity of cells in a control without microparticles and the metabolic activity of cells that were exposed to the microparticles. The ratio of these concentrations was plotted as the “cell viability” in the y-axis of Figure 2.5. No toxicity was observed at even the highest concentrations after 4 h, so a longer incubation time of 24 h was studied and shown in Figure 5. At the expected working concentrations of microparticles minimal toxicity was observed. Interestingly, at the highest concentration of 1 mg of microparticles per mL of solution where the wells containing HEK293 cells were beginning to become saturated with microparticles, the cell viability was still 57 %. This suggests that polysulfenamides have low toxicity and are therefore suitable for drug, gene, and vaccine delivery applications.

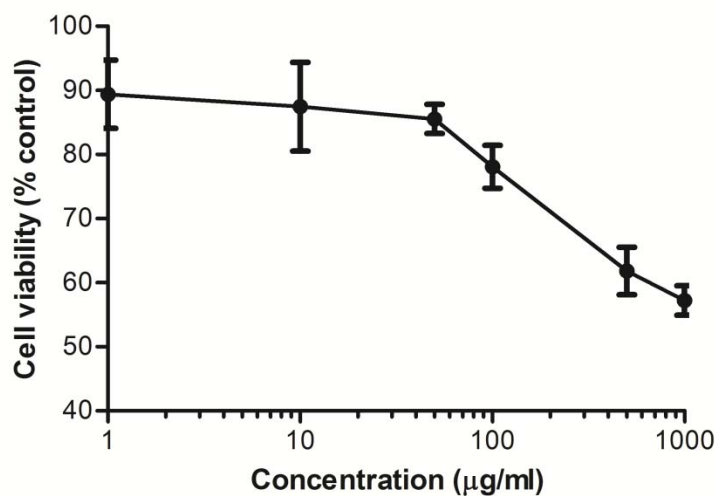


Figure 2.5 Cytotoxicity of microparticles fabricated with the structure shown in entry 2 of Table 1 towards HEK293 cells. Microparticles were suspended in media immediately before addition into cells. Cells were incubated with the microparticles for 24 hours at 37 °C in a humidified 5% CO₂-containing atmosphere. Cell viability was determined by MTS assay and expressed as percentage of control (without microparticles).

Conclusions

In conclusion, we described the synthesis of polymers that are the first to possess sulfenamides along their backbone and can be used as drug delivery vehicles. These polymers are exciting because they possess many of the right characteristics to be useful in drug delivery such as their stability at physiological pH and ease of degradation under acidic conditions. These polymers can be readily functionalized to express new functional groups, a characteristic that is not possible with the functional groups present on the backbone of polyesters typically used in this field. These microparticles were readily internalized by two different cell lines and possessed minimal toxicity. We believe that the introduction of sulfenamides in the synthesis of polymers will provide new opportunities to synthesize more complex drug delivery vehicles that will have real applications in medicine.

Experimental Section

Materials and Methods

Materials

Polyethylenimine (PEI, Mw 25 kDa) and phosphate buffer saline (PBS) are products of Sigma-Aldrich (St. Louis, MO). Dulbecco's Modified Eagle's Medium (DMEM) was obtained from Gibco BRL (Grand Island, NY). LysoTracker® Green was obtained from Invitrogen (Eugene, Oregon, USA). Paraformaldehyde (16% solution, EM grade) was obtained from Electron Microscopy Services (Hatfield, PA) and Vectashield mounting medium for fluorescence with DAPI was a product of Vector Laboratories (Burlingame, CA). 1-Hexanethiol, 1,6-hexanedithiol, 2-mercaptoethyl ether, *N*-benzylmethylamine, *N*-ethylmethylamine, *N,N'*-dimethyl-1,6-hexanediamine, *N*-chlorosuccinimide, triethylamine, ethylenediamine, benzoic acid, *p*-toluenesulfonic acid, acetic acid, and sulfonyl chloride were purchased from Aldrich or Acros Organics at their highest purity and used as received. HPLC-grade chloroform purchased from Acros Organics was used as the GPC solvent after filtering it through a glass frit. All other solvents were reagent grade and purchased from Acros Organics. Piperazine (99%) was purchased from Aldrich. It was purified by sublimation under vacuum at 130 °C. *N,N'*-Diethylethylenediamine (95%) was purchased from Aldrich and distilled under vacuum at 30 °C. Genduran silica gel 60 (230-400 mesh) and basic alumina Brockman activity I (60-325 mesh) were purchased from Fisher Scientific and used for column chromatography.

Cell culture

Human embryonic kidney cells (HEK293) and JAWSII were obtained from American Type Culture Collection (ATCC, Rockville, MD). HEK293 cells were maintained in DMEM supplemented with 10% fetal bovine serum (FBS) and gentamycin

sulfate at $50 \mu\text{g ml}^{-1}$. JAWSII were maintained in Alpha MEM with ribonucleosides, deoxyribonucleosides, 4 mM L-glutamine, 1 mM sodium pyruvate, 5 ng/ml murine GM-CSF, and 20% fetal bovine serum (FBS). Cells were incubated at 37°C in a humidified 5% CO_2 -containing atmosphere.

Characterization of small molecules and polysulfenamides

^1H and ^{13}C NMR spectra were recorded on a Bruker DPX 300 at 300 MHz and 75 MHz, respectively. CDCl_3 was used as NMR solvent with tetramethylsilane (TMS) as an internal standard. HR ESI-MS data were recorded on a Waters Q-ToF Premier instrument in positive ion mode and HR EI-MS data were recorded on a Waters GCT Premier instrument. Size exclusion chromatography (SEC) was performed using chloroform as the mobile phase (1.00 mL min^{-1}) at 40°C . A Waters 515 HPLC pump and two Waters columns (Styragel HR4 and HR5E) were used in series. A DAWN EOS 18 angle laser light scattering detector from Wyatt Corp. to measure light scattering and a Wyatt Optilab DSP to measure changes in refractive index were used to measure absolute molecular weights of polymers. Polystyrene standards ($1,260 \text{ g mol}^{-1}$, $3,790 \text{ g mol}^{-1}$, $13,000 \text{ g mol}^{-1}$, and $30,300 \text{ g mol}^{-1}$) were used to generate a calibration curve to measure relative molecular weights of some polysulfenamides as indicated in Table 1.

Synthesis of Small Molecules and Polymers

Hexanesulfenyl chloride

Alkylsulfenyl chlorides were prepared according to a literature procedure.⁹⁷ Since they quickly returned to thiols after being exposed to air, alkylsulfenyl chlorides were used *in situ* for the preparation of sulfenamides. Sulfuryl chloride (6.28 g, 0.047 mol) was added dropwise to a solution of hexanethiol (5 g, 0.042 mol) in CH_2Cl_2 (30 mL) at 0°C under nitrogen and stirred for 2 h 45 min. ^1H NMR (CDCl_3): δ 0.90 (t, 3H, $J = 6.8 \text{ Hz}$),

1.39 (m, 6H), 1.78 (m, 2H), 3.11 (t, 2H, $J = 7.1$ Hz). ^{13}C NMR (CDCl_3): δ 14.03, 22.52, 27.83, 28.02, 31.31, 41.52.

2,2'-Oxydiethanesulfenyl dichloride

2-Mercaptoethyl ether (3 g, 0.022 mol) was reacted with a solution of sulfuryl chloride (6.15 g, 0.046 mol) in CH_2Cl_2 (30 mL) following the previous procedure. ^1H NMR (CDCl_3): δ 3.33 (t, 4H, $J = 6.3$ Hz), 3.88 (t, 4H, $J = 6.2$ Hz). ^{13}C NMR (CDCl_3): δ 40.92, 68.10.

N-Ethylmethyl-hexanesulfenamide (Molecule A)

A solution of hexanesulfenyl chloride (6.45 g, 0.042 mol) in CH_2Cl_2 (30 mL) was slowly added to a solution of *N*-ethylmethylamine (7.50 g, 0.13 mol) in CH_2Cl_2 (50 mL) at 0 °C under nitrogen and stirred for 7 h. The reaction was diluted with anhydrous Et_2O (130 mL) and washed with saturated NaCl solution in water (3 x 50 mL). The organic phase was dried over anhydrous MgSO_4 sulfate and evaporated to give a brown oil. The product was isolated by vacuum distillation at 30 °C to yield a colorless oil (3.93 g, 53% yield). ^1H NMR (CDCl_3): δ 0.89 (t, 3H, $J = 6.8$ Hz), 1.14 (t, 3H, $J = 7.2$ Hz), 1.35 (m, 6H), 1.54 (m, 2H), 2.65 (t, 2H, $J = 7.2$ Hz), 2.75 (s, 3H), 2.82 (q, 2H, $J = 7.1$ Hz). ^{13}C NMR (CDCl_3): δ 13.79, 14.09, 22.58, 28.27, 28.89, 31.59, 31.86, 46.82, 53.93. HRMS calcd for $\text{C}_9\text{H}_{21}\text{NS}$: 175.1395. Found: 175.1392.

N,N'-Ethylmethyl-bis(2-mercaptoethyl)disulfenamide

A solution of 2,2'-oxydiethanesulfenyl dichloride (4.49 g, 0.022 mol) in CH_2Cl_2 (30 mL) was reacted with a solution of *N*-ethylmethylamine (7.70 g, 0.13 mol) in CH_2Cl_2 (50 mL) following the previous procedure. The extract was filtered through basic alumina to yield a colorless oil (3.29 g, 60% yield). ^1H NMR (CDCl_3): δ 1.13 (t, 6H, $J = 7.1$ Hz), 2.74 (s, 6H), 2.82 (m, 8H), 3.67 (t, 4H, $J = 7.1$ Hz). ^{13}C NMR (CDCl_3): δ 13.70, 32.68, 46.89, 54.13, 70.01. HRMS calcd for $\text{C}_{10}\text{H}_{24}\text{N}_2\text{OS}_2$: 252.1321. Found: 252.1324.

N-(Hexanethio)succinimide (Molecule B)⁹⁸

Hexanethiol (3 g, 25.37 mmol) was added dropwise to a solution of *N*-chlorosuccinimide (3.36 g, 26.64 mmol) in CH₂Cl₂ (70 mL) at 0 °C under nitrogen and stirred for 20 min. The solution changed to a yellow-green color and immediately became cloudy. A solution of triethylamine (2.82 g, 27.91 mmol) in CH₂Cl₂ (10 mL) was added dropwise to the reaction. After the mixture was stirred for 2.5 h, it was washed with a saturated NaCl solution in water (4 x 30 mL). The organic layer was dried over anhydrous MgSO₄ and evaporated to give a colorless oil. The product was isolated by column chromatography using silica gel and 20% EtOAc in hexanes to yield a colorless oil (4.73 g, 87% yield). ¹H NMR (CDCl₃): δ 0.88 (t, 3H, *J* = 6.6 Hz), 1.28 (m, 4H), 1.40 (m, 2H), 1.54 (m, 2H), 2.85 (m, 6H). ¹³C NMR (CDCl₃): δ 13.99, 22.45, 27.90, 28.11, 28.61, 31.28, 37.62, 177.23. HRMS calcd for C₁₀H₁₇NO₂S: 215.0980. Found: 215.0979.

(2,2'-Oxydiethenthio)disuccinimide

2-Mercaptoethyl ether (10 g, 0.072 mol) was reacted with a solution of *N*-chlorosuccinimide (20.28 g, 0.15 mol) in CH₂Cl₂ (300 mL) and a solution of triethylamine (16.10 g, 0.16 mol) in CH₂Cl₂ (55 mL) following the previous procedure. The mixture was purified by column chromatography using 95% EtOAc in hexanes to yield a white solid (11.42 g, 48% yield). ¹H NMR (CDCl₃): δ 2.78 (s, 8H), 2.95 (t, 4H, *J* = 5.9 Hz), 3.68 (t, 4H, *J* = 5.9 Hz). ¹³C NMR (CDCl₃): δ 28.68, 36.93, 70.90, 177.29. HRMS calcd for C₁₂H₁₆N₂O₅S₂ + Na⁺: 355.0398. Found: 355.0387.

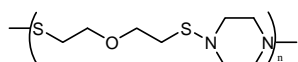
N,N'-(Hexanethio)disuccinimide

1,6-Hexanedithiol (7 g, 0.047 mol) was reacted with a solution of *N*-chlorosuccinimide (13.06 g, 0.098 mol) in CH₂Cl₂ (230 mL) and a solution of triethylamine (10.37 g, 0.102 mol) in CH₂Cl₂ (35 mL) following the previous procedure to give a brown solid. The solid was recrystallized from methanol (350 mL) 3 times to yield a white solid (9.90 g, 62% yield). ¹H NMR (CDCl₃): δ 1.47 (m, 8H), 2.83 (m, 12H).

^{13}C NMR (CDCl_3): δ 27.62, 27.65, 28.62, 37.48, 177.26. HRMS calcd for $\text{C}_{14}\text{H}_{20}\text{N}_2\text{O}_4\text{S}_2 + \text{Na}^+$: 367.0762. Found: 367.0757.

N-Benzylmethyl-hexanesulfenamide (Molecule C)

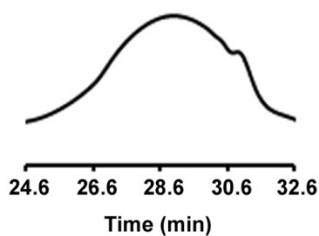
N-Benzylmethylamine (1.11 g, 9.19 mmol) was added to a solution of molecule B (1.94 g, 9.01 mmol) in CH_2Cl_2 (2.5 mL) and stirred at room temperature for 19 h. The reaction was diluted with anhydrous Et_2O (30 mL) and washed with water (4 x 20 mL). The organic phase was dried over anhydrous MgSO_4 and evaporated to give a yellowish oil (1.7 g, 81% yield). ^1H NMR (CDCl_3): δ 0.89 (t, 3H, $J = 6.8$ Hz), 1.34 (m, 6H), 1.56 (m, 2H), 2.69 (m, 5H), 4.01 (s, 2H), 7.28 (m, 5H). ^{13}C NMR (CDCl_3): δ 14.07, 22.56, 28.26, 28.80, 31.56, 32.88, 45.97, 65.47, 127.25, 128.23, 128.68, 138.90. HRMS calcd for $\text{C}_{14}\text{H}_{23}\text{NS}$: 237.1551. Found: 237.1541.

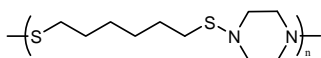


Polymer A

Piperazine (0.176 g, 2.05 mmol) was added to a stirred solution of (2,2'-oxydiethenthio)disuccinimide. (0.71 g, 2.05 mmol) in CHCl_3 (3.5 mL) and reacted at room temperature for 24 h. The polymer was precipitated into methanol (35 mL) and washed with methanol 3 times. The polymer was dried under vacuum to yield a white powder. ^1H NMR (CDCl_3): δ 2.86 (t, 4H, $J = 6.8$ Hz), 2.97 (s, 8H), 3.65 (t, 4H, $J = 6.9$ Hz). ^{13}C NMR (CDCl_3): δ 32.92, 57.28, 70.10.

(Mw: 3,700 g / mol, PDI: 1.42)

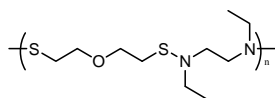
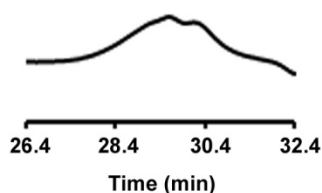




Polymer B

N,N'-(Hexanethio)disuccinimide (3 g, 8.71 mmol) in CHCl_3 (19 mL) was reacted with piperazine (0.75 g, 8.71 mmol) following the previous procedure to yield a white powder. ^1H NMR (CDCl_3): δ 1.40 (m, 4H), 1.56 (m, 4H), 2.69 (t, 4H, $J = 7.5$ Hz). ^{13}C NMR (CDCl_3): δ 28.62, 28.82, 32.17, 57.30.

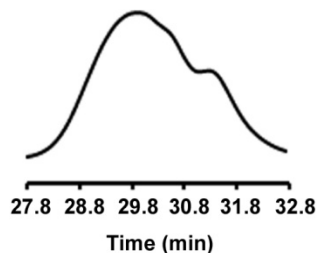
(M_w : 6,300 g / mol, PDI: 1.22)

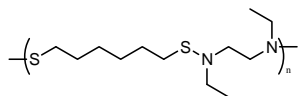


Polymer C

(2,2'-Oxydiethenthio)disuccinimide (0.625 g, 1.77 mmol) in CH_2Cl_2 (1.5 mL) was reacted with *N,N'*-diethylethylenediamine (0.21 g, 1.77 mmol) following the previous procedure. After evaporating the solvent, the polymer was precipitated into methanol (10 mL) and washed with methanol (15 mL). The polymer was dried under vacuum to yield a yellowish oil. ^1H NMR (CDCl_3): δ 1.14 (t, 6H, $J = 6.9$ Hz), 2.77 (t, 4H, $J = 7.1$ Hz), 2.90 (q, 4H, $J = 7.0$ Hz), 3.04 (s, 4H), 3.65 (t, 4H, $J = 7.2$ Hz). ^{13}C NMR (CDCl_3): δ 14.27, 35.14, 53.66, 56.79, 69.98.

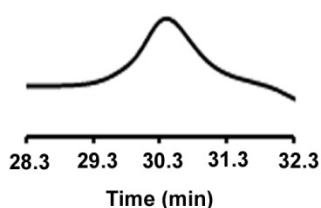
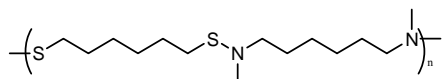
(M_w : 2,300 g / mol, PDI: 1.60)



Polymer D

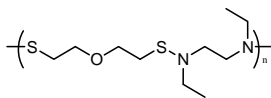
N,N'-(Hexanethio)disuccinimide (1 g, 2.90 mmol) in CHCl_3 (5 mL) was reacted with *N,N'*-diethylethylenediamine (0.34 g, 2.90 mmol) following the previous procedure. The polymer was precipitated into methanol (10 mL). The polymer was redissolved in a minimal amount of CHCl_3 and precipitated into methanol (2 mL) to yield a yellowish oil after drying it under vacuum. ^1H NMR (CDCl_3): δ 1.14 (t, 6H, $J = 7.1$ Hz), 1.40 (m, 4H), 1.54 (m, 4H), 2.60 (t, 4H, $J = 7.4$ Hz), 2.90 (q, 4H, $J = 7.1$ Hz), 3.05 (s, 4H). ^{13}C NMR (CDCl_3): δ 13.99, 27.92, 28.91, 34.27, 53.23, 56.52.

(M_w : 3,700 g / mol, PDI: 1.06)

Polymer E

N,N'-(Hexanethio)disuccinimide (1 g, 2.90 mmol) in CHCl_3 (6 mL) was reacted with *N,N'*-dimethyl-1,6-hexanediamine (0.42 g, 2.90 mmol) following the previous procedure. The polymer was precipitated into methanol (10 mL). The polymer was redissolved in a minimal amount of CHCl_3 and precipitated into methanol (7 mL) to yield a yellowish oil after drying it under vacuum. ^1H NMR (CDCl_3): δ 1.31 (m, 4H), 1.41 (m, 4H), 1.55 (m, 8H), 2.64 (t, 4H, $J = 7.4$), 2.76 (m, 10H). ^{13}C NMR (CDCl_3): δ 26.87, 28.18, 28.40, 28.89, 31.68, 47.12, 59.87.

Polymer C from a disulfenamide.



N,N'-Ethylmethyl-bis(2-mercaptoethyl)disulfenamide (1.34 g, 5.32 mmol) was reacted with *N,N'*-diethylethylenediamine (0.62 g, 5.32 mmol) in refluxing benzene (5 mL) for 24 h. After evaporating the solvent, the polymer was precipitated into methanol (2 x 15 mL). The polymer was dried under vacuum to yield a yellowish oil (0.12 g). ^1H NMR (CDCl_3): δ 1.14 (t, 6H, $J = 6.9$ Hz), 2.77 (t, 4H, $J = 7.1$ Hz), 2.90 (q, 4H, $J = 7.0$ Hz), 3.04 (s, 4H), 3.65 (t, 4H, $J = 7.2$ Hz). ^{13}C NMR (CDCl_3): δ 14.27, 35.14, 53.66, 56.79, 69.98.

Kinetic Reactions with Sulfenamides and Thiosuccinimides

Kinetics of molecule A and *N*-benzylmethylamine (Figure

2.1c)

Molecule A (71.1 mg, 406 μmol) was dissolved in 1.75 mL of CD_3OD and 1 mL (40.7 mg, 232 μmol) of the solution was transferred to a NMR tube. After the addition of *N*-benzylmethylamine (28.1 mg, 232 μmol), the reaction was monitored by ^1H NMR spectroscopy.

Kinetics of molecule B and *N*-benzylmethylamine (Figure

2.1d)

Molecule B (29.0 mg, 135 μmol) was dissolved in 2 mL of CD_2Cl_2 and 0.69 mL (10 mg, 46.4 μmol) of the solution was transferred to a NMR tube. *N*-Benzylmethylamine (37.7 mg, 311 μmol) was dissolved in 2 mL of CD_2Cl_2 , from which 0.30 mL (5.6 mg, 46.4 μmol) was withdrawn and added to the NMR tube. The reaction was monitored by ^1H NMR spectroscopy.

Kinetics of reaction between *N,N'*-
(hexanethio)disuccinimide and piperazine (Figure 2.1e)

N,N'-(Hexanethio)disuccinimide (48.4 mg, 141 μmol) was dissolved in 1 mL of CDCl_3 . Piperazine (12.6 mg, 155 μmol) was added and the reaction was monitored by ^1H NMR spectroscopy.

Degradation of Sulfenamides

Kinetics of the degradation of molecule C under neutral
conditions (Figure 2.2a)

Molecule C (363.2 mg, 1.53 mmol) was dissolved in 3.3 mL of CD_3OD , from which 0.5 mL (55.1 mg, 232 μmol) was transferred to a NMR tube. After adding an additional 0.5 mL of CD_3OD , ^1H NMR spectra were recorded at room temperature every few days. After 33 days, 15 % of molecule C degraded to yield *N*-benzylmethylamine.

This procedure was also followed but the NMR tube was added to a heat bath at 40 $^\circ\text{C}$. The reaction showed 27 % degradation of molecule C to *N*-benzylmethylamine after 33 days.

For the kinetics in C_6D_6 at room temperature, a solution of molecule C (33.9 mg, 143 μmol) in 0.7 mL of C_6D_6 was added to a NMR tube and ^1H NMR spectra were recorded every few days for 30 days. The NMR spectra did not change which demonstrated that <3% of molecule C degraded.

Kinetics of the degradation of molecule C with benzoic
acid in CD_3OD

Molecule C (103.5 mg, 436 μmol) was dissolved in 0.94 mL of CD_3OD and 0.5 mL (55.1 mg, 232 μmol) was transferred to a NMR tube. Benzoic acid (202.5 mg, 1.66 mmol) was dissolved in 0.72 mL of CD_3OD , from which 0.5 mL (141.8 mg, 1.16 mmol) was withdrawn and added to the NMR tube. The ^1H NMR spectrum after 4 min showed

51 % conversion of molecule C to protonated *N*-benzylmethylamine. This reaction was too rapid to monitor the kinetics.

Degradation of molecule C with acetic acid in water

(Figure 2.2b)

Acetic acid (0.44 g, 7.37 mmol) was added to a solution of molecule C (0.25 g, 1.05 mmol) in D₂O (4 mL) and stirred at room temperature for 41 h. The protonated *N*-benzylmethylamine was soluble in D₂O but the other organic products were not soluble. The reaction was extracted with Et₂O (20 mL) and washed with water (4 x 10 mL). The organic layer was dried over anhydrous MgSO₄ and evaporated to give a yellowish oil (122 mg). A ¹H NMR spectrum was obtained of this reaction mixture prior to chromatography to characterize the distribution of products. The products were separated by column chromatography using 4 % EtOAc in hexanes to give *S*-hexyl hexanesulfinate (molecule D in Figure 2b; 84 mg) and a mixture (28 mg) of hexyl disulfide and byproducts. Molecule D was fully characterized as described below.

Molecules E and F were only small components of this reaction mixture and were not obtained in sufficient yield and purity for full characterization. Rather, they were obtained as pure solids from the next reaction described below and were fully characterized at that point. Their presence when molecule C was decomposed with acetic acid was based on their peaks in the ¹H NMR spectrum which made them simple to identify.

S-hexyl hexanesulfinate (molecule D): ¹H NMR (CDCl₃): δ 0.90 (m, 6H), 1.37 (m, 12H), 1.80 (m, 4H), 3.13 (m, 4H). ¹³C NMR (CDCl₃): δ 13.97, 14.00, 22.39, 22.48, 23.43, 28.27, 28.28, 30.82, 31.22, 31.32, 32.91, 56.23. HRMS calcd for C₁₂H₂₆OS₂: 250.1425. Found: 250.1416.

Degradation of molecule C with *p*-toluenesulfonic acid in water

p-Toluenesulfonic acid (0.24 g, 1.24 mmol) was added to a solution of molecule C (0.30 g, 1.24 mmol) in D₂O (4 mL) and stirred at room temperature for 16 h. The reaction was extracted with anhydrous Et₂O (20 mL) and washed with water (4 x 10 mL). The organic layer was dried over anhydrous MgSO₄ and evaporated to give a yellowish oil (116 mg). The distribution of products was checked by ¹H NMR spectroscopy prior to chromatography. The products were isolated through column chromatography using 4 % EtOAc in hexanes to give three main products; hexyl disulfide (molecule F in Figure 2b; 49.1 mg), *S*-hexyl hexanesulfinate (molecule D in Figure 2b; 16.4 mg), *S*-hexyl hexanesulfonate (molecule E in Figure 2b; 37.3 mg). The ¹H and ¹³C NMR spectra of these compounds matched those reported in the literature and are described below.⁹⁹⁻¹⁰¹

Hexyl disulfide: ¹H NMR (CDCl₃): δ 0.89 (t, 6H, *J* = 7.0 Hz), 1.48 (m, 12H), 1.67 (m, 4H), 2.68 (t, 4H, *J* = 7.4 Hz). ¹³C NMR (CDCl₃): δ 14.05, 22.56, 28.23, 29.20, 31.45, 39.21. HRMS calcd for C₁₂H₂₆S₂: 234.1476. Found: 234.1469

S-hexyl hexanesulfonate: ¹H NMR (CDCl₃): δ 0.90 (m, 6H), 1.38 (m, 12H), 1.69 (m, 2H), 1.92 (m, 2H), 3.13 (t, 2H, *J* = 7.4 Hz), 3.29 (t, 2H, *J* = 8). ¹³C NMR (CDCl₃): δ 13.94, 13.97, 22.32, 22.45, 23.49, 27.66, 28.26, 29.63, 31.15, 31.21, 36.28, 62.71. HRMS calcd for C₁₂H₂₆O₂S₂: 266.1374. Found: 266.1367.

Characterization of Microparticles

All of the microparticles were prepared polymer with the structure shown in entry 2 of Table 2.1.

Preparation of microparticles

Blank microparticles were prepared by oil-in-water (o/w) single emulsion, solvent evaporation technique. Briefly, 300 mg of polymer was dissolved in 3.5 mL of chloroform in a heated waterbath (55 °C). This organic phase was then emulsified with

35 mL of 1% (w/v) mowiol® at 13,500 rpm for 1 min using an IKA Ultra-Turrax T25 basic homogenizer (IKA, Wilmington, NC). The mixture was stirred overnight to evaporate the organic phase. The microparticles were then washed three times with deionized water (5000 rpm for 10 min) and lyophilized (Labconco FreeZone 4.5, Kansas City, MI). Microparticles were stored at -20 °C until use.

For *in vitro* particle uptake studies, 2 mg of Rhodamine B (Sigma, St. Louis, MO) was dissolved along with the polysulfenamide in chloroform prior to the formation of the oil-in-water single emulsion. The rhodamine labeled particles were washed and collected as described above.

Surface morphology

Microparticle morphology was assessed by scanning electron microscopy (SEM, Hitachi S-4000). Air-dried microparticles were placed on silicon wafers mounted on SEM specimen stubs. The stubs were coated with ~5 nm of gold by ion beam evaporation followed by imaging using SEM operated at 3 kV accelerating voltage.

Particle size and zeta potential

Microparticle size and zeta potential was measured using the Zetasizer Nano ZS (Malvern, Southborough, MA). The microparticles were suspended in deionized water at a concentration of 1 mg ml⁻¹. The zeta potential was measured using folded capillary cell in automatic mode and the size was measured using a disposable sizing cuvette (DTS0012). The size was measured at 25 °C at a 173° scattering angle.

Crosslinking with polyethylene imine (PEI)

PEI crosslinking was carried out by adding PEI into a suspension of microparticles in deionized water (1 mg ml⁻¹). The solution was vortexed for 30 sec and left at 4 °C for 5 h. The microparticles were washed with deionized water and collected

by centrifugation (7000 rpm for 10 min). The zeta potential of the crosslinked particles was measured as described above.

In vitro analysis of microparticle degradation

For *in vitro* analysis, ~85 mg of the microparticles was suspended in either phosphate buffer saline (PBS, pH 7.4) or acetate buffer (pH 4). The samples were agitated at 37 °C, 150 rpm in a horizontal shaker (C24 incubator shaker, New Brunswick Scientific, Edison, NJ). At specific time points, the samples were centrifuged for 10 min at 7000 rpm. The pellet was washed three times with deionized water and lyophilized. The dry weight of the pellet was recorded and percentage weight loss was calculated for each sample. In addition, the samples were also analyzed by scanning electron microscopy to observe change in surface morphology of microparticles.

Particle uptake

Uptake of rhodamine-labeled microparticles was studied in JAWSII cells and HEK293 cells. Chambers were initially coated with 300 µL of poly L-lysine (0.1% w/v) overnight. Following coating, ~ 1 x 10⁴ cells were seeded per well and incubated overnight at 37 °C in a humidified 5% CO₂-containing atmosphere. Rhodamine labeled particles were added to the media at a concentration of 50 micrograms per well. The particles were incubated with the cells for ~ 18 h. Cells were washed three times with sterile PBS and fixed with 4% paraformaldehyde. The nucleus was stained with DAPI. Vectashied mounting medium was added onto slide and sealed with coverslip. The samples were imaged using LSM710 confocal microscope (Carl Zeiss MicroImaging).

Cytotoxicity evaluation of microparticles

The cytotoxicity of polymer microparticles was evaluated using the MTS assay. HEK293 cells were seeded in a 96 well plate at a density of 1 x 10⁴ cells/well and incubated for 24 hours at 37 °C in a humidified 5% CO₂-containing atmosphere.

Following this, the cells were incubated with 200 μ L of complete DMEM containing various concentrations of microparticles. The particles were incubated at 4 h and 24 h to study the time-dependent effect on toxicity of the microparticles. MTS solution in PBS was added to each well and incubated for 4 h. The optical density of the sample was measured at 490 nm using a Spectramax plus microplate spectrophotometer (Molecular Device). The values obtained for cell viability represent the average of eight values. Cell viability (%) was calculated as [(mean absorbance of the sample – reference absorbance)]/mean absorbance of the control] \times 100.

Statistical analysis

Group data are reported as mean \pm SD. Differences between groups were analyzed by two-tailed unpaired t test. Levels of significance were accepted at the $P < 0.05$ level. Statistical analyses were performed using Prism 3.02 software (Graphpad Software, Inc., San Diego, CA)

(This work was submitted to *Proc. Natl. Acad. Sci. USA*, 2011.)

CHAPTER 3
SYNTHESIS OF POLYMERS WITH BIODEGRADABLE N-S-N
BONDS

Introduction

This chapter describes work that builds on our synthesis of polysulfenamides to synthesize the first polymers with NSN bonds along their backbones. In our prior work we synthesized polysulfenamides primarily from dithiosuccinimides and secondary diamines as shown in Figure 3.1a. These polymers were stable in methanol but readily

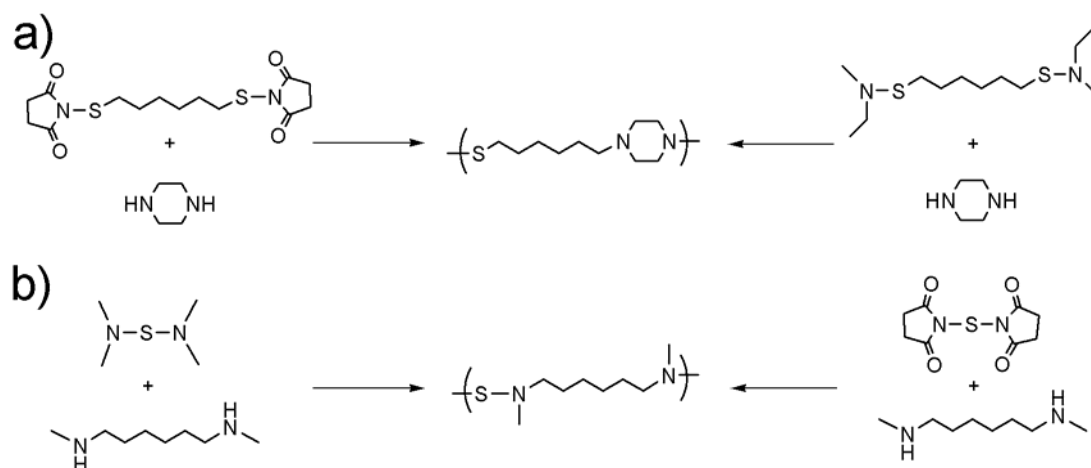


Figure 3.1 The synthesis of polysulfenamides and polymers with NSN bonds.

degraded under acidic conditions. To further explore the types of polymers that could be synthesized with SN bonds, we synthesized two sulfur transfer reagents and developed methods to synthesize polymers with NSN bonds (Figure 3.1b). No examples of these polymers had been reported in the literature, so our syntheses are unique. In this chapter we will report the synthesis of two sulfur transfer reagents, their rates of reaction with a

secondary amine in various solvents, and the characterization of a set of polymers with NSN bonds.

Results and Discussion

Synthesis and Reactions of Sulfur Transfer Reagents.

The synthesis of polymers with NSN bonds required the synthesis of sulfur transfer reagents that would readily react with diamines. Based on the success of synthesizing polymers with SN bonds, two approaches to sulfur transfer reagents were investigated based on the use of succinimides and ethylmethylamine as leaving groups. In prior work, amines readily reacted with activated thiols to yield molecules with SN bonds according to Figure 3.2. These reactions were robust and high yielding so the synthesis of two types of sulfur transfer reagents was completed as shown in Figure 3.3.

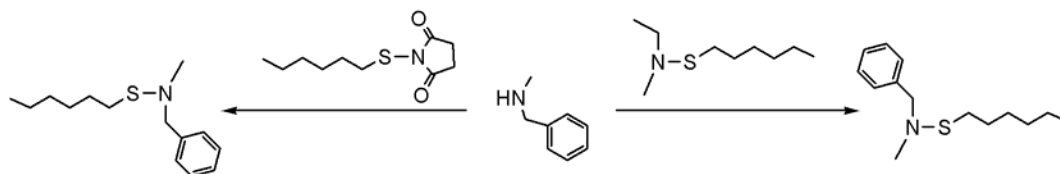


Figure 3.2 Two approaches to synthesize SN bonds that were successful in our prior work.

Molecule B was initially explored as a sulfur transfer reagent based on the rapid reactions of thiosuccinimides with secondary amines in our prior work. A literature procedure was followed to synthesize molecules A and B. The synthesis of A had a crude yield of 81% and yielded a clean intermediate that was carried onto the next step without need for further purification. Although the synthesis of B was straightforward, its

purification was challenging because of its poor solubility in many solvents. Molecule B was mostly insoluble in benzene, chloroform, and methylene chloride but dissolved when briefly heated in DMSO. Molecule B was cleaned by washing the crude product with hexanes and an isolated yield of 69% was obtained. Replacement of *N*-chlorosuccinimide with *N*-chlorophthalimide in the second step yielded a diphthalimide sulfur transfer reagent that was more insoluble than B.

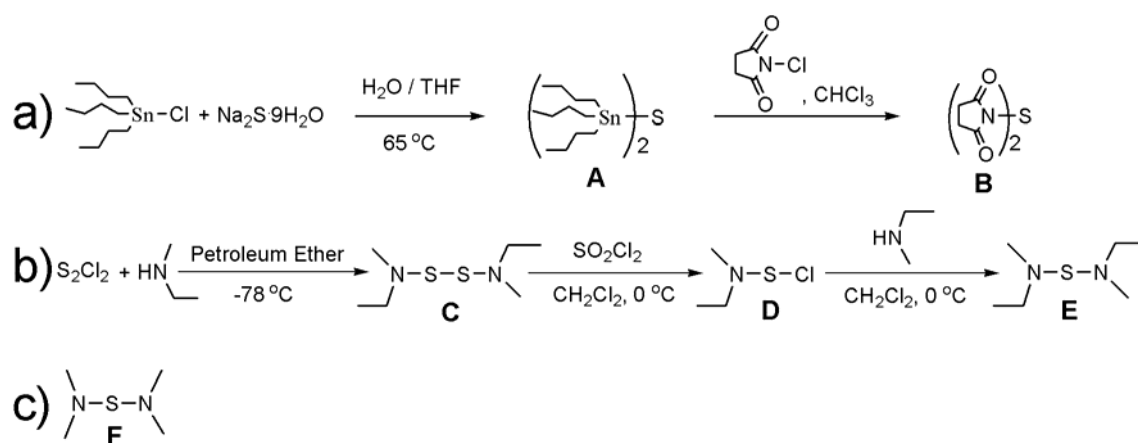


Figure 3.3 The synthesis of two sets of sulfur transfer reagents. a) The synthesis of a dithiosuccinimide. b) and c) The synthesis of two examples of bis-aminosulfides.

Although B was partially soluble in DMSO, it was not used to synthesize polymers for several reasons. First, many of the polymers that were anticipated will possess poor solubilities in DMSO. Second, the synthesis of B had poor atom efficiency. The addition of one sulfur (atomic weight: 32 g mol⁻¹) to two amines to yield two S-N bonds along the backbone of a polymer would require the use of two equivalents of tributyltin chloride (MW: 326 g mol⁻¹) and two equivalents of *N*-chlorosuccinimide (MW: 134 g mol⁻¹). Thus, significant amounts of waste are produced for each NSN bond

synthesized using molecule B. Also, the poor solubility of molecule B made it challenging to purify it to the level needed for a step polymerization. For instance, it decomposed within minutes when heated in CDCl_3 and $\text{DMSO-}d_6$.

A second sulfur transfer reagent was synthesized (E in Figure 3.3) based on a literature precedent. In the first step, an excess of ethylmethylamine was reacted with sulfur chloride at $-78\text{ }^\circ\text{C}$. Reactions run at $0\text{ }^\circ\text{C}$ had unidentified side products, but the reaction at $-78\text{ }^\circ\text{C}$ yielded C in high purity. Molecule C could be carried onto the next step without purification or it could be purified by distillation. In the second step, C was reacted with SO_2Cl_2 to yield D that was not isolated. Rather, D was slowly added to ethylmethylamine to yield the sulfur transfer reagent E. This procedure was followed to synthesize F using dimethylamine in both steps. Both E and F were isolated as clean products as shown by ^1H NMR spectroscopy, and they were readily further purified by distillation. The yield of the second step was 32% for E and 46% for F.

Kinetics of Transamination Reactions

To synthesize polymers via transamination reactions between E or F and secondary diamines, the kinetics of reactions between E and benzylmethylamine were studied in four solvents (Figure 3.4). Benzylmethylamine was chosen for these reactions because of the easily identified benzylic CH_2 group that shifted downfield in the ^1H NMR spectra when proceeding from benzylmethylamine to H to I. The chemical shifts of the peaks are given in the experimental section for each solvent.

Four reactions between molecule E and two molar equivalents of benzylmethylamine were studied and the rate constants were measured in CD_2Cl_2 (rate constant = $7.81 \times 10^{-5}\text{ M}^{-1}\text{ s}^{-1}$), $\text{DMSO-}d_6$ ($4.89 \times 10^{-5}\text{ M}^{-1}\text{ s}^{-1}$), CDCl_3 ($2.79 \times 10^{-5}\text{ M}^{-1}\text{ s}^{-1}$), and C_6D_6 ($5.47 \times 10^{-6}\text{ M}^{-1}\text{ s}^{-1}$). The rate constants were found using the data points for conversions of less than 10% and with the assumption that the reaction was irreversible. Although the reaction was reversible, this assumption is typically used in to find rate

constants for reactions that have proceeded to low conversions.⁹⁶ In Figure 3.4b the conversion was the number of S-N(CH₃)(Bn) bonds divided by the total number of S-N bonds.

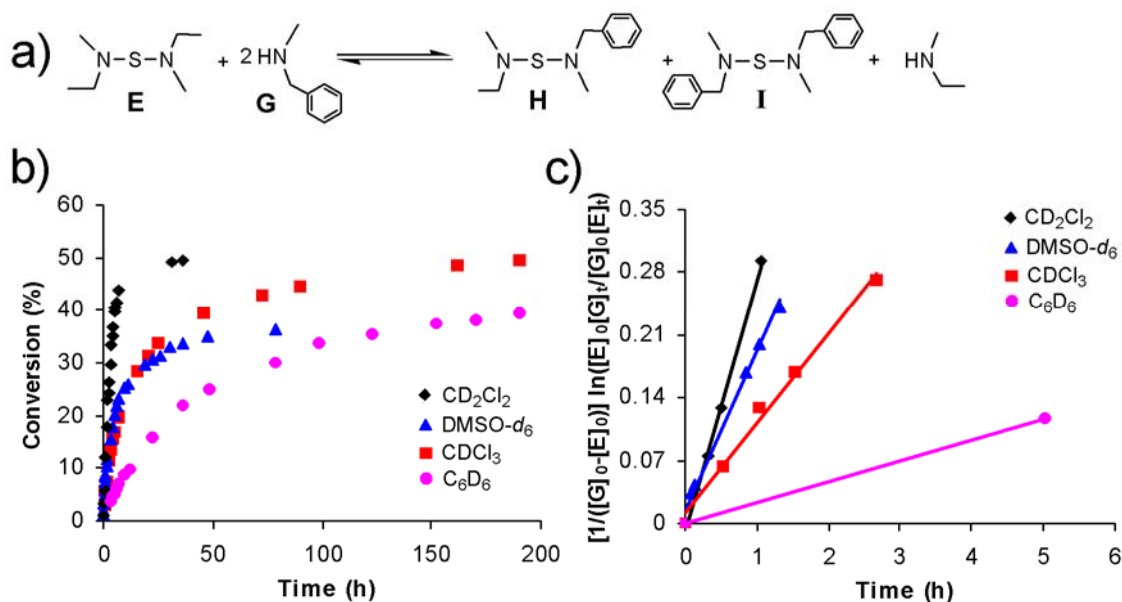


Figure 3.4 Kinetics of transamination reactions. a) The reaction that was studied in a sealed NMR tube. b) The conversion of the transamination reactions as a function of time. The conversion was defined as the sum of the S-N(CH₃)Bn bonds divided by the sum of all of the S-N bonds for molecules E, H, and I. c) The plot of the initial data points to find the rate constants for each solvent.

Although the reaction was most rapid in CD₂Cl₂ and reached equilibrium in 14 h, small amounts of unidentified side products were visible. The presence of side products made methylene chloride a poor choice for the polymerization. The reaction in CDCl₃ took 8 days to reach equilibrium and the reaction in C₆D₆ did not reach equilibrium after 8 days. Despite the slower rates for reactions in these solvents, the reactions were clean and no side products were observed. The reaction in DMSO-*d*₆ also did not show any side products even after 3 days, but this reaction reached 37% conversion and did not

proceed any further. The final conversion was less than 50% because molecule I had limited solubility in DMSO- d_6 due to the apolar structure of molecule I and the polar structure of DMSO- d_6 . The ^1H NMR spectra of this reaction in DMSO- d_6 showed a lower than expected concentration of molecule I even after three days.

The reaction between molecule E and benzylmethylamine reached 51% conversion in 17 h when run at 40 °C in an uncapped NMR tube, but prolonged reaction times resulted in a slow increase in conversion. To lower the boiling point of the free amine to allow the reaction to go to a higher conversion, molecule F with dimethylamine (boiling point 7 °C) as the leaving group was used rather than molecule E with ethylmethylamine (boiling point 36-37 °C) as the leaving group.

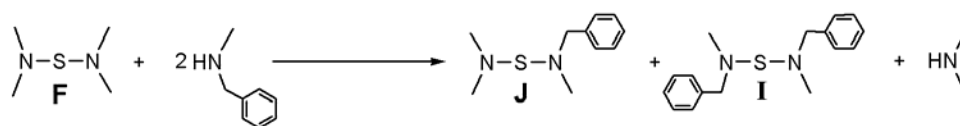


Figure 3.5 Transamination reactions with dimethylamine as the leaving group.

Reactions between molecule F and benzylmethylamine were studied in CDCl_3 , DMSO- d_6 , and C_6D_6 in vented reaction vessels to allow the dimethylamine to boil off (Figure 3.5). Each of the reactions in Table 3.1 did not show any impurities even when heated to 85 °C for extended periods of time. The conversions for the reactions were high for each solvent for reactions at 50 °C, but went to quantitative conversions for reactions in C_6D_6 at 85 °C.

Table 3.1 Transamination reactions of molecule F and benzylmethylamine.

Entry	Solvent	Temperature (°C)	Reaction time (h)	^a Conversion (%)
1	CDCl ₃	50	24	39
2	CDCl ₃	50	72	93
3	DMSO- <i>d</i> ₆	50	73	84
4	C ₆ D ₆	50	24	41
5	C ₆ D ₆	50	72	84
6	C ₆ D ₆	85	24	>97

^aThe conversion was defined as the sum of the S-N(CH₃)Bn bonds divided by all of the S-N bonds in molecules F, J, and I.

Synthesis of Polymers with NSN Bonds

Polymers with NSN bonds were synthesized by reaction of secondary diamines and molecule F at elevated temperatures (Table 3.2). These polymerizations were run for 24 to 96 h and the resulting polymers were characterized by GPC against polystyrene standards, ¹H NMR spectroscopy, and ¹³C NMR spectroscopy.

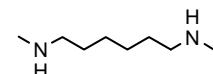
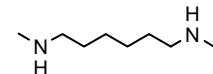
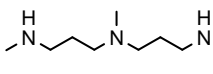
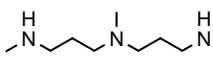
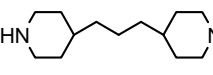
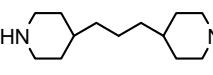
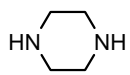
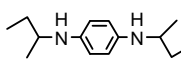
The polymers synthesized in entries 1, 2, 5, and 6 had high molecular weights and degrees of polymerization. The degree of polymerization was determined using the molecular weight measured by GPC and by end group analysis in ¹H NMR spectroscopy. The separate values for the degree of polymerization agreed with each and demonstrated that these reactions cleanly proceeded to high conversions.

The polymer synthesized in entries 3 and 4 had limited stability. The polymer was isolated by removing the solvent under vacuum and characterized without further purification. When this polymer was precipitated into methanol and water, it rapidly degraded as shown by the presence of numerous, unidentified peaks in the ¹H NMR

spectra. The internal tertiary amine was believed to be the source of the instability of this polymer.

The polymerization with piperazine (entry 7) yielded an insoluble polymer in all solvents. The monomer in entry 8 failed to react with molecule F

Table 3.2 Synthesis of N-S-N bond polymers.

Entry	Diamine	Solvent	Temperature (°C)	Reaction time (h)	M_n^a (g mol ⁻¹)	PDI ^a	Yield (%)	DP ^b (%)	DP ^c (%)
1		C ₆ H ₆	85	24	5,600	3.7	75	98	99
2		C ₆ H ₆	85	24	5,200	3.4	97	98	99
3		C ₆ H ₆	85	72	810	1.6	97	87	97
4		C ₆ H ₆	85	96	1,600	1.6	89	93	98
5		CHCl ₃	60	72	12,400	6.6	88	99	98
6		CHCl ₃	60	96	7,200	3.3	95	98	98
^d 7		C ₆ H ₆	85			-			
^e 8		C ₆ H ₆	85			-			

^aThe relative M_n and PDI were measured versus polystyrene standards using a calibration curve and the reflective index peaks of the polymer. ^bThe degree of polymerization based on the values for M_n . ^cThe degree of polymerization based on ¹H NMR spectra. ^dThe polymer was insoluble. ^eNo polymerization occurred.

Degradation of the N-S-N Bond

In preliminary work, molecule E was stable in C_6D_6 for 37 days and $DMSO-d_6$ for 35 days (Figure 3.6). No evidence of degradation was observed by 1H NMR spectroscopy in these solvents. In contrast, some degradation was observed in $CDCl_3$ and a 10:1 (v:v) mixture of $DMSO-d_6/D_2O$. In future work the degradation of the NSN bond in water will be studied.

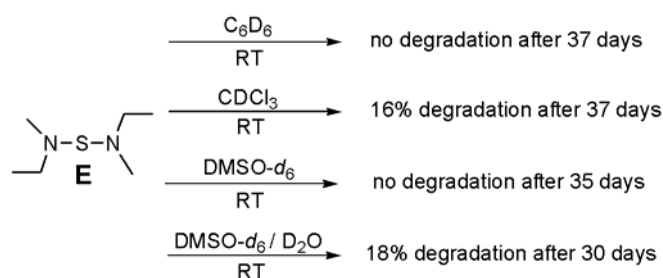


Figure 3.6 Degradation of N-S-N bond: Molecule D was added to C_6D_6 , $CDCl_3$, $DMSO-d_6$, and $DMSO-d_6 / D_2O$ (10/1 v/v) to study how rapidly it degraded.

Conclusions

This chapter described our work to synthesize the first polymers with NSN bonds along their backbones. We synthesized these polymers to apply them as new biodegradable polymers in biomedical applications similar to how the polysulfenamides were applied. This project is not complete, but rather, it is an excellent start. Before publication of this work, more complex polymers will be synthesized and the degradation of the NSN bond will be studied in more detail. Specifically, the degradation of a molecule with an NSN bond will be investigated in water to learn if it degrades rapidly

under acidic conditions. Our work has shown that these polymers can be synthesized and that they are stable to many conditions and our future work will build on these results.

Experimental Section

Materials and Methods

Materials

Sodium sulfide nonahydrate ($\text{Na}_2\text{S}\cdot 9\text{H}_2\text{O}$), tributyltin chloride, *N*-chlorosuccinimide, sulfur monochloride (S_2Cl_2), sulfurly chloride (SO_2Cl_2), *N*-ethylmethylamine, *N*-benzylmethylamine, *N,N'*-dimethyl-1,6-hexanediamine, *N,N'*-bis[3-(methylamino)propyl]mentylamine, 4,4'-trimethylenedipiperidine, *N,N'*-di-*sec*-butyl-*p*-phenylenediamine, dimethylamine, *p*-toluenesulfonyl chloride, and 3-methoxypropylamine were purchased from Aldrich or Acros Organics at their highest purity and used as received. HPLC grade chloroform purchased from Fisher Scientific was used as the GPC solvent after filtering it through a glass frit. All other solvents including petroleum ether (39 ~ 56 °C) were reagent grade and purchased from Fisher Scientific. Because dimethylamine is a gas at room temperature, it was condensed inside a graduate cylinder in a - 78 °C bath before using it. Piperazine (99%) was purchased from Aldrich and was purified by sublimation under vacuum at 130 °C. Genduran silica gel 60 (230-400 mesh) and Basic Alumina Brockman Activity I (60-325 mesh) purchased from Fisher Scientific were used for all column chromatography.

Characterization

^1H and ^{13}C NMR spectra were recorded on a Bruker DPX 300 at 300 MHz and 75 MHz respectively. CDCl_3 and $\text{DMSO}-d_6$ were used as NMR solvent with tetramethylsilane (TMS) as an internal standard. HR ESI-MS data were recorded on a Waters Q-ToF Premier instrument in positive ion mode and HR EI-MS data were recorded on a Waters GCT Premier instrument. Size exclusion chromatography (SEC)

was performed using tetrahydrofuran as the mobile phase (1.00 mL min^{-1}) at $25 \text{ }^\circ\text{C}$. A Shimadzu LC-10AT HPLC pump and one Varian column (PLgel $5 \mu\text{m}$ MIXED-D) were used in series. A Shimadzu RID-10A refractive index detector and a Shimadzu SCL-10A system controller were used to measure molecular weights of polymers based on a polystyrene standard calibration curve.

Synthesis of Small Molecules and Polymers

Bis(tributyltin) sulfide (Molecule A)

This molecule was prepared according to a literature procedure.¹⁰² A solution of sodium sulfide nonahydrate ($\text{Na}_2\text{S}\cdot 9\text{H}_2\text{O}$) (42.0 g, 175 mmol) in deionized water (34.8 ml) was prepared by heating it with a heat gun. This solution was added to a solution of tributyltin chloride (28.5 g, 87.4 mmol) in THF (174 mL). Extra deionized water (17.4 mL) was used to transfer the $\text{Na}_2\text{S}\cdot 9\text{H}_2\text{O}$ to the flask. The mixture was reacted at $65 \text{ }^\circ\text{C}$ for 5 h. After cooling the reaction, the organic layer was evaporated. The residue was extracted with Et_2O . The extract was dried over anhydrous MgSO_4 and evaporated to give a colorless oil (21.8 g, 81% yield). ^1H NMR (CDCl_3): δ 0.91 (t, 18H, $J = 7.2 \text{ Hz}$), 1.08 (m, 12H), 1.34 (m, 12H), 1.55 (m, 12H). ^{13}C NMR (CDCl_3): δ 13.66, 15.85, 27.17, 28.68.

Bis(succinimide) sulfide (Molecule B)¹⁰²

N-chlorosuccinimide (2.22 g, 16.6 mmol) was slowly added to a solution of molecule A (5.08 g, 8.30 mmol) in CHCl_3 (22 mL) at $0 \text{ }^\circ\text{C}$ and stirred. After 1.7 h, the ice bath was removed and the reaction was stirred for 8 h. A yellow solid precipitated along the wall of flask. The CHCl_3 was decanted. The yellow solid was washed with hexanes 3 times and dried under vacuum to give a crude yellow solid (1.30 g, 69% yield). ^1H NMR ($\text{DMSO}-d_6$): δ 2.57 (s, 8H). ^{13}C NMR ($\text{DMSO}-d_6$): δ 29.55, 179.47.

N,N'-Dithiobis-ethylmethylanine (Molecule C)¹⁰³

A solution of *N*-ethylmethylanine (10.5 g, 178 mmol) in petroleum ether (400 mL) was cooled to -78 °C. To this solution, sulfur monochloride (6.00 g, 44.4 mmol) was added dropwise for 10 min. The solution was stirred for 20 min at -78 °C and another 35 min at room temperature. The mixture was washed with an aqueous NaCl solution. The organic layer was dried over anhydrous MgSO₄ and evaporated to give a yellow–green oil (7.00 g). The product was isolated by vacuum distillation at 30–35 °C to yield a colorless oil (6.20 g, 78% yield). ¹H NMR (CDCl₃): δ 1.14 (t, 6H, *J* = 7.2 Hz), 2.64 (s, 6H), 2.69 (q, 4H, *J* = 7.1 Hz). ¹³C NMR (CDCl₃): δ 13.81, 46.28, 53.54. HRMS calcd for C₆H₁₆N₂S₂: 180.0755. Found: 180.0759.

N-Ethylmethylsulfenyl chloride (Molecule D)¹⁰⁴

A solution of molecule C (4.81 g, 26.7 mmol) in CH₂Cl₂ (70 mL) was precooled to 0 °C for 40 min under nitrogen. Sulfuryl chloride (3.96 g, 29.4 mmol) was added dropwise to the solution for 17 min under N₂. The reaction was stirred for 30 min at 0 °C and another 50 min at room temperature to yield a crude product (6.70 g, 53.4 mmol), which was used *in situ* for the preparation of Molecule E.

Bis(*N*-ethylmethyl)sulfide (Molecule E)¹⁰⁴

A solution of Molecule D (6.70 g, 53.4 mmol), in CH₂Cl₂ (40 mL) was slowly added to a solution of *N*-ethylmethylanine (7.89 g, 13.3 mmol) in CH₂Cl₂ (60 mL) at 0 °C under nitrogen and stirred for 1 h. The reaction was washed with an aqueous NaCl solution. The organic phase was dried over anhydrous MgSO₄ and evaporated to give a yellow–green oil (4.22 g). The product was purified by distillation under vacuum at room temperature to yield a colorless oil (2.53 g, 32% yield). ¹H NMR (CDCl₃): δ 1.14 (t, 6H, *J* = 7.2 Hz), 2.95 (s, 6H), 3.11 (q, 4H, *J* = 7.1 Hz). ¹³C NMR (CDCl₃): δ 14.24, 46.29, 54.89. HRMS calcd for C₆H₁₆N₂S: 148.1034. Found: 148.1033.

N,N'-Dithiobis-dimethylamine¹⁰³

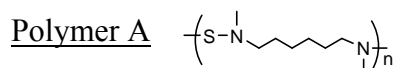
A solution of dimethylamine (8.01 g, 178 mmol) in anhydrous Et₂O (400 mL) was cooled to -78 °C. Sulfur monochloride (6.00 g, 44.4 mmol) was added dropwise to the solution for 14 min. The solution was stirred for 30 min at -78 °C and another 30 min at room temperature. The mixture was washed with an aqueous NaCl solution. The organic layer was dried over anhydrous MgSO₄ and evaporated to give a colorless oil (6.66 g, 99% yield), which was used directly for the preparation of *N*-dimethylsulfenly chloride without further purification. ¹H NMR (CDCl₃): δ 2.63 (s, 12H). ¹³C NMR (CDCl₃): δ 48.31. HRMS calcd for C₄H₁₂N₂S₂: 152.0442. Found: 152.0444.

N-Dimethylsulfenly chloride¹⁰⁴

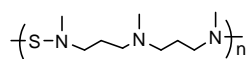
A solution of *N,N'*-dithiobis-dimethylamine (6.03 g, 39.6 mmol) in anhydrous Et₂O (50 mL) was cooled to 0 °C for 1 h under N₂. Sulfuryl chloride (5.88 g, 43.6 mmol) was added dropwise to the solution under N₂. The reaction was stirred for 36 min at 0 °C and another 50 min at room temperature to give a crude product (8.84 g, 79.2 mmol), which was used *in situ* for the preparation of Molecule F.

Bis(*N,N'*-dimethyl) sulfide (Molecule F)¹⁰⁴

A solution of *N*-dimethylsulfenly chloride (8.84 g, 79.2 mmol) in anhydrous Et₂O (50 mL) was slowly added to a solution of dimethylamine (17.9 g, 39.6 mmol) in anhydrous Et₂O (75 mL) at - 5 °C to - 7 °C under N₂ and stirred for 1.2 h. The reaction was washed with a saturated NaCl solution in water. The organic phase was dried over anhydrous MgSO₄ and the solvent was blown off after freezing the product at - 5 °C to - 7 °C to give yellow-green oil (7.00 g). Further purification was achieved by distillation under vacuum at 30 °C to yield a colorless oil (4.39 g, 46% yield). ¹H NMR (CDCl₃): δ 3.02 (s, 12H). ¹³C NMR (CDCl₃): δ 49.69. HRMS calcd for C₄H₁₂N₂S: 120.0721. Found: 120.0719.

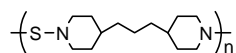


Molecule F (0.942 g, 7.83 mmol) was reacted with *N,N'*-dimethyl-1,6-hexanediamine (1.13 g, 7.83 mmol) in refluxing benzene (11 mL) at 85 °C for 24 h. After evaporating the solvent, the polymer was precipitated into methanol (10 mL). The polymer was dried under vacuum to yield a brown oil (1.02 g, 75 % yield). ^1H NMR (CDCl_3): δ 1.29 (m, 4H), 1.54 (m, 4H), 2.94 (s, 6H), 3.07 (t, 4H, $J = 7.2$ Hz). ^{13}C NMR (CDCl_3): δ 26.88, 28.86, 46.90, 61.05.



Polymer B

Molecule F (0.186 g, 1.55 mmol) was reacted with *N,N'*-bis[3-(methylamino)propyl]mentylamine (0.268 g, 1.55 mmol) in refluxing benzene (1.4 mL) at 85 °C for 72 h. After evaporating the solvent, the polymer was directly dried under vacuum to yield a brown oil (0.310 g, 97 % yield). ^1H NMR (CDCl_3): δ 1.71(m, 4H), 2.21 (s, 3H), 2.32 (t, 4H, $J = 7.5$ Hz), 2.95 (s, 6H), 3.12 (t, 4H $J = 7.1$ Hz). ^{13}C NMR (CDCl_3): δ 25.59, 42.43, 46.90, 55.38, 59.01.



Polymer C

Molecule F (0.186 g, 1.55 mmol) was reacted with 4,4'-trimethylenedipiperidine (0.326 g, 1.55 mmol) in CHCl_3 (1.6 mL) at 60 °C for 72 h. After evaporating the solvent and redissolving the polymer in CH_2Cl_2 (4 mL), the polymer was precipitated into methanol (8 mL) to yield a white-yellow powder (0.330 g, 88 % yield). ^1H NMR (CDCl_3): δ 1.22(m, 12H), 1.59 (m, 4H), 3.08 (t, 4H, $J = 11.0$ Hz), 3.44 (m, 4H). ^{13}C NMR (CDCl_3): δ 23.68, 34.02, 34.96, 36.72, 58.57. Anal. calcd for $\text{C}_{13}\text{H}_{24}\text{N}_2\text{S}$: C, 64.95; H, 10.06; N, 11.65; S, 13.34. Found: C, 64.70; H, 9.97; N, 11.76; S, 13.44.

Calculation of Degree of Polymerization Based on ^1H NMR Spectroscopy.

The degree of polymerization of polymer A was measured by the ratio of the peak corresponding to the terminal *N*-dimethyl (2.99 ppm) and the peak corresponding to the *N*-methyl (2.94 ppm) of the polymer chain. The degree of polymerization of polymer B was measured by the ratio of the peak corresponding to the terminal *N*-dimethyl (3.01 ppm) and the peak corresponding to the *N*-methyl (2.21 ppm) of the polymer chain. The degree of polymerization of polymer C was measured by the ratio of the peak corresponding to the terminal *N*-dimethyl (2.97 ppm) and peaks corresponding to piperazine (3.44 ppm) of the polymer chain.

Kinetic Reactions with Molecule E and *N*- Benzylmethylamine

Molecule E (46.3 mg, 312 μmol) was dissolved in 1.35 mL of CD_2Cl_2 and 1 mL (34.4 mg, 232 μmol) of the solution was transferred to a NMR tube. After the addition of *N*-benzylmethylamine (56.3 mg, 464 μmol) and sealing the NMR tube with a rubber septum, ^1H NMR spectra were periodically recorded for 3 days. The reaction was monitored by conversion of the benzyl hydrogens in *N*-benzylmethylamine at 3.71 ppm to the benzyl hydrogens for molecule H at 4.31 ppm and for molecule I at 4.38 ppm.

The same procedure was also followed for the kinetics of this reaction in CDCl_3 . The conversion from molecule E to molecule H and I was monitored by comparing the benzyl peak (3.74 ppm) of *N*-benzylmethylamine with the benzyl peak (4.32 ppm) of molecule H and the benzyl peak (4.38 ppm) of molecule I for 10 days.

For the kinetics in $\text{DMSO}-d_6$, molecule E (51.3 mg, 345 μmol) was dissolved in 1.49 mL of $\text{DMSO}-d_6$, from which 1 mL (34.4 mg, 232 μmol) was added to a NMR tube. After adding *N*-benzylmethylamine (56.3 mg, 464 μmol) and sealing the NMR tube with a rubber septum, the reaction was monitored by ^1H NMR spectroscopy for 5 days. The

conversion was observed by comparing the benzyl hydrogens in *N*-benzylmethylamine at 3.63 ppm with the benzyl hydrogens for molecule H at 4.29 ppm and for molecule I at 4.36 ppm.

For the kinetics in C₆D₆, molecule E (49.4 mg, 333 μmol) was dissolved in 1.44 mL of C₆D₆ and 1 mL (34.4 mg, 232 μmol) was added to a NMR tube, followed the addition of *N*-benzylmethylamine (56.3 mg, 464 μmol) and sealing the NMR tube with a rubber septum. The conversion from molecule E to molecule H and I was monitored by comparing the benzyl hydrogens in *N*-benzylmethylamine at 3.62 ppm with the benzyl hydrogens for molecule H at 4.34 ppm and for molecule I at 4.36 ppm for 8 days.

Transamination Reaction of Molecule F and *N*-Benzylmethylamine

N-benzylmethylamine (153 mg, 1.26 mmol) was added to a solution of molecule F (75.8 mg, 631 μmol) in 1.26 mL of CDCl₃. After connecting a condenser to the reactor, the mixture was reacted at 50 °C in air and the reaction was monitored by ¹H NMR spectroscopy every 24 h showing 9% conversion to J and 88% conversion to I after 72 h.

The same procedure was followed for the reaction of molecule F (88.3 mg, 735 μmol) and *N*-benzylmethylamine (178 mg, 1.47 mmol) in 1.47 mL of DMSO-*d*₆ showing 13% conversion to J and 77 % conversion to I after 72 h and the reaction of molecule F (82.3 mg, 685 μmol) and *N*-benzylmethylamine (166 mg, 1.37 mmol) in 1.37 mL of C₆D₆ showing 17% conversion to J and 75% conversion to I after 72 h.

For a reaction at 85 °C, molecule F (89.9 mg, 748 μmol) and *N*-benzylmethylamine (181 mg, 1.50 mmol) were reacted in 1.5 mL of refluxing C₆D₆ for 24 h to yield a 3% conversion to J and 97% conversion to I.

Degradation of N-S-N Bonds

Solutions of molecule E (43.4 mg in 1.26 ml of CDCl₃, 49.8 mg in 1.35 mL of DMSO-*d*₆/D₂O (10/1 v/v), 45.3 mg in 1.32 mL of C₆D₆, 48.4 mg in DMSO-*d*₆) were

prepared, from which 1 mL of the solutions were transferred to separate NMR tubes. After 37 days, 15% of molecule E in CDCl_3 degraded to unidentified products (1.18-1.32 ppm and 2.55-2.78 ppm). The degree of degradation was calculated using the residual peak of CDCl_3 at 7.27 ppm as an internal standard. 18 % of molecule E in $\text{DMSO-d}_6/\text{D}_2\text{O}$ (10/1 v/v) degraded to unknown products (1.03-1.07 ppm, 2.33 ppm, 2.55 ppm and 2.60-2.70 ppm) after 30 days and the degree of degradation was calculated using the residual peak of DMSO-d_6 at 2.50 ppm as an internal standard. The NMR spectra in C_6D_6 and DMSO-d_6 did not change after 37 days and 35 days, respectively.

CHAPTER 4
SYNTHESIS OF COMPLEX ARCHITECTURES OF COMB BLOCK
COPOLYMERS AND THEIR ASSEMBLY IN THE SOLID STATE

Abstract

The synthesis of comb block copolymers by ring-opening metathesis polymerization (ROMP), ring-opening polymerization (ROP), and atom transfer radical polymerization (ATRP) is described. Block copolymers were synthesized by the ROMP of oxanorbornene and norbornene monomers followed by hydrogenation of the olefins along the backbone. One block of these diblock copolymers possessed initiators either for the ROP of (3*S*)-*cis*-3,6-dimethyl-1,4-dioxane-2,5-dione or the ATRP of butyl acrylate. The synthesis and characterization of comb polymers with arms composed of poly(lactic acid) and poly(butyl acrylate) are described. These polymers had well defined peaks in the size exclusion chromatography spectra which indicated that no homo polymers were synthesized. A comb block copolymer with polymeric arms of poly(styrene-*b*-vinylpyridine) is described. Vinylpyridine was polymerized from a comb polymer with poly(styrene) arms by ATRP at high dilution of the comb polymer. Finally, the assembly of a series of comb polymers with tri- and tetra-block copolymers as backbones and possessing poly(styrene) arms is described.

Introduction

Comb polymers are an interesting morphology of polymers that often possess molecular weights in excess of one million grams per mole (Figure 4.1).¹⁰⁵⁻¹¹⁷ Because these polymers have large molecular weights and possess radii measured in the tens of nanometers, they are interesting nanomaterials that are nearly monodisperse and possess well-defined distributions of functional groups. Comb polymers possess one or two polymeric arms attached to each monomer unit along a backbone polymer that often results in significant steric crowding between the arms and elongation of the backbone

polymer such that comb polymers may be shaped as cylinders. Recently, we and others synthesized complex architectures of comb polymers including those that possessed dendrimer wedges as arms, liquid crystalline arms, arms with hydrogen bonding motifs, and a block copolymer backbone that resulted in comb block copolymers.¹¹⁸⁻¹²⁵ Comb block copolymers are an interesting motif because they offer the ability to extend the assembly of block copolymers in the solid state to morphologies that possess domain sizes in excess of 100 nm. Linear block copolymers assemble in the solid state into ordered morphologies with domain sizes that are measured in the tens of nanometers.^{126, 127} Reaching larger domain sizes requires the use of additives such as low molecular weight homopolymers, solvents, or nanoparticles that often lead to a decrease in the degree of order and an increase in defects.¹²⁸⁻¹⁴⁰ Comb block copolymers offer an opportunity to reach domain sizes well in excess of 100 nm without the use of additives. In recent work, we demonstrated that comb block copolymers possessing arms composed of poly(styrene) assembled into ordered arrays in the solid state with domain sizes up to 258 nm.^{114, 121, 123} These were the largest domain sizes for assembled polymers that did not require the use of additives.

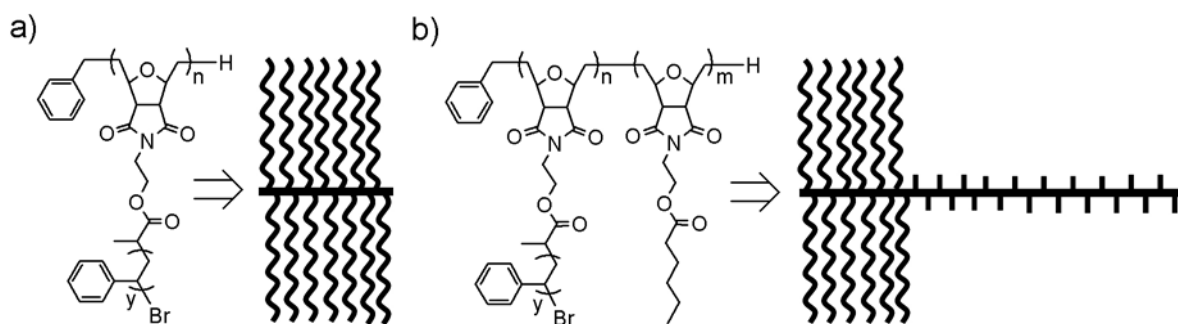


Figure 4.1 Architectures of comb polymers. a) A chemical structure and schematic of a comb polymer with poly(styrene) arms is shown. b) A comb block copolymer is shown with a schematic of its structure.

The synthesis of comb polymers typically involves the use of one or more living/controlled polymerization methods including atom transfer radical polymerization (ATRP), radical addition-fragmentation transfer polymerization, ring-opening polymerization (ROP), and ring-opening metathesis polymerization (ROMP).¹⁴¹ The development of the Grubbs catalysts has spurred advances in comb polymers such that metathesis has been used to synthesize both the backbone and, less commonly, the arms.^{108, 141} In our prior work, we used ROMP with the Grubbs first generation catalyst to synthesize block copolymers exposing initiators for ATRP and ROP with degrees of polymerization exceeding 2,000.^{114, 120-123} Additionally, the olefins along the polymer were hydrogenated in situ to yield stable, robust polymers that were used as backbone polymers. Both the polymerization of the backbone polymer and its hydrogenation were accomplished in one pot with high degrees of hydrogenation (>97%). In more recent work, Grubbs reported the synthesis of comb block copolymers directly from the polymerization of macromonomers using the G3 catalyst.^{108, 142, 143}

This chapter primarily reports the synthesis of new sets of high molecular weight comb block copolymers possessing new polymeric arms that increase the complexity of what can be synthesized in this field. In our prior work, polystyrene arms were synthesized from a backbone polymer to yield comb block copolymers that assembled in the solid state into ordered arrays.^{114, 123} These polymers demonstrated that it was possible to assemble comb block copolymers with molecular weights in excess of two million grams per mole and that these morphologies could be understood based on analogy to those assembled from linear block copolymers. To generate more functional arrays of comb block copolymers, the use of different monomers in their synthesis must be included. Here, the synthesis of comb block copolymers with arms composed of poly(butyl acrylate), poly(lactic acid), and poly(styrene-*b*-vinylpyridine) are described and the assembly of a variety of comb triblock copolymers is shown. The substitution of poly(styrene) arms for other polymers allowed the formation of comb polymers with

arms possessing either a low T_g (the T_g for poly(styrene) is 95 °C and for poly(butyl acrylate) it is -49 °C) or arms that could be readily etched from a final assembly such as those with poly(lactic acid) arms. These new comb polymers extend the possible applications of this architecture by allowing for functionally diverse polymers to be used.

Experimental Section

Materials and Methods

Materials

Styrene, n-butyl acrylate, 4-vinylpyridine, ethylenediamine, copper(I) bromide, copper(II) bromide, *N,N,N',N'',N'''*-pentamethyldiethylenetriamine (PMDETA), and Sn(II) 2-ethylhexanoate were purchased from Aldrich or Across Organics at their highest purity and used as received. HPLC grade chloroform purchased from Fisher Scientific was used as the GPC solvent after filtering it through a glass frit. All other solvents were reagent grade and purchased from Fisher Scientific. (3*S*)-*cis*-3,6-Dimethyl-1,4-dioxane-2,5-dione (98%) was purchased from Aldrich and was purified by recrystallization from ethyl acetate three times and stored under N₂ in a glovebox. 2-Methoxyethyl ether and CH₂Cl₂ were freeze-pump-thawed three times before being taken into the glove box, poured over aluminum oxide, and stored. Genduran silica gel 60 (230-400 mesh) and Basic Alumina Brockman Activity I (60-325 mesh) purchased from Fisher Scientific were used for all column chromatography.

Characterization

¹H and ¹³C NMR spectra were recorded on a Bruker DPX 300 at 300 MHz and 75 MHz, respectively. CDCl₃ was used as NMR solvent with tetramethylsilane (TMS) as an internal standard. Size exclusion chromatography (SEC) was performed using CHCl₃ as the mobile phase (1.00 mL min⁻¹) at 40 °C. A Waters 515 HPLC pump and two Waters columns (Styragel HR 4 and HR 5E) were used in series. A DAWN EOS 18 angle laser

light scattering detector, Wyatt-QELS detector to measure quasi-elastic light scattering, and Wyatt Optilab DSP to measure changes in refractive index were used to measure absolute molecular weights of the polymers. The Zimm plot of comb block copolymers was measured and the second virial coefficient of $1.16 \times 10^{-3} \text{ mol mL g}^{-2}$ was found for comb block copolymers with poly(butyl acrylate) arms. Polymers with poly(4-vinylpyridine) showed significant adsorption in the GPC column resulting in a systematic error of retention time of the polymers. The degree of polymerization of the poly(4-vinylpyridine) block was measured by the ratio of peaks corresponding to the phenyl ring (6.3-7.1 ppm) and peaks corresponding to the pyridine ring (8.1-8.6 ppm) in the ^1H NMR spectra. Images from scanning electron microscopy were obtained using a Hitachi S-4800 at accelerating voltages between 1 to 5 kV.

Synthesis of Comb Block Copolymers

Synthesis of comb block copolymers with poly(butyl acrylate) arms

The same procedure was applied for all entries in Table 1. The synthesis of entry 13 is described. CuBr (20.9 mg, 0.145 mmol) and a stir bar were added to a Schlenk flask which was connected to a Schlenk manifold. Butyl acrylate (71.7 g, 0.56 mol) was poured over aluminum oxide to remove inhibitor and was added to the Schlenk flask. PMDETA (27.7 mg, 0.16 mmol) was added, and the reaction was degassed by three freeze-pump-thaw cycles. The reaction flask was then placed in a 50 °C oil bath for 10 min, and the block copolymer backbone (0.5 g, 0.73 μmol) was dissolved in 10 mL of acetone and transferred to the flask under flowing N_2 . The reaction was heated at 50 °C for 3.5 h and cooled in an ice bath for 15 min. The reaction was filtered through a column filled with silica gel to remove the copper complex and the remaining butyl acrylate was removed through vacuum distillation. The polymer was redissolved in 10 mL of THF and precipitated into methanol to yield a colorless polymeric gel. GPC: $M_n = 651,000 \text{ g mol}^{-1}$,

PDI = 1.08. $^1\text{H NMR}$ (CDCl_3): δ 0.91 (m, 5.6H), 1.37 (m, 6H), 1.59 (broad peak, 8.7H), 1.96 (broad peak, 4.6H), 2.25 (t, 2.9H, $J = 7.5$ Hz), 3.12 (broad peak, 2H), 3.73 (broad peak, 2H), 3.85 (broad peak, 2H), 4.02 (broad peak, 1.9H), 4.23 (broad triplet, 2H, $J = 5.1$ Hz).

Synthesis of comb block copolymers with poly(lactic acid)

arms

The same procedure was followed for all entries in Table 2. The synthesis of entry 2 is described. The block copolymer backbone (0.4 g, 0.13 mmol), *L*-lactide (0.77g, 5.34 mmol), and 2-methoxyethyl ether (13 ml) were added to a Schlenk flask in a glovebox. After sealing the Schlenk flask, it was removed from the glovebox, attached to a Schlenk manifold, and heated to 110 °C for 30 min. Sn(II) 2-ethylhexanoate (10.3 mg, 25.4 μmol) was added under flowing N_2 and the reaction was stirred for 3 h. After cooling the reaction in an ice bath, it was precipitated into methanol. The polymer was redissolved in minimal CH_2Cl_2 and precipitated again into methanol to yield a white, polymeric powder. GPC: $M_n = 817,500 \text{ g mol}^{-1}$, PDI = 1.14. $^1\text{H NMR}$ (CDCl_3): δ 0.87 (t, 3H, $J = 6.8$ Hz), 1.25 (broad peak, 18H), 1.58 (m, 31H), 1.97 (broad peak, 4H), 3.11 (broad peak, 2H), 3.43 (broad peak, 2H), 3.63 (broad peak, 0.7H), 3.80 (broad peak, 2H), 5.16 (q, 8.7H, $J = 7.0$)

Synthesis of comb block copolymers with poly(styrene-

block-4-vinylpyridine) arms

CuBr (5.1 mg, 35.3 μmol) and a stir bar were added to a Schlenk flask which was connected to a Schlenk manifold. 4-Vinylpyridine (85.7g, 0.82 mol) was distilled under vacuum at 30 °C and added to the Schlenk flask. PMDETA (24.4 mg, 0.14 mmol) and the comb block copolymer with polystyrene arms (0.6 g, 0.236 μmol) in 30 mL of distilled 4-vinylpyridine were added, and the reaction was degassed by three freeze-pump-thaw cycles. The reaction vessel was then placed in a 50 °C oil bath and stirred for

1.5 h under flowing N₂. After cooling the reaction in an ice bath, it was filtered through a column filled with basic alumina (the upper layer) and silica gel (the lower layer) to remove copper complex. The polymer was precipitated into the mixture of hexane (400 mL) and Et₂O (400 mL). After decanting the solvents, the polymer was redissolved in 100 mL of CH₂Cl₂ and precipitated again into 600 mL of hexane. This procedure of purifying the polymer was repeated one more time to yield a peach-colored powder. M_n (cal) = 3,951,000 g mol⁻¹. ¹H NMR (CDCl₃): δ 0.88 (m, 4.8H), 1.61 (broad peak, 57.5H), 2.25 (t, 2.8H, *J* = 7.5 Hz), 3.11 (broad peak, 2H), 3.73 (broad peak, 2H), 3.85 (broad peak, 2H), 4.23 (broad triplet, 2H, *J* = 4.8 Hz), 6.66 (broad peak, 52.1H), 8.30 (broad peak, 9.7H).

Results and Discussion

Synthesis of Comb Block Copolymers with Arms

Composed of Poly(butyl acrylate)

Comb block copolymers with poly(butyl acrylate) arms were synthesized as shown in Figure 4.2. The backbone polymer was synthesized and hydrogenated in one pot as previously described, and poly(butyl acrylate) arms were grown from these polymers using ATRP (Table 4.1).^{114, 122, 123} Although butyl acrylate is readily polymerized under standard ATRP conditions, the synthesis of comb polymers were run under very dilute conditions to avoid cross-linking that led to insoluble polymers. In these polymerizations, the ratio of butyl acrylate to each ATRP initiator along the backbone was 3800:1 and the polymerizations went to approximately 1% to 6% conversions. Reactions at lower ratios of butyl acrylate to ATRP initiator resulted in cross-linked polymers.

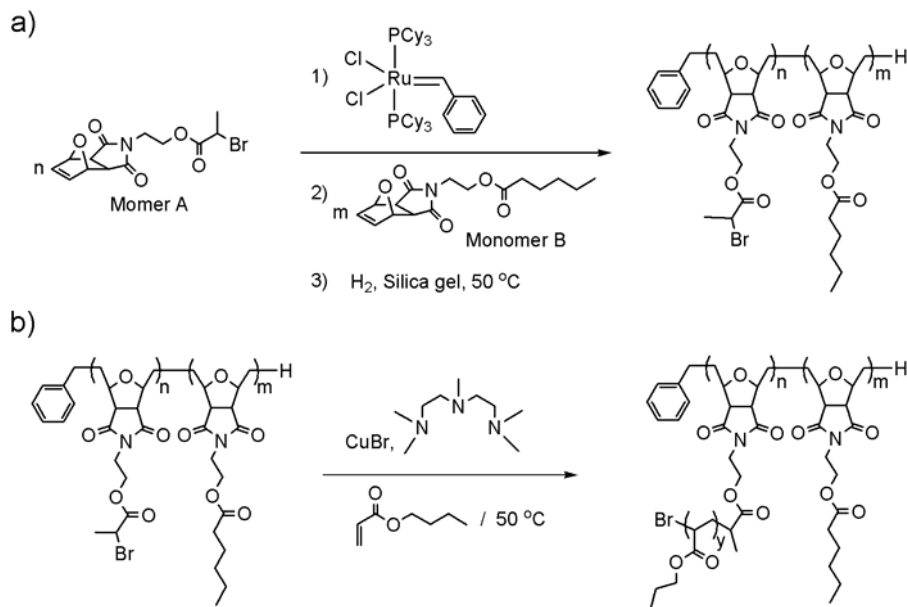


Figure 4.2 Synthesis of a comb block copolymer with poly(butyl acrylate) arms. a) How the backbone polymer was synthesized in one pot. b) How poly(butyl acrylate) arms were grown from the backbone polymer.

The physical characteristics of the polymers were measured using SEC connected to a laser light scattering apparatus to find the absolute molecular weight (Figure 4.3). We and others have shown that comb polymers characterized by SEC using poly(styrene) standards in the absence of light scattering underestimate the molecular weight by up to an order of magnitude.^{114, 122, 123, 144} The backbone polymers all possessed low PDIs which was consistent with prior work. The PDIs of the comb polymers were also reasonable and low which indicated that little to no cross-linking occurred during synthesis of the arms. Furthermore, the absence of any low molecular weight peaks demonstrated that poly(butyl acrylate) was only grown from the backbone polymer.

Table 4.1 Synthesis of comb block copolymers with poly(butyl acrylate) arms.

Entry	°A:B	Backbone Polymer			Comb Block Copolymer			Poly(butyl acrylate) Arms		
		^b Predicted M _n (kg mol ⁻¹)	^c Measured M _n (kg mol ⁻¹)	PDI	^d Predicted M _n (kg mol ⁻¹)	^e Measured M _n (kg mol ⁻¹)	PDI	^f R _z (nm)	^g Predicted M _n (g mol ⁻¹)	^h Calculated M _n (g mol ⁻¹)
1	200:2000	688	737	1.03	2,560	1,920	1.41	85	9,360	5,930
2					1,230	1,000	1.30	87	2,690	1,330
3					1,680	1,990	1.22	71	5,000	6,240
4					1,610	1,330	1.30	59	4,610	2,990
5					1,770	1,390	1.30	56	5,380	3,250
6	200:2000	688	699	1.02	1,480	1,360	1.02	46	3,970	3,330
7					2,360	2,490	1.50	89	8,330	8,940
8					1,280	1,670	1.32	65	2,950	4,860
9					1,300	1,400	1.27	63	3,080	3,500
10	150:1500	516	674	1.05	1,020	1,020	1.17	46	3,330	2,310
11					1,480	1,710	1.21	50	6,410	6,910
12	100:1500	499	453	1.02	922	1,070	1.10	41	4,220	6,120
13					665	651	1.08	39	1,670	1,980
14					1,690	1,260	1.22	42	11,900	8,090
15					1,840	1,940	1.23	47	13,500	14,900
16	500:1500	637	812	1.02	2,180	2,660	1.33	67	3,080	3,690

^aThe number of monomers A and B along the backbone polymer. ^bThe predicted molecular weight from the composition of the backbone. ^cThe molecular weight was measured by SEC with light scattering to find the absolute molecular weight. ^dThe predicted molecular weight from the composition of the backbone polymer and amount of poly(butyl acrylate) as determined by ¹H NMR spectroscopy. ^eThe root-mean-square radii of comb block copolymers measured by light scattering. ^fThe predicted molecular weight of the arms based on the known composition of the backbone polymer and the ¹H NMR spectra of the comb polymers. ^gThe calculated molecular weights based on the molecular weights of the comb and backbone polymers measured by SEC.

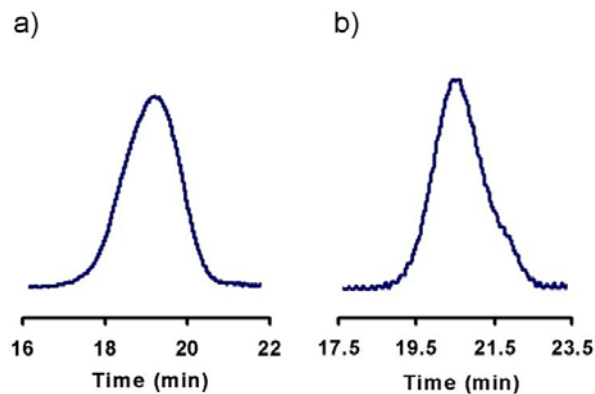


Figure 4.3 SEC micrographs of comb polymers with a) poly(butyl acrylate) arms and b) poly(lactic acid) arms.

The characterization of these comb polymers was further accomplished using ^1H NMR spectroscopy to provide more evidence for their structures. Because the molecular weights and compositions of the backbone polymers were known to a high degree of accuracy, the chemical composition of the comb polymer by ^1H NMR spectroscopy was used to predict the molecular weight of the comb polymer and the poly(butyl acrylate) arms. The predicted molecular weight for the comb polymers agreed well with the measured molecular weights which indicated that the comb polymer had the structure shown in Figure 4.2.

It was not possible to separate the arms from the backbone polymer to characterize them independently from the comb polymers, but the molecular weights of the arms were calculated by two different methods. First, the molecular weight of the arms were predicted based on the composition and measured molecular weight of the backbone polymer and the composition of the comb polymer as measured by ^1H NMR spectroscopy. For instance, it was straightforward to measure the number of moles of butyl acrylate that had polymerized relative to the number of moles of the backbone polymer by ^1H NMR spectroscopy, and from this data the “predicted Mn” for the arms were calculated (Table 4.1). The values for the “calculated Mn” for the arms were calculated from the composition and measured molecular weight of the backbone polymer and the molecular weight of the comb polymer. These numbers agreed well with each other and demonstrated that the arms had molecular weights of a couple thousand to nearly fifteen thousand grams per mole.

As a further proof for the structure of these polymers, the root-mean-square radii of the comb polymers were measured. These values were in the tens of nanometers which was consistent with other comb polymers with these molecular weights.^{114, 122, 123}

Synthesis of Comb Block Copolymers with Arms

Composed of Poly(lactic acid)

Comb block copolymers with arms composed of poly(lactic acid) were synthesized following a procedure reported earlier (Figure 4.4).^{120, 122} One critical aspect of this polymerization was that the backbone polymer was dissolved in methylmethoxyether with (3*S*)-*cis*-3,6-dimethyl-1,4-dioxane-2,5-dione prior to the addition of the Sn catalyst. In experiments where the backbone polymer was not first fully dissolved, a cross-linked polymer was isolated.

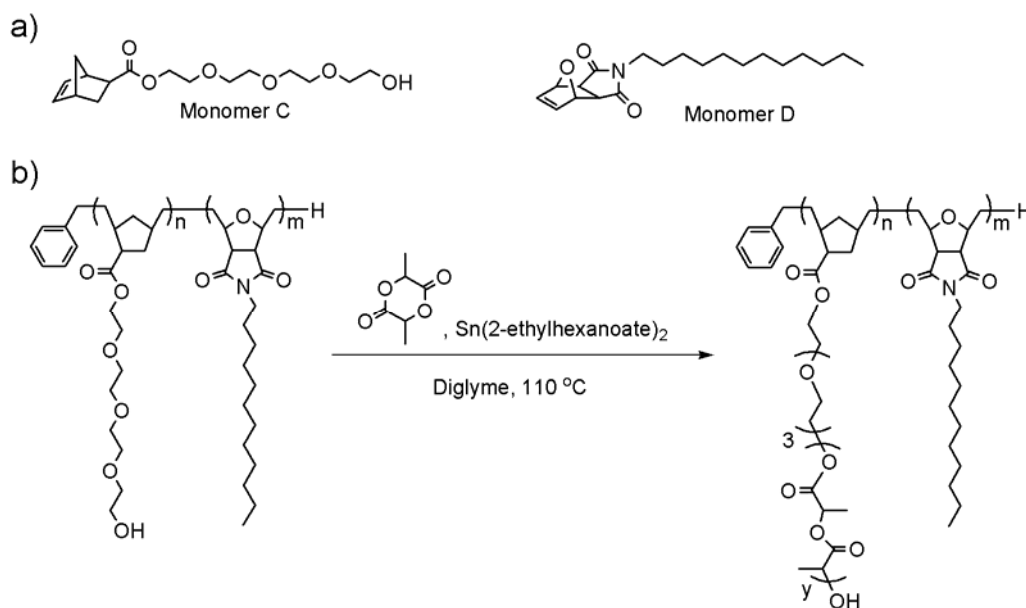


Figure 4.4 Synthesis of a comb block copolymer with poly(lactic acid) arms. a) The monomers that were used to synthesize the backbone polymer for comb polymers with poly(lactic acid) arms. b) The polymerization to yield comb block copolymers is shown.

In contrast to the polymerization of butyl acrylate, the polymerizations of *L*-lactide were run to near quantitative conversions. The reason for this difference is that two carbon centered radicals can combine to yield cross-links between comb polymers in the growth of poly(butyl acrylate) arms by ATRP, but the opportunities for cross-links in the synthesis of comb polymers with poly(lactic acid) arms is much lower. In fact, a transesterification reaction between poly(lactic acid) arms on comb polymers does not yield cross-links unless the reaction occurs with the ester bond in the backbone polymer (Figure 4.5).

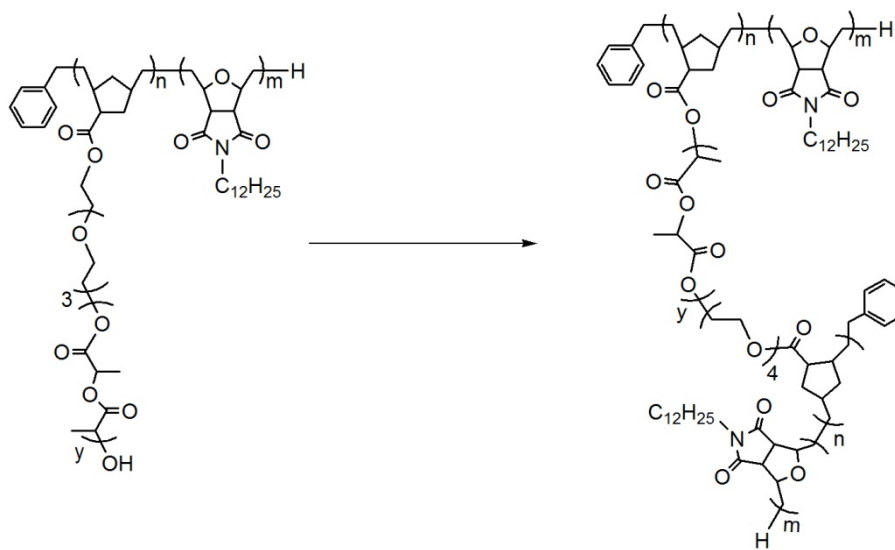


Figure 4.5 Cross-links between the comb polymers will only occur when transesterification occurs with the ester group in the backbone polymer.

Table 4.2 Synthesis of comb block copolymers with poly(lactic acid) arms.

Entry	°C:D	Backbone Polymer			Comb Block Copolymer				Poly(lactic acid) Arms	
		^b Predicted	^c Measured	PDI	^d Predicted	^e Measured	PDI	^g R _z (nm)	^f Predicted	^h Calculated
		M _n (kg mol ⁻¹)	M _n (kg mol ⁻¹)		M _n (kg mol ⁻¹)	M _n (kg mol ⁻¹)			M _n (g mol ⁻¹)	M _n (g mol ⁻¹)
1	100:1000	367	519	1.38	555	838	1.13	39	1,870	3,190
2					814	818	1.14	41	4,470	2,290
3					1,450	1,770	1.22	93	10,800	12,600
4					929	1,100	1.22	56	5,620	5,810
5					900	952	1.10	40	5,330	4,330
6	100:1000	367	396	1.23	999	1,110	1.19	54	6,340	7,140
7					913	1,030	1.19	48	5,480	6,300
8					567	524	1.30	44	2,020	1,280
9	150:1500	547	616	1.37	1,290	1,170	1.17	40	4,900	3,700
10					1,480	1,290	1.29	45	6,230	4,510
11					789	764	1.20	46	1,590	987
12					874	734	1.09	29	2,160	787
13	100:2000	698	679	1.33	1,250	1,560	1.23	51	5,480	8,850
14					919	1,460	1.22	55	2,160	7,770

^aThe number of monomers C and D along the backbone polymer. ^bThe predicted molecular weight from the composition of the backbone. ^cThe molecular weight was measured by SEC with light scattering to find the absolute molecular weight. ^dThe predicted molecular weight based on the composition of the backbone and amount of poly(lactic acid) as determined by ¹H NMR spectroscopy. ^eThe root-mean-square radii of comb block copolymers are shown. ^fThe predicted molecular weights based on the known composition of the backbone polymer and the ¹H NMR spectra of the comb polymers. ^gThe calculated molecular weights based on the molecular weights of the comb and backbone polymers measured by SEC.

The characterization of comb polymers with poly(lactic acid) arms possessed many of the same challenges as comb polymers with poly(butyl acrylate) arms (Table 4.2). The biggest limitation was that the arms could not be separated and characterized independent of the backbone polymer. The molecular weight of the comb polymers was measured using SEC with light scattering detectors and it was also calculated using the composition and molecular weight of the backbone polymer and the composition of the comb polymers by ¹H NMR spectroscopy. The calculated and measured molecular weights for the comb polymers agreed with a reasonable degree of accuracy. The

predicted and calculated molecular weights for the poly(lactic acid) arms were also in reasonable agreement and demonstrated that these polymers possessed the structures shown in Figure 4.4. The SEC micrographs of the comb polymers did not show a low molecular peak which demonstrated that the poly(lactic acid) grew from the backbone polymer (Figure 4.3).

Synthesis of Comb Block Copolymers with Block Copolymer Arms

To further extend the types and complexities of comb polymers that could be synthesized, two comb polymers with arms composed of block copolymers were synthesized (Figure 4.6). The starting comb polymers contained polystyrene arms and were synthesized and characterized by SEC as described previously. The ends of the polystyrene arms possessed ATRP initiators that were used to grow poly(vinylpyridine) to demonstrate how to introduce more functionality into the comb polymers.

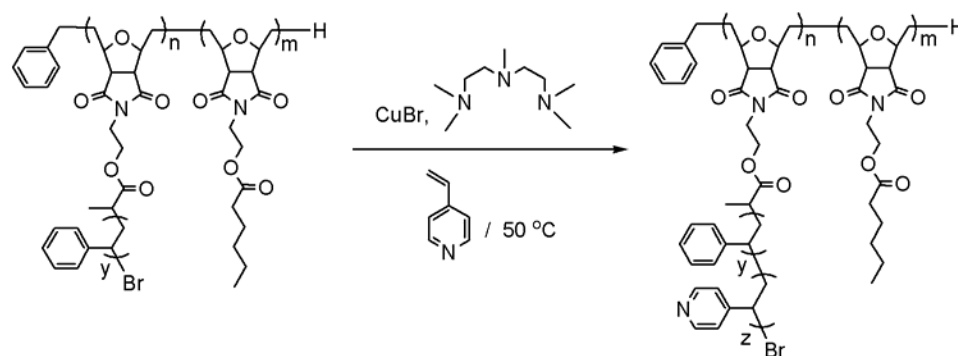


Figure 4.6 Vinylpyridine was polymerized from comb block copolymers with poly(styrene) arms.

The polymerization of vinylpyridine was challenging due to the formation of cross-links that led to insoluble comb polymers. To overcome these cross-links, the initial comb polymer was dissolved in a large excess of vinylpyridine prior to the introduction of Cu and PMDETA. Furthermore, the ratio of vinylpyridine to ATRP initiator was 23,000:1 which represented a six fold increase from the ratio of butyl acrylate to ATRP initiator used in the synthesis of comb polymers with poly(butyl acrylate) arms. After 1.5 h of heating at 50 °C, the reaction was quenched and the product was isolated as a solid. The polymer was repeatedly precipitated and filtered to ensure that no free poly(vinylpyridine) was present.

Similar to reports by others, the characterization of the final comb polymer by SEC was not possible because it did not pass through the SEC columns.^{145, 146} The lack of a peak in the SEC further demonstrated that the vinylpyridine had grown from the comb polymer because the starting comb polymer with poly(styrene) arms had very strong peaks both in the light scattering and refractive index detectors. The composition of the final polymer was found by ¹H NMR spectroscopy and the molecular weight of the comb polymer was calculated using this spectrum and the molecular weight and composition of the initial comb polymer. Two different comb polymers were used as starting materials and two different final polymers were produced. The first comb polymer that was used as a starting material had a M_n of 2,550,000 g mol⁻¹ and polystyrene arms with a M_n of 13,500 g mol⁻¹. After polymerization of vinylpyridine, the comb polymer was calculated to have a molecular weight of 3,500,000 g mol⁻¹ and the M_n of each poly(styrene-*b*-vinylpyridine) arm was 19,800 g mol⁻¹. The second comb polymer that was used as a starting material possessed a M_n of 1,360,000 g mol⁻¹ and poly(styrene) arms with M_n of 5,600 g mol⁻¹. After polymerization of vinylpyridine, the comb polymer was calculated to possess a M_n of 1,450,000 g mol⁻¹ and the M_n of each poly(styrene-*b*-vinylpyridine) arm was 6,300 g mol⁻¹.

Assembly of Comb Triblock Copolymers with Polystyrene Arms

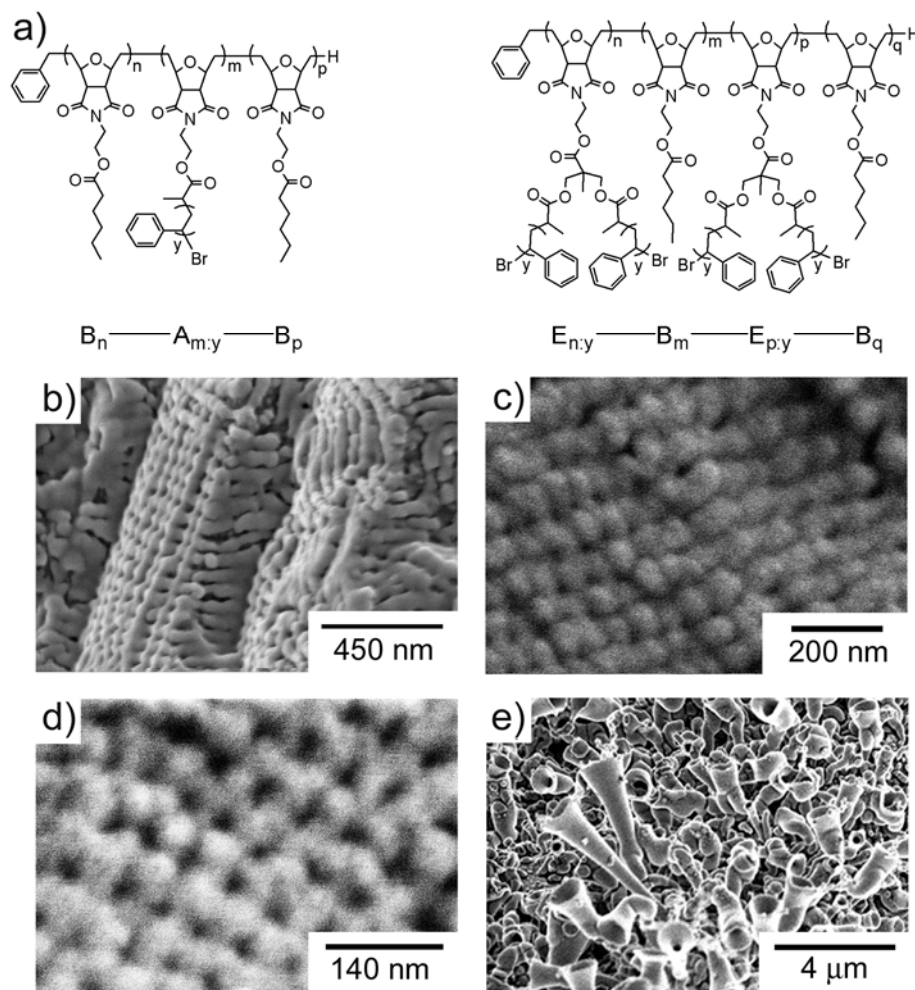


Figure 4.7 Comb block copolymers and their morphologies. a) Two examples of comb polymers with poly(styrene) arms that were assembled in the solid state. The capitalized letters refers to the monomer units along the backbone and the subscript letters refer to the degree of polymerization along the backbone and polystyrene arms as shown. b) An SEM micrograph of an assembled array of a comb polymer with composition of $B_{500}A_{100:3950}B_{500}$ is shown. c) and d) SEM micrographs of an assembled array of a comb polymer with a composition of $A_{50:5190}B_{1000}A_{50:5190}$ is shown. e) A SEM micrograph of an assembled array of a comb polymer with composition of $B_{500}A_{100:4710}B_{500}$ is shown.

The synthesis of a series of comb tri- and tetra-block copolymers with arms composed of polystyrene were described previously (Figure 4.7).¹¹⁴ These polymers were

synthesized in a similar manner to the comb polymers with poly(butyl acrylate) arms in a two pot approach where the backbone was synthesized first followed by the ATRP of styrene to yield the final comb polymers.

These polymers readily assembled in the solid state into ordered morphologies. Although some of the morphologies were easily understood based on their SEM micrographs, many of these polymers assembled into more complex morphologies. The complexity was expected based on analogies to the morphologies assembled from linear triblock copolymers which are often very interesting and complex. In Figure 4.7 four of the SEM micrographs are shown to illustrate the complexity of these assemblies and many more are provided in the supporting information. The complexity of the morphologies exceeded our ability to characterize them by SEM; we provide these micrographs to illustrate that many complex morphologies are possible.

Conclusions

The synthesis of three new sets of comb block copolymers were reported that expanded the complexity and functional groups that could be realized with this architecture. The synthesis and characterizations of comb polymers with poly(butyl acrylate), poly(lactic acid), poly(styrene-*b*-vinylpyridine) arms were described and demonstrate that a wide range of these polymers can be realized. The challenging synthesis of comb polymers with block copolymer arms was overcome by the high dilution of the comb polymers in vinylpyridine followed by an ATRP polymerization. To demonstrate some potential applications of these polymers, the assembly in the solid state of comb tri- and tetrablock copolymers with poly(styrene) arms was described. These polymers represent a new approach to achieve the ordered assembly of complex morphologies in the solid state with domain sizes exceeding 100 nm. The use of the new, functional polymers described in this paper will open up new possibilities for their applications.

Supporting Information

Series of Comb Tri- and Tetra-Block Copolymers with
Polystyrene Arms

Structure and Characterization

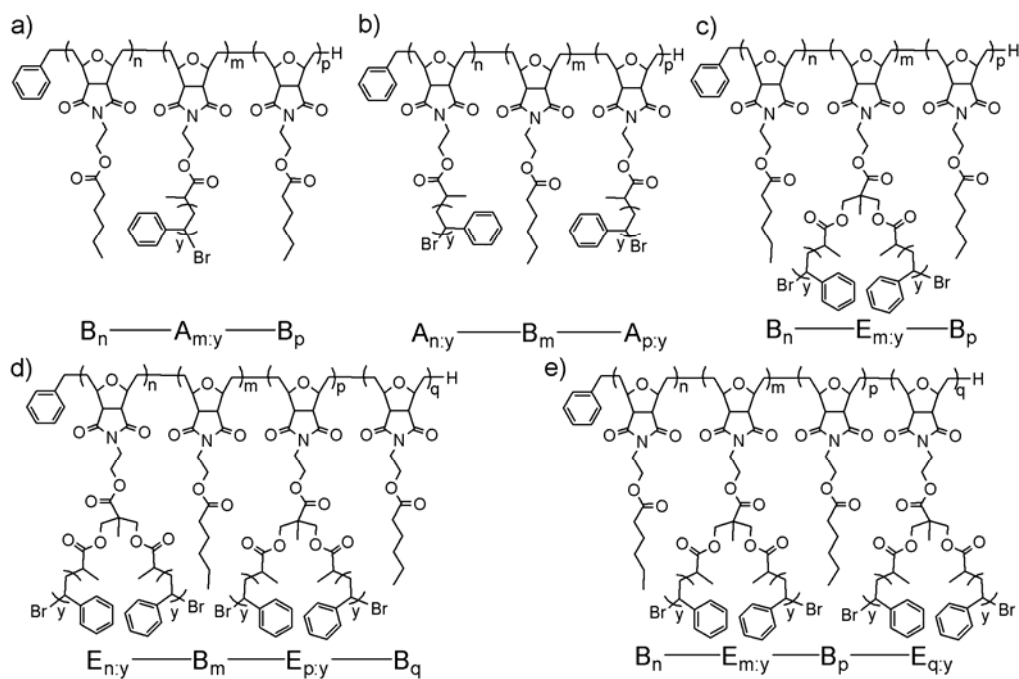


Figure 4.8 Structure of multi-block comb polymers.

Table 4.3 Characterization of multi-block comb polymers.

Entry	^a Backbone Polymer	^b Predicted M_n (kg mol ⁻¹)	^c Measured M_n (kg mol ⁻¹)	PDI	R_z (nm)	R_h (nm)	^d Arms M_n (g mol ⁻¹)	^d PDI of arms
1	B ₅₀₀ A _{100:1430} B ₅₀₀	487	552	1.14	56.5	45.5	1,430	1.14
2	B ₅₀₀ A _{100:4630} B ₅₀₀	807	1,270	1.27	41.2	26.8	4,630	1.02
3	B ₅₀₀ A _{100:3950} B ₅₀₀	739	756	1.15	51.6	22.4	3,950	1.04
4	B ₅₀₀ A _{100:11400} B ₅₀₀	1,480	2,080	1.16	37.2	26.0	11,400	1.02
5	A _{50:5190} B ₁₀₀₀ A _{50:5190}	863	614	1.21	38.6	21.7	5,190	1.28
6	B ₅₀₀ E _{100:2740} B ₅₀₀	917	753	1.16	29.3	20.0	2,740	1.10
7	B ₅₀₀ E _{100:6810} B ₅₀₀	1,730	1,590	1.17	31.0	22.7	6,810	1.18
8	B ₅₀₀ E _{100:7280} B ₅₀₀	1,830	1,510	1.14	27.8	21.5	7,280	1.06
9	E _{50:1830} B ₁₀₀₀ E _{50:1830}	732	477	1.20	33.9	19.7	1,830	1.20
10	E _{50:4700} B ₁₀₀₀ E _{50:4700}	1,310	983	1.17	38.6	21.7	4,700	1.04
11	E _{50:4750} B ₁₀₀₀ E _{50:4750}	1,320	726	1.17	32.4	18.5	4,750	1.13
12	E ₂₀ B ₂₀₀ E ₁₀ B ₂₀₀	210	214	1.15	12.0	10.8		
13	E _{20:4050} B ₂₀₀ E _{10:4050} B ₂₀₀	385	314	1.18	21.2	13.6	4,050	1.08
14	E ₁₀₀ B ₇₅₀ E ₁₀ B ₂₀₀	520	528	1.19	31.8	19.4		
15	B ₂₀₀ E _{10:3820} B ₇₅₀ E _{100:3820}	1,080	820	1.13	30.0	19.1	3,280	1.19
16	E ₁₀₀ B ₇₅₀ E ₁₀ B ₂₀₀	1,500	1,720	1.15	33.9	22.2		
17	B ₅₀₀ A _{100:3240} B ₅₀₀	656	655	1.03	22.3	17.6	3,240	1.06
18	B ₃₀₀ A _{100:8710} B ₃₀₀	1,030	1,300	1.10	24.1	16.6	8,710	1.02
19	B ₃₀₀ A _{100:13200} B ₃₀₀	1,190	1,180	1.13	29.7	19.5	13,200	1.02
20	B ₅₀₀ A _{100:7420} B ₅₀₀	1,200	1,020	1.06	24.8	17.9	7,420	1.05
21	B ₅₀₀ A _{100:3800} B ₅₀₀	750	581	1.08	24.4	16.8	3,800	1.04
22	B ₅₀₀ A _{100:4710} B ₅₀₀	875	614	1.08	20.7	16.5	4,710	1.04

^aThe letters refer to the monomers. The subscripts refer to the degree of polymerization of each monomer and the styrene in the arms as shown in Figure 4.1. ^bThe predicted molecular weight of the comb polymers from the known molecular weight of the backbone polymer and the ratio of styrene to monomers in the backbone as measured by ¹H NMR spectroscopy. ^cMeasured by SEC with light scattering and RI detectors. ^dThe molecular weight and PDI of the arms were found by cleaving the arms from the backbone polymer and characterizing them by SEC as described in our prior work.

Self-assembly and characterization of multi-block

copolymer films

Polymers were dissolved in CH₂Cl₂ (9 mL) at concentrations from 8 to 30 mg mL⁻¹. The solvent was allowed to vaporize at room temperature to form thin films inside glass vials. These films were exposed to CH₂Cl₂ under vacuum for three days. The films were frozen in liquid nitrogen, fractured, mounted on an aluminum holder with the fractured interior facing upward and then stained with RuO₄ vapor. The samples were

imaged by scanning electron microscopy (SEM) on a Hitachi S-4800 at accelerating voltages between 2 to 5 kV.

SEM Micrographs for the Polymers in Table 4.3

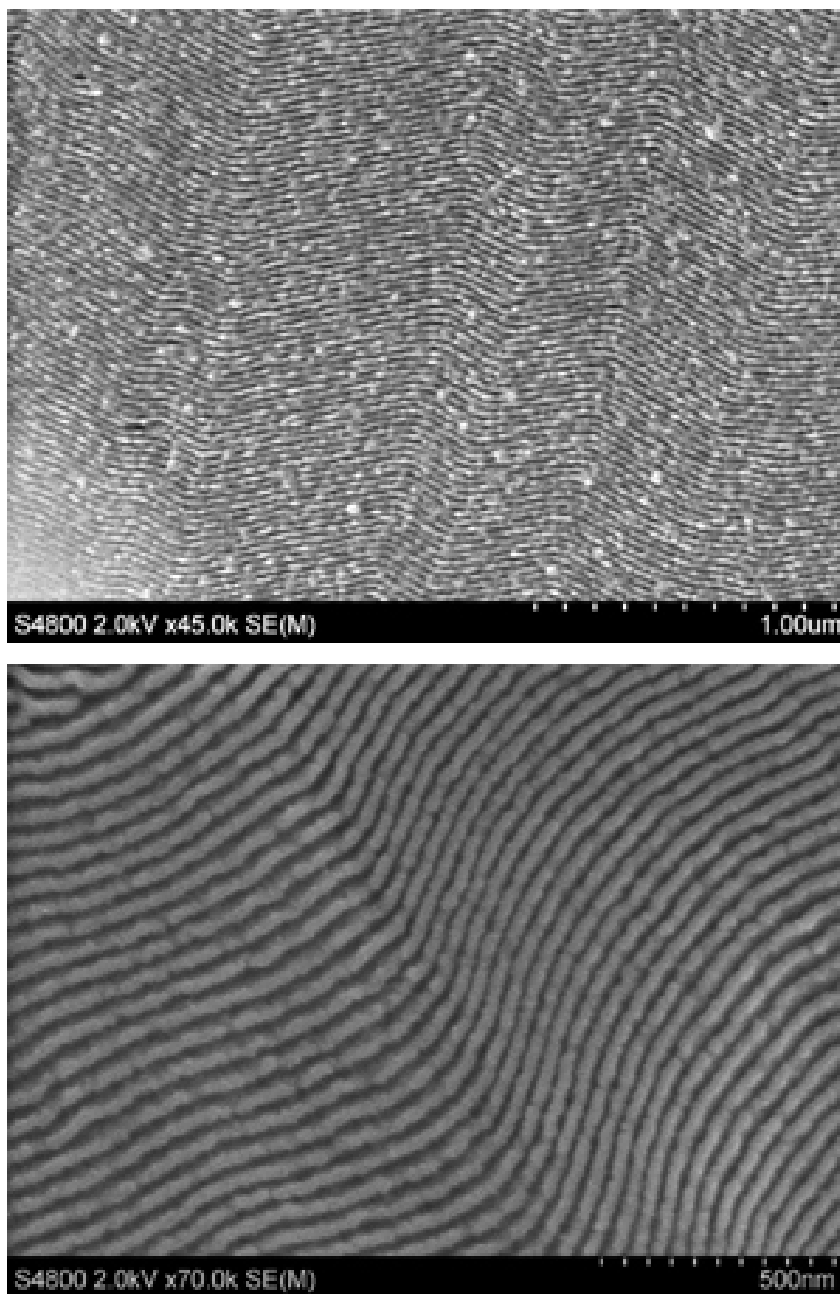


Figure 4.9 SEM micrographs of entry 1.

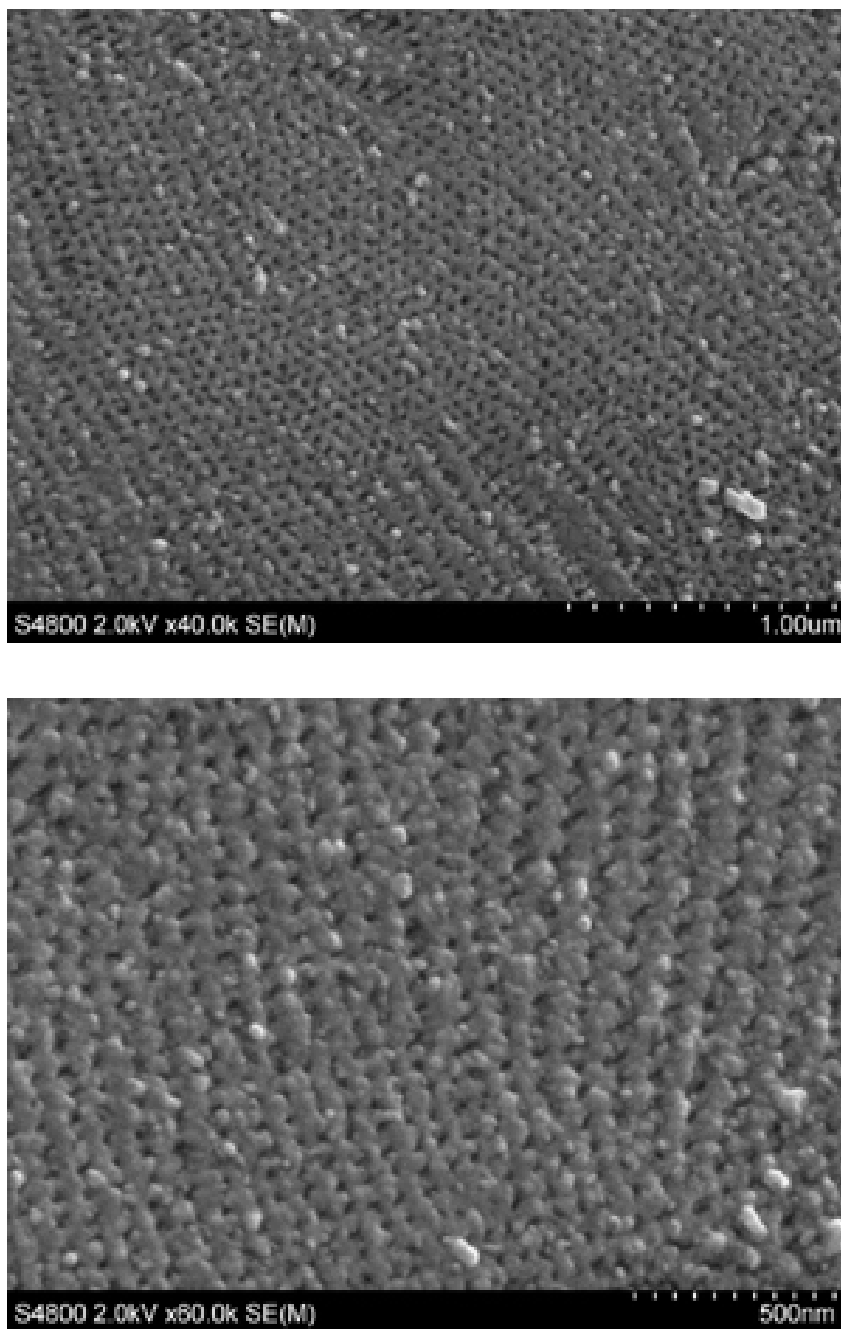


Figure 4.10 SEM micrographs of entry 2.

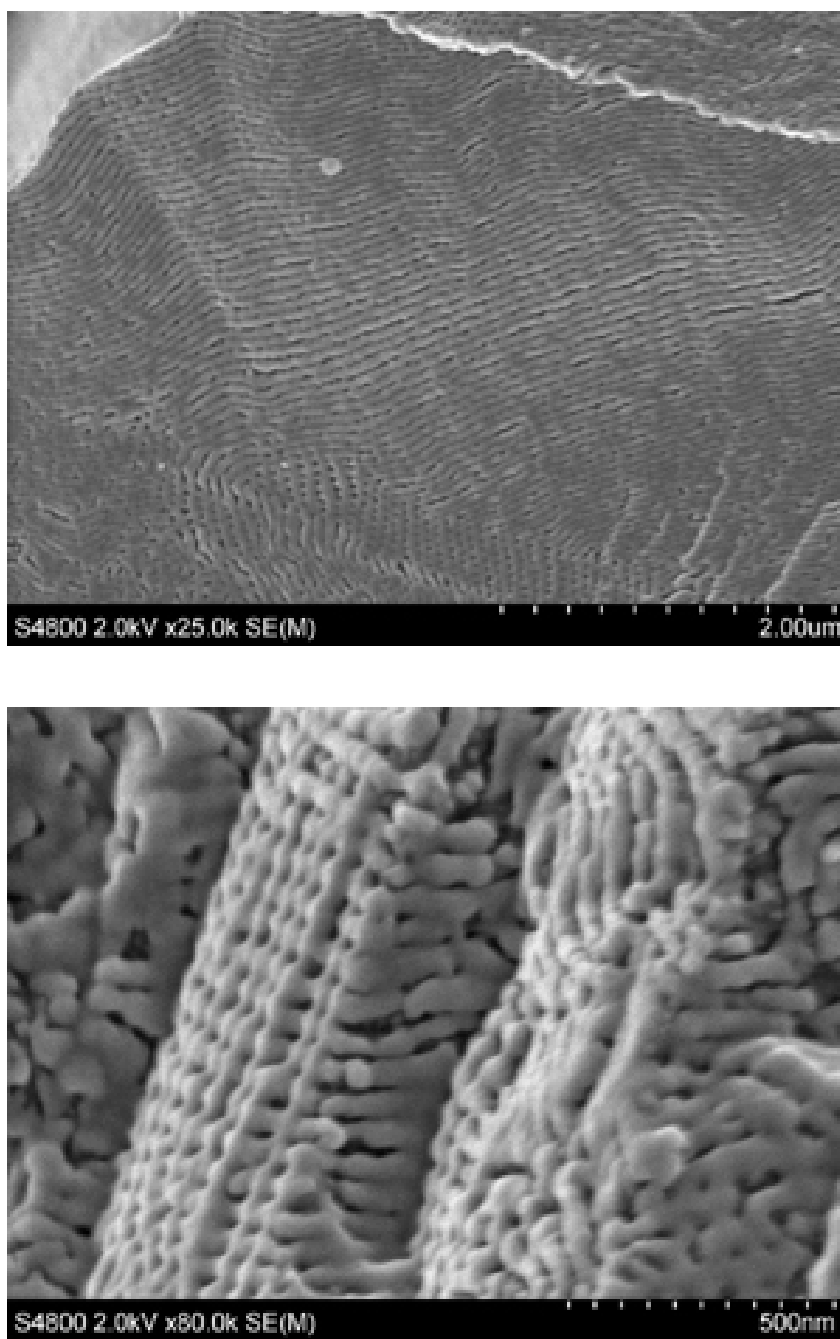


Figure 4.11 SEM micrographs of entry 3.

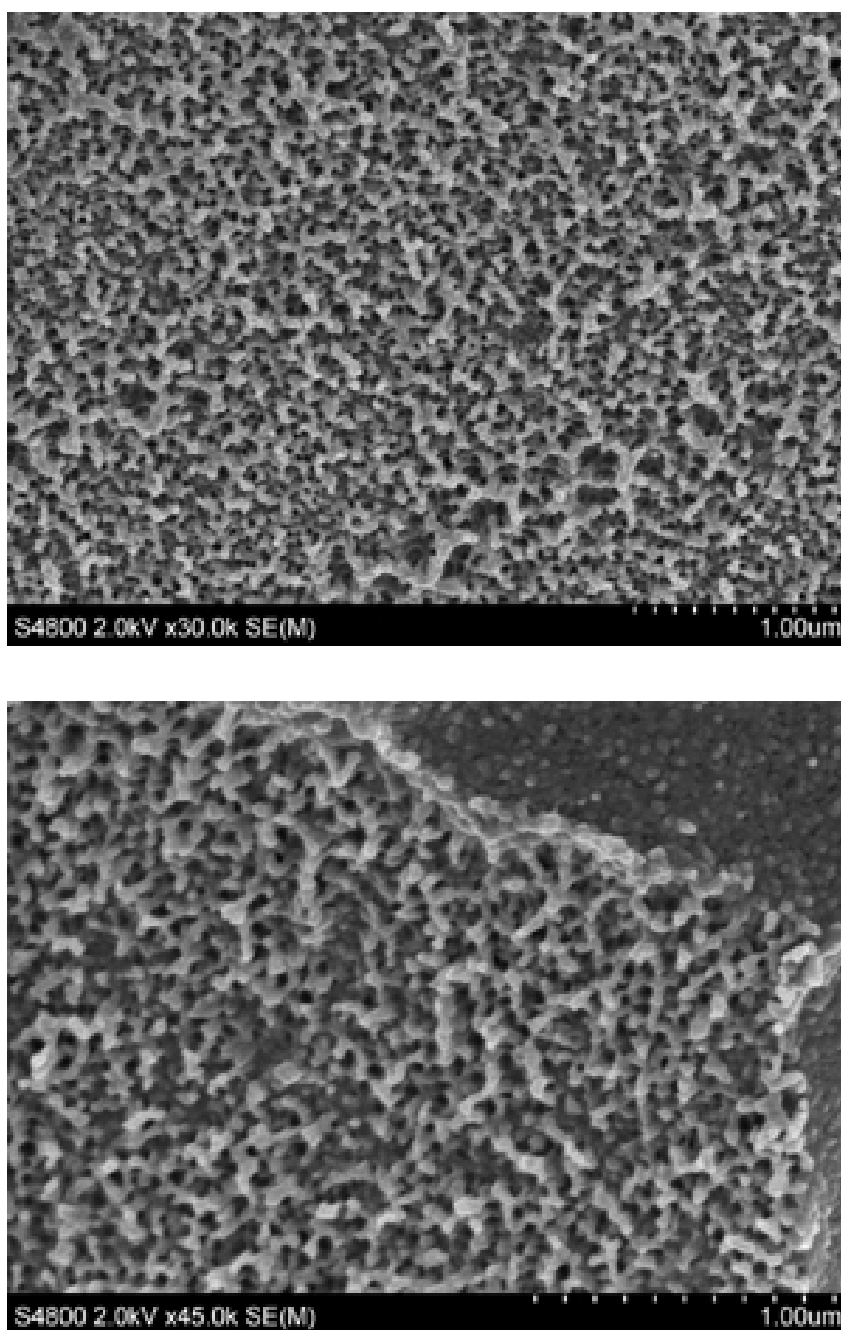


Figure 4.12 SEM micrographs of entry 4.

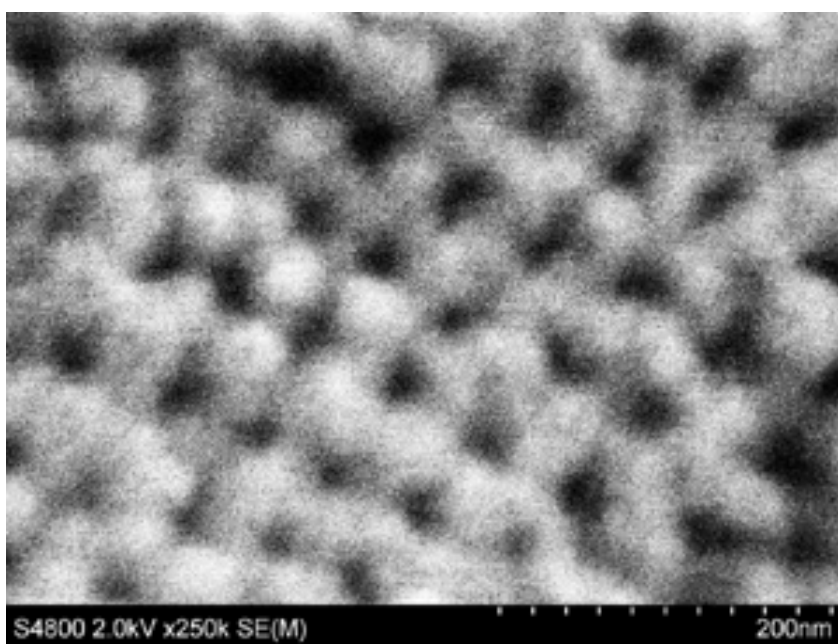
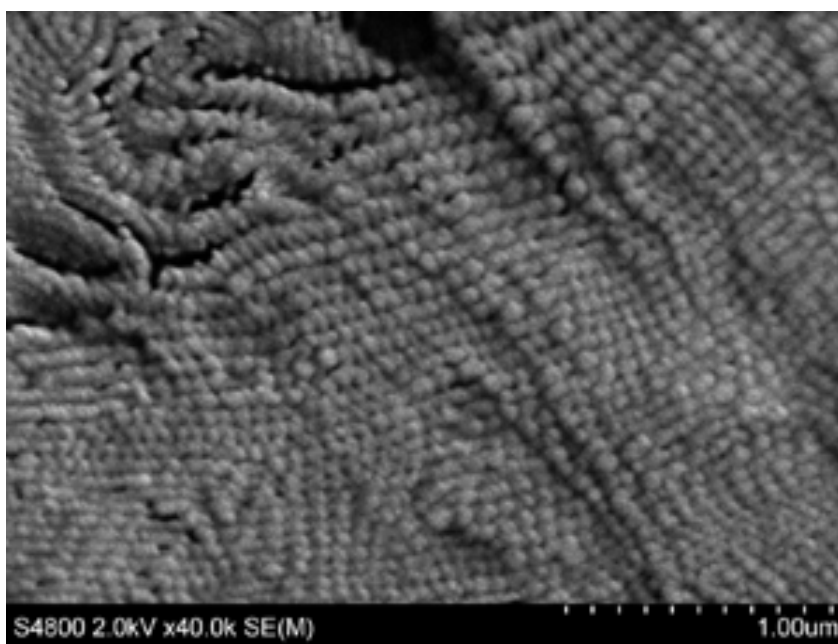


Figure 4.13 SEM micrographs of entry 5.

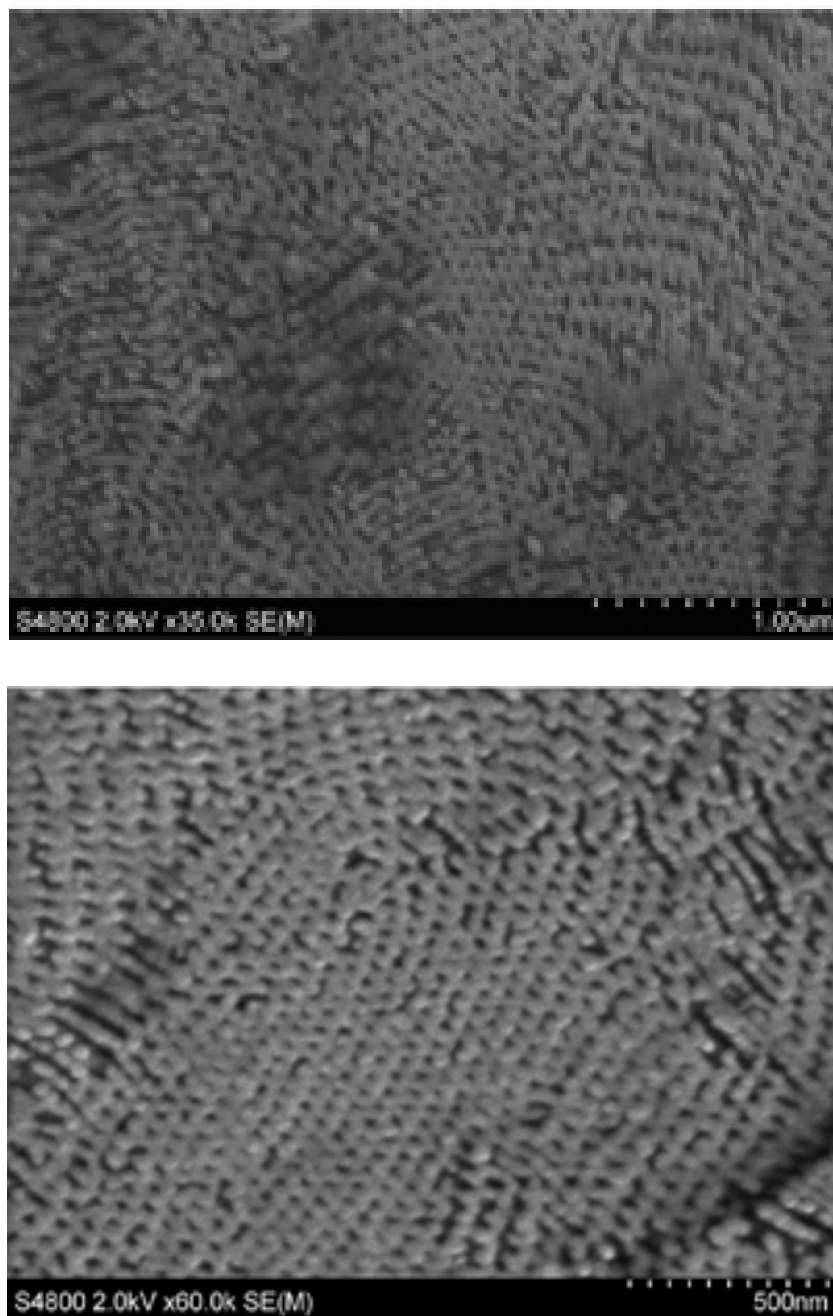


Figure 4.14 SEM micrographs of entry 6.

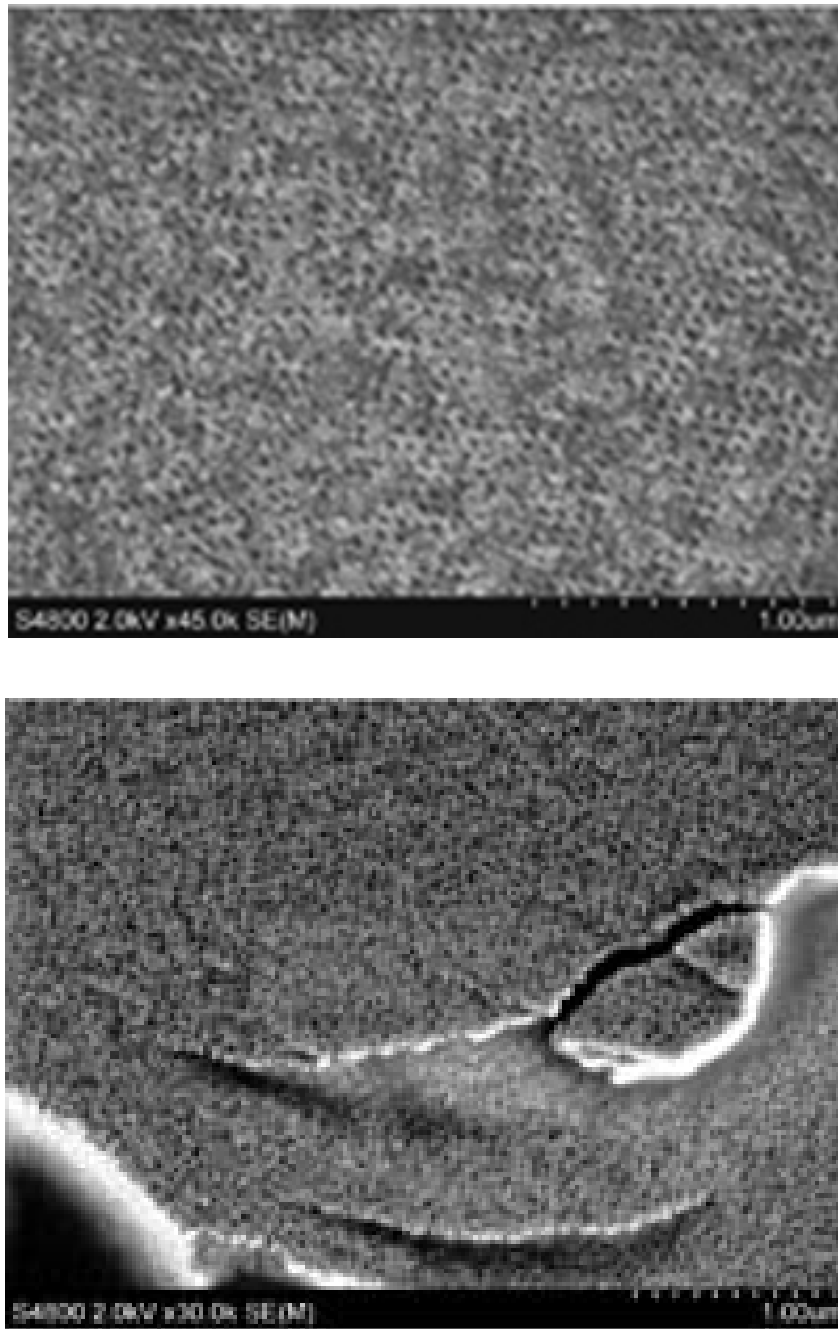


Figure 4.15 SEM micrographs of entry 7.

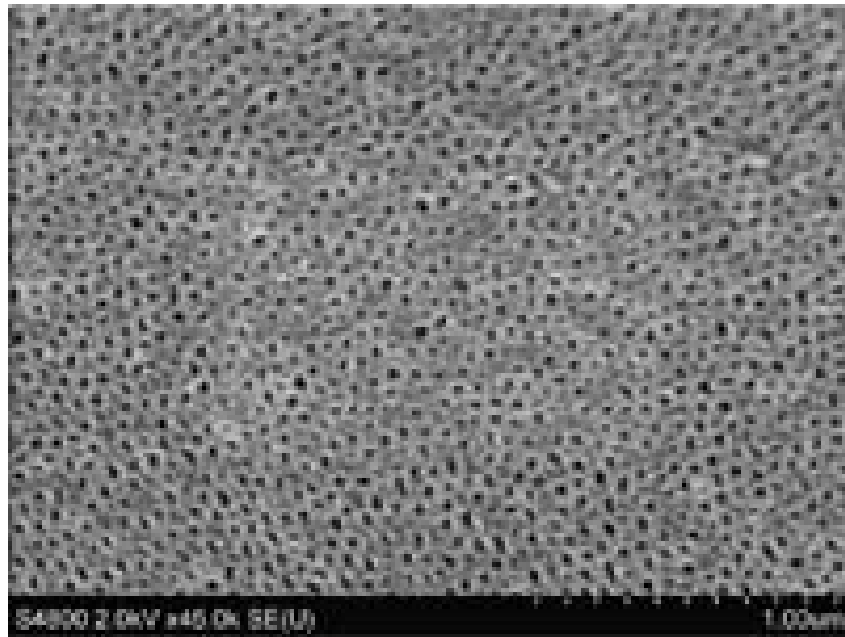
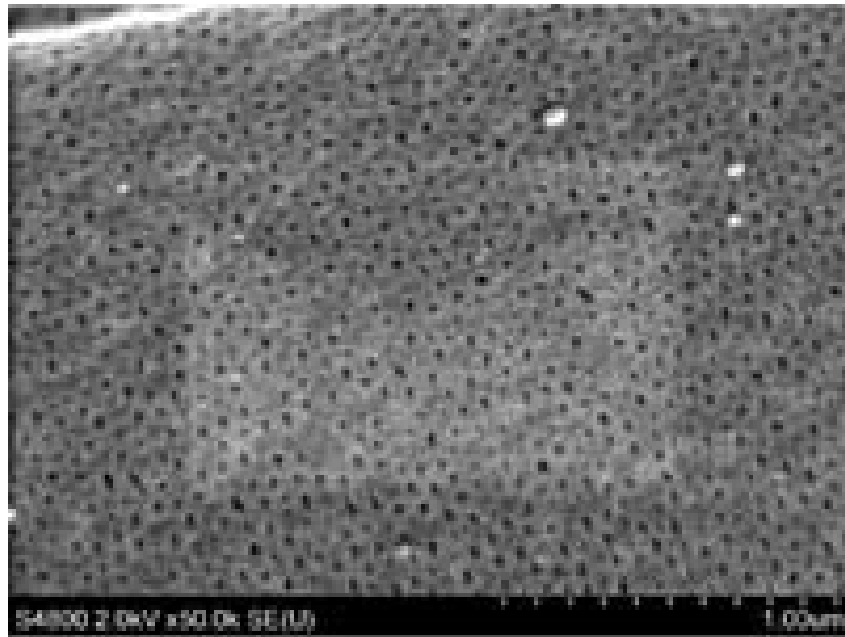


Figure 4.16 SEM micrographs of entry 8.

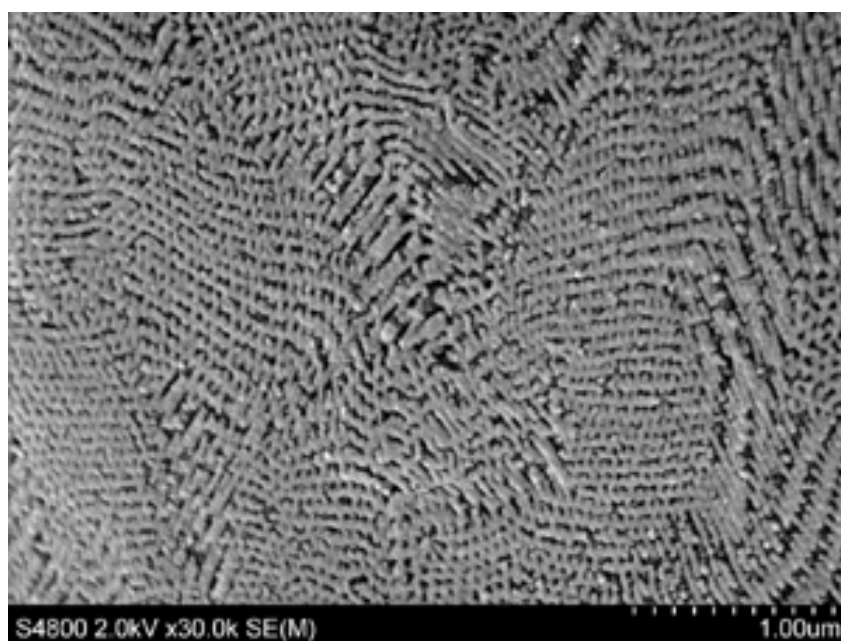
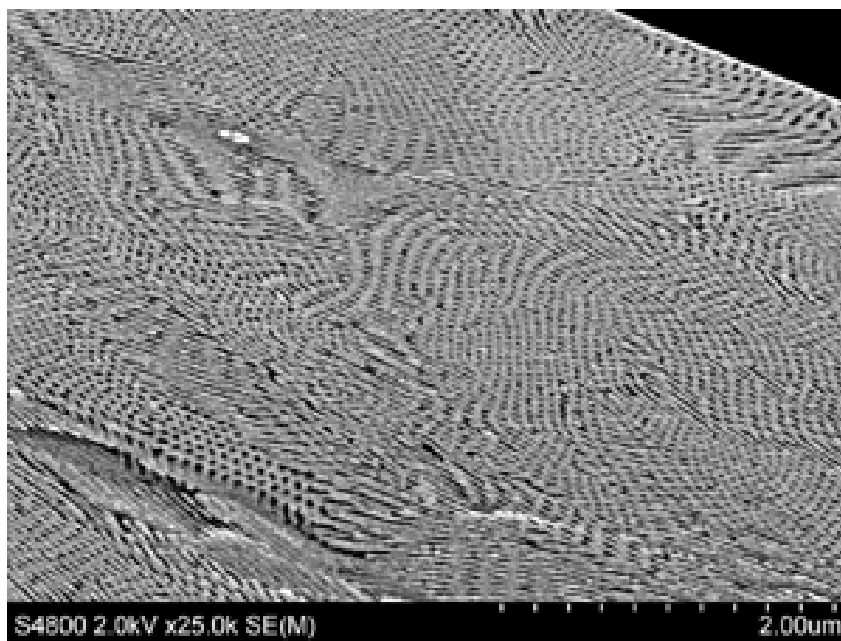


Figure 4.17 SEM micrographs of entry 9.

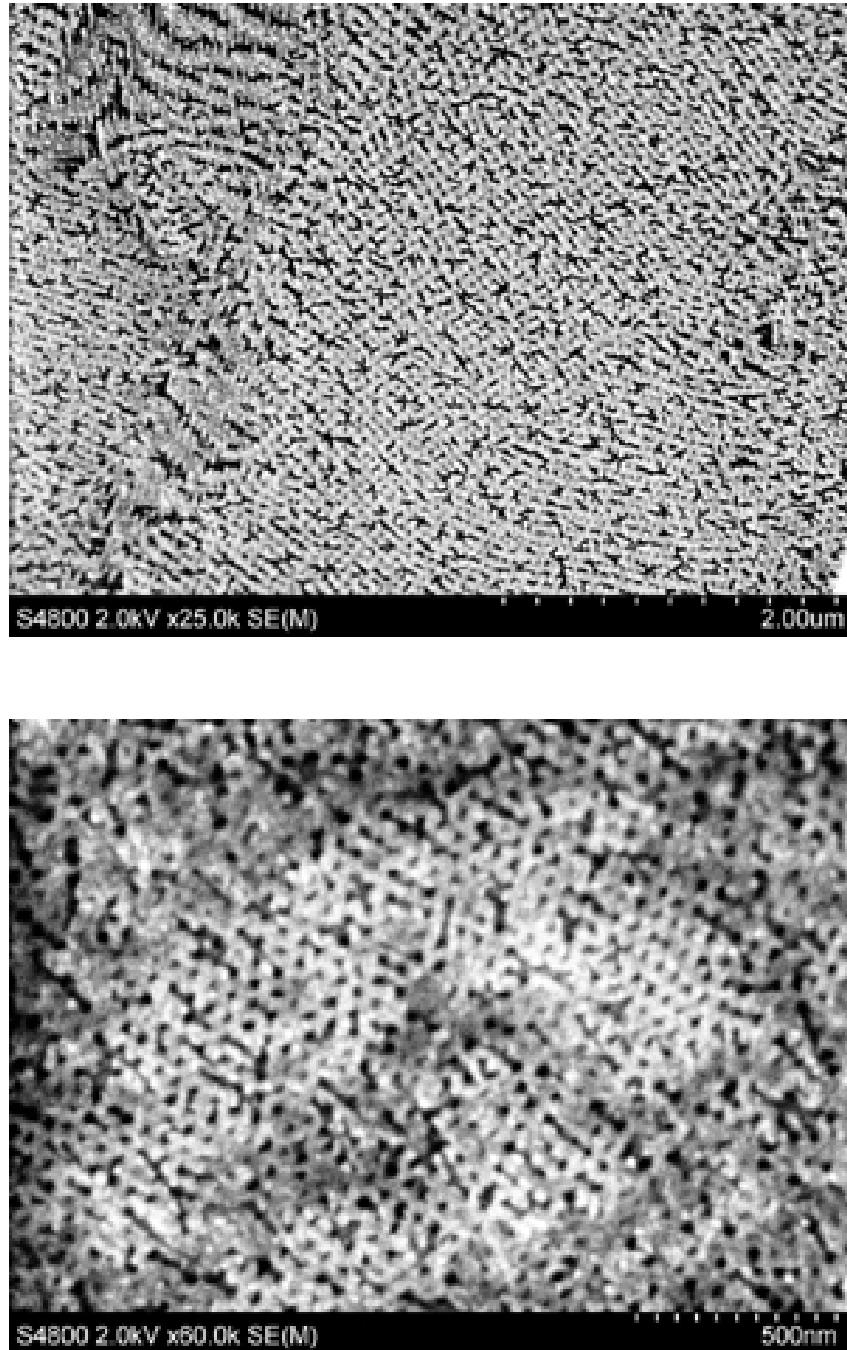


Figure 4.18 SEM micrographs of entry 10.

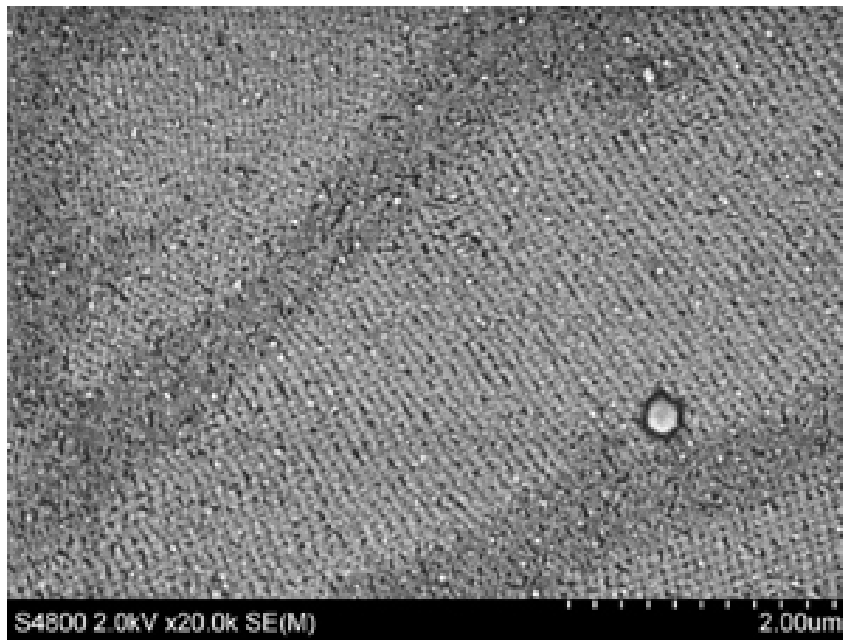


Figure 4.19 The SEM micrograph of entry 11.

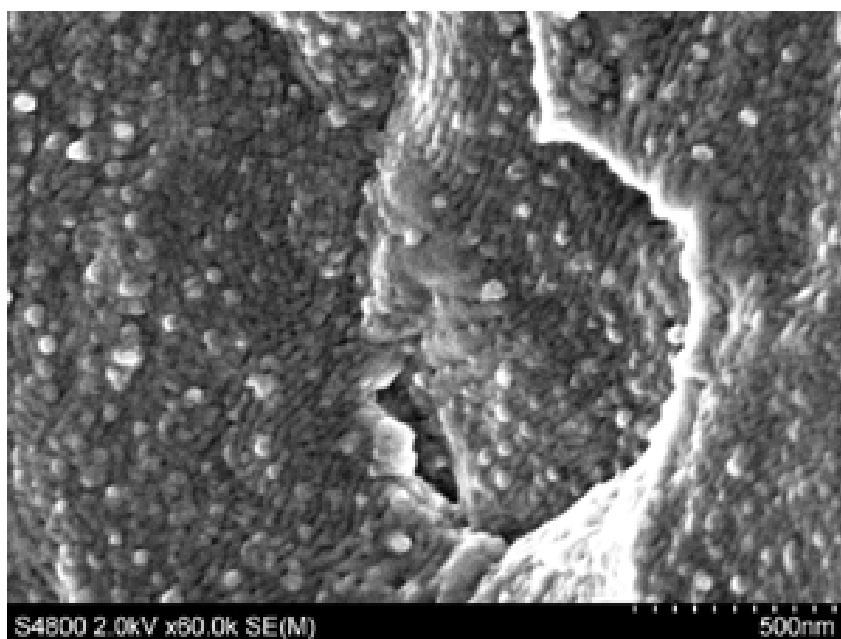
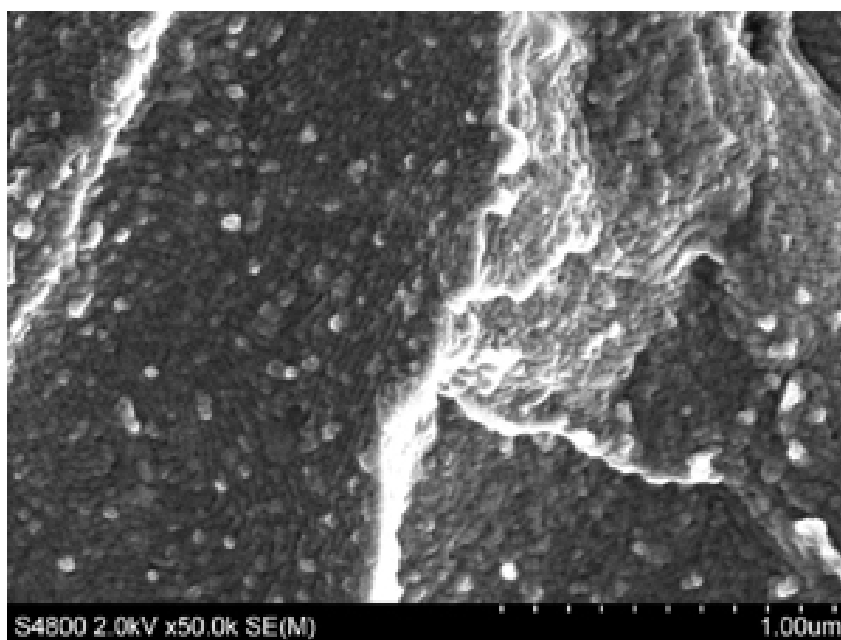


Figure 4.20 SEM micrographs of entry 12.

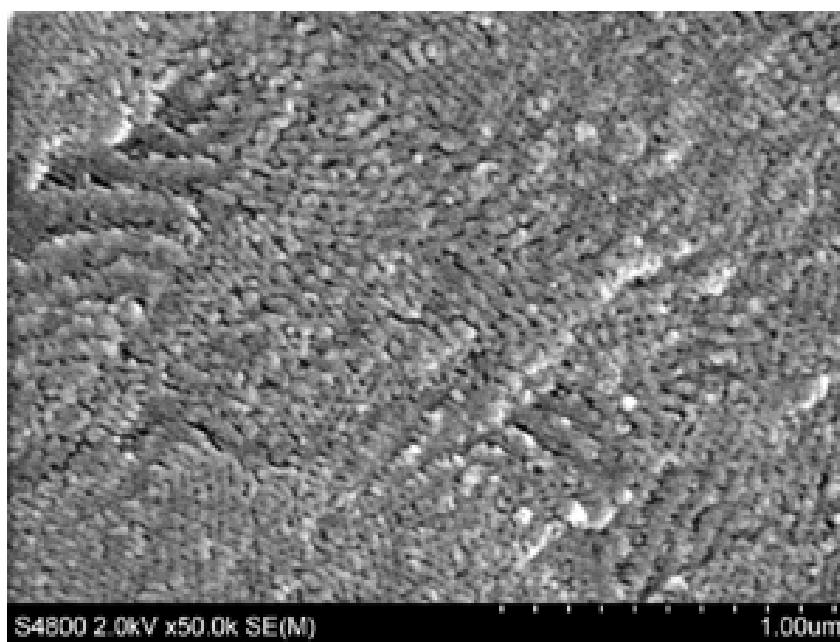


Figure 4.21 SEM micrographs of entry 13.

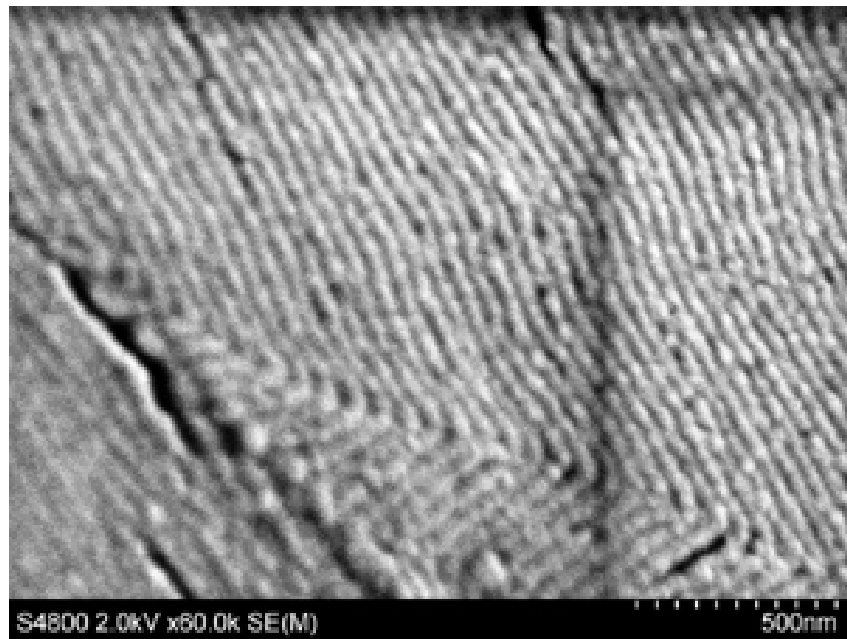
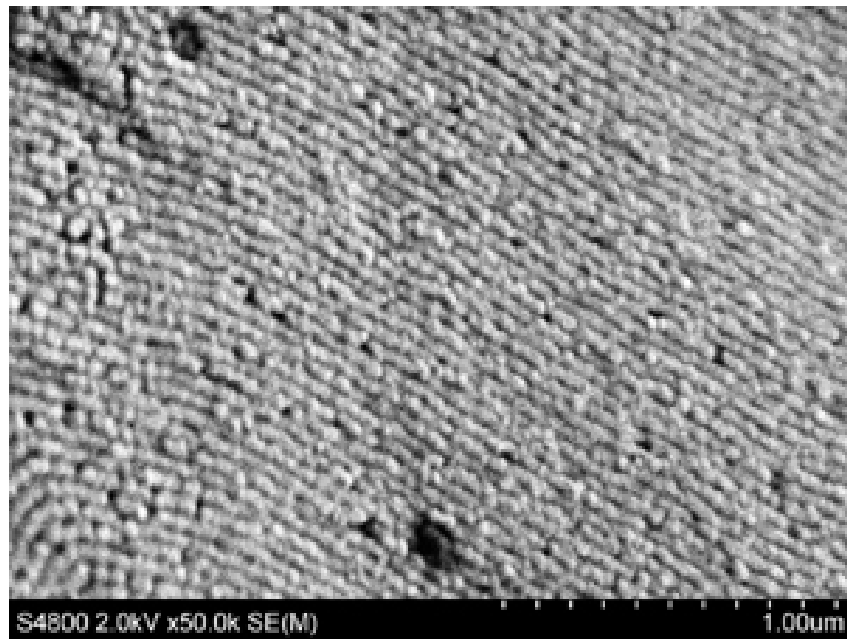


Figure 4.22 SEM micrographs of entry 14.

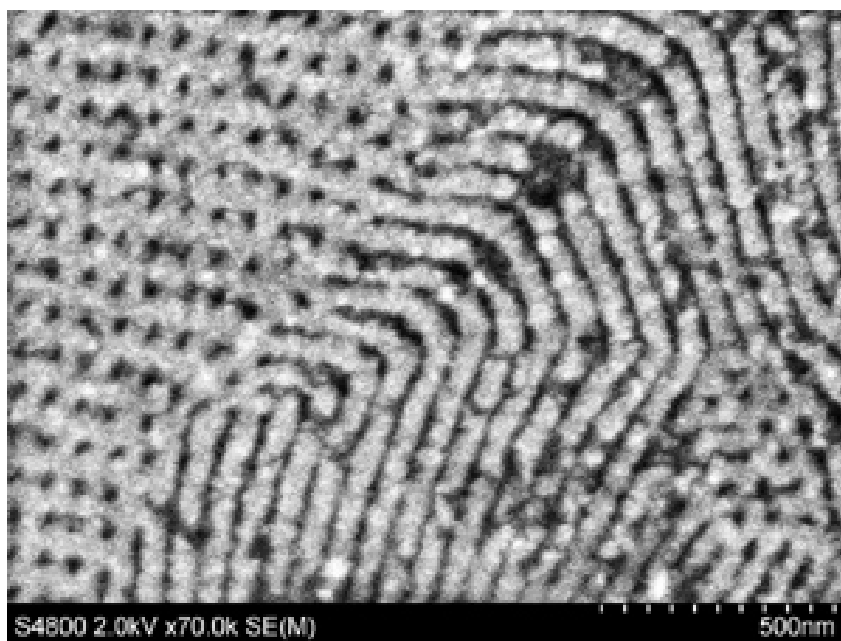
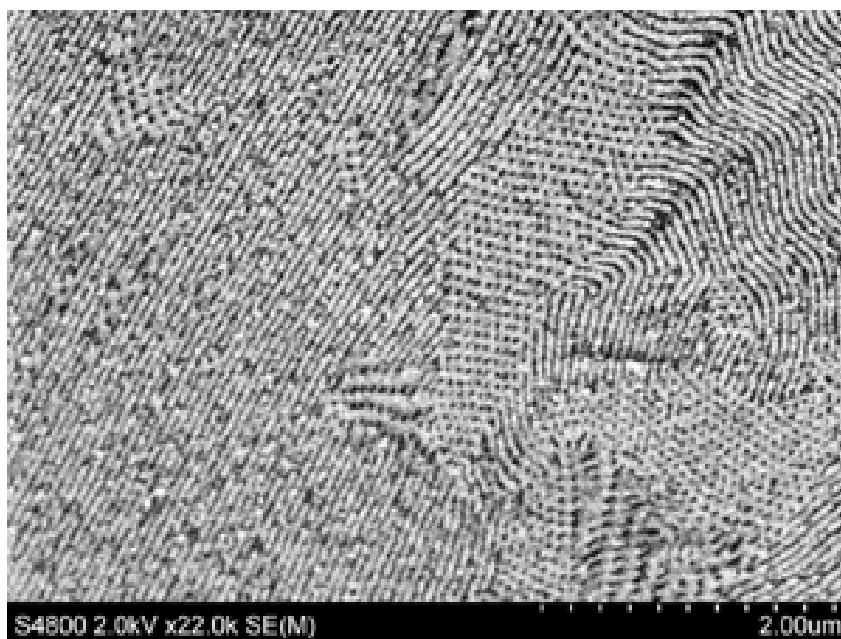


Figure 4.23 SEM micrographs of entry 15.

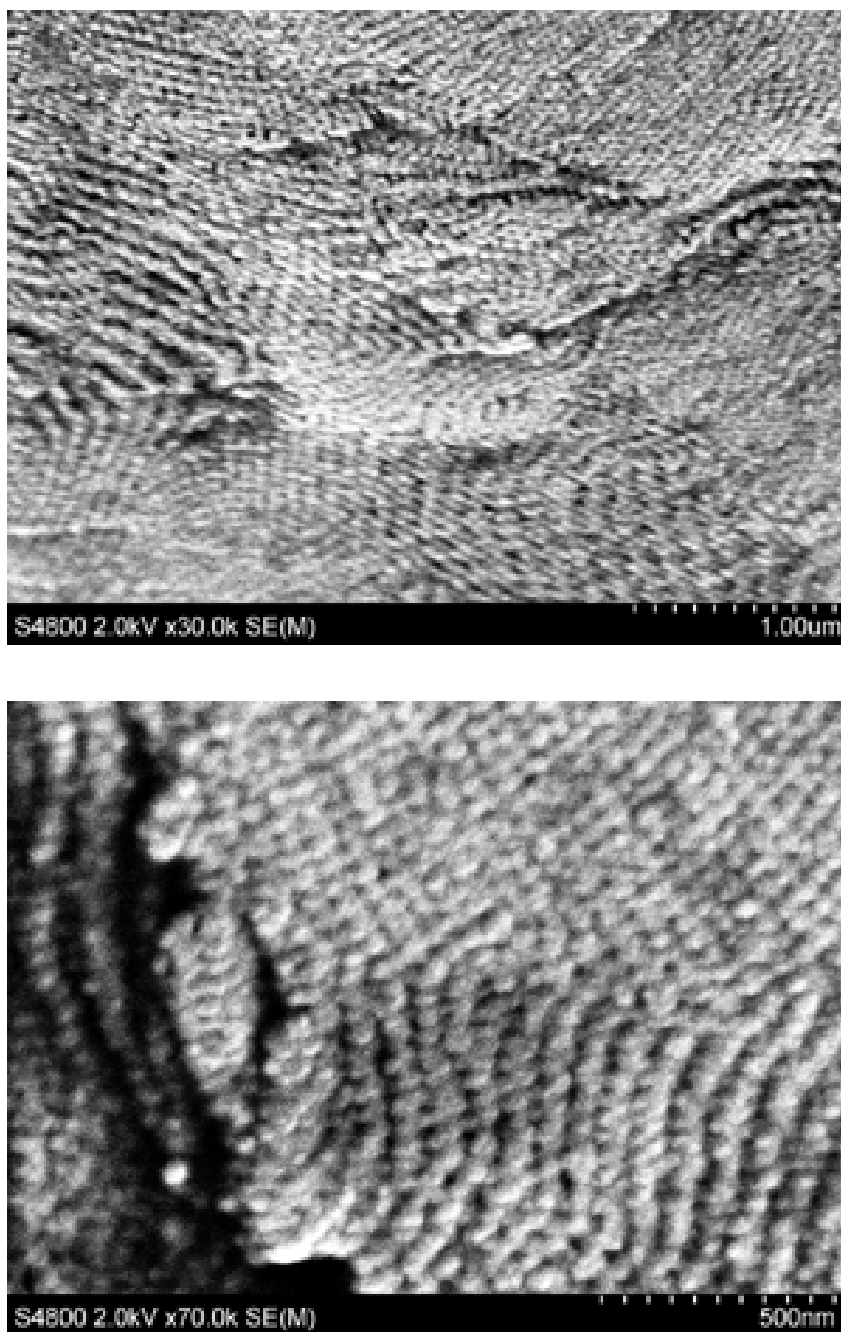


Figure 4.24 SEM micrographs of entry 16.

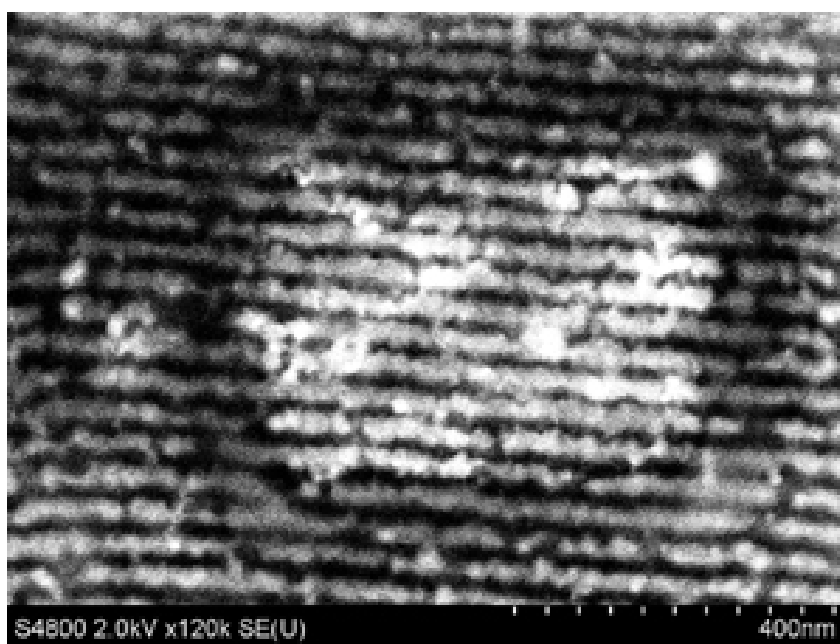


Figure 4.25 SEM micrographs of entry 17.

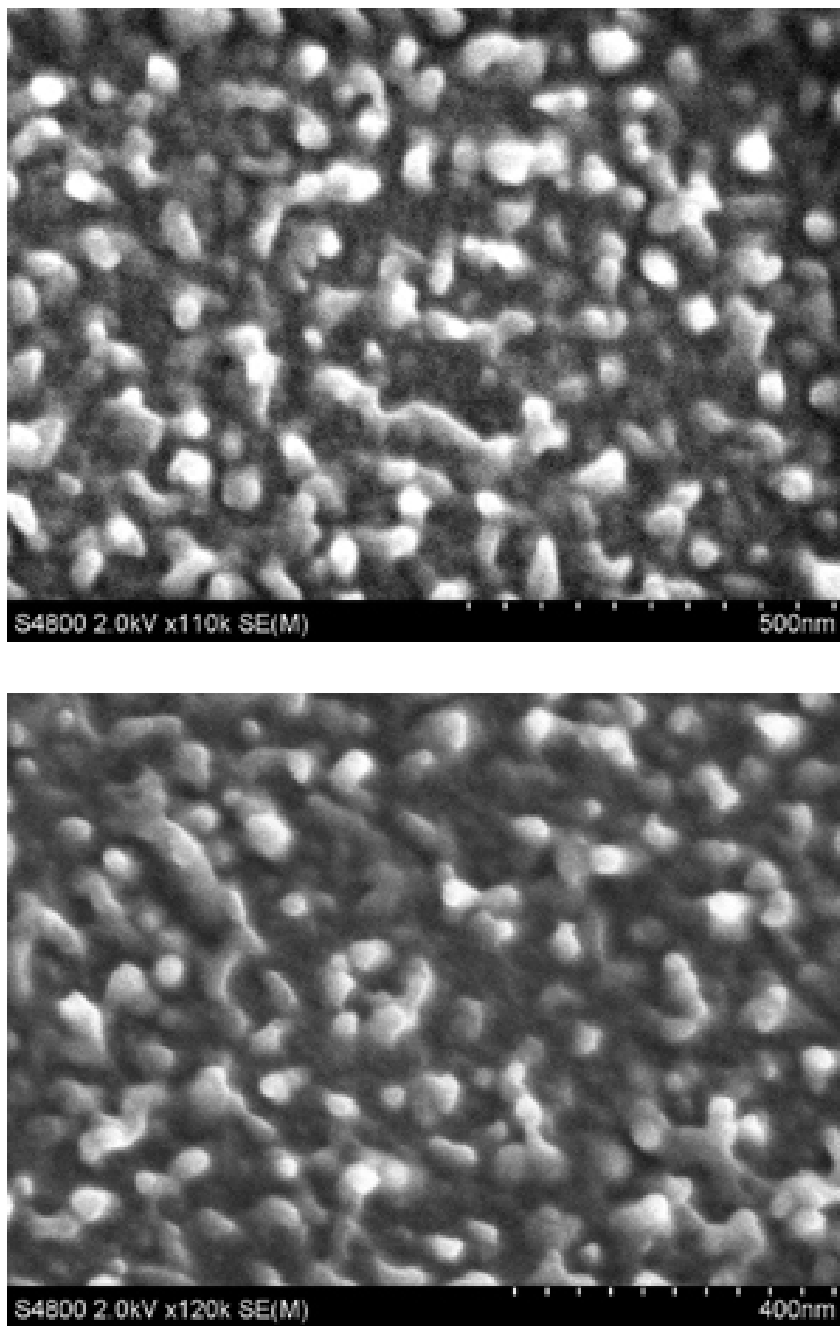


Figure 4.26 SEM micrographs of entry 18.

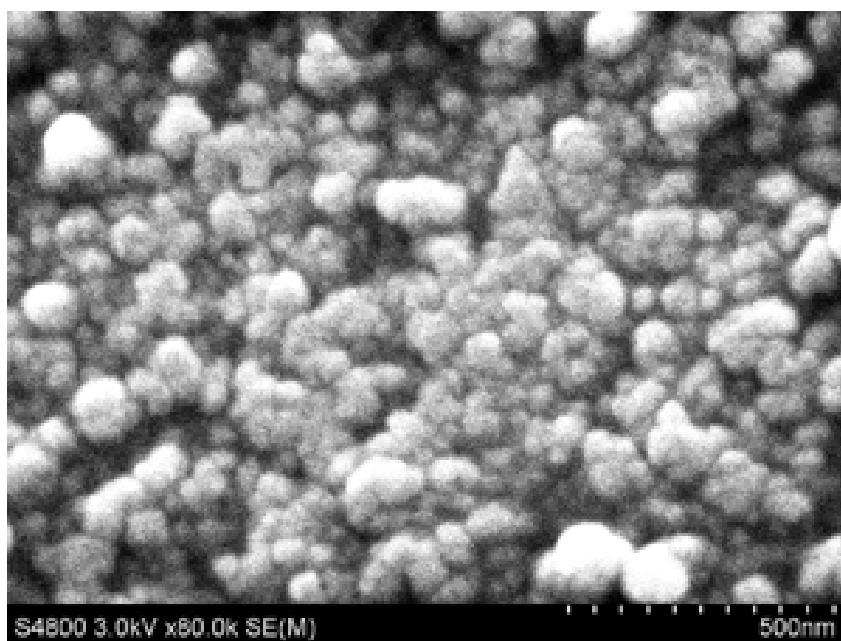
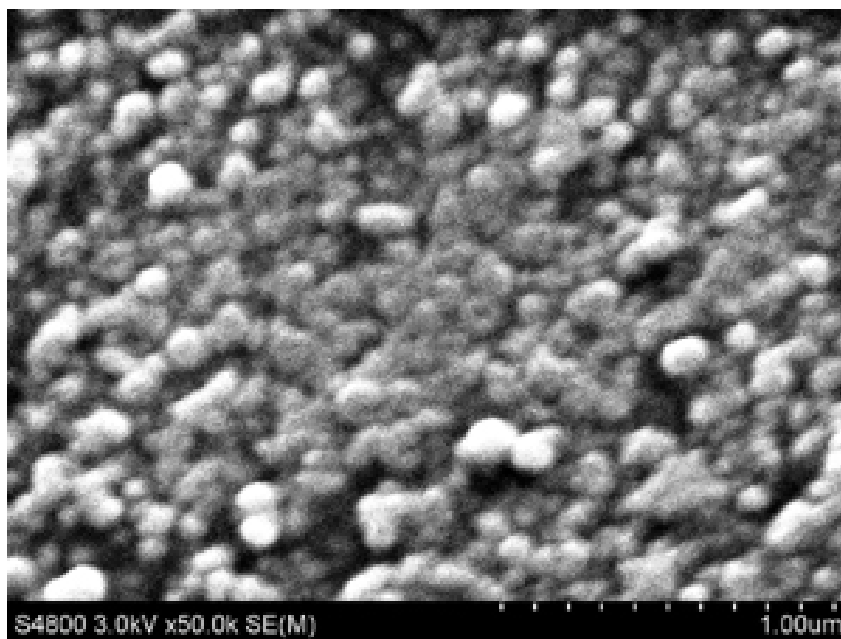


Figure 4.27 SEM micrographs of entry 19.

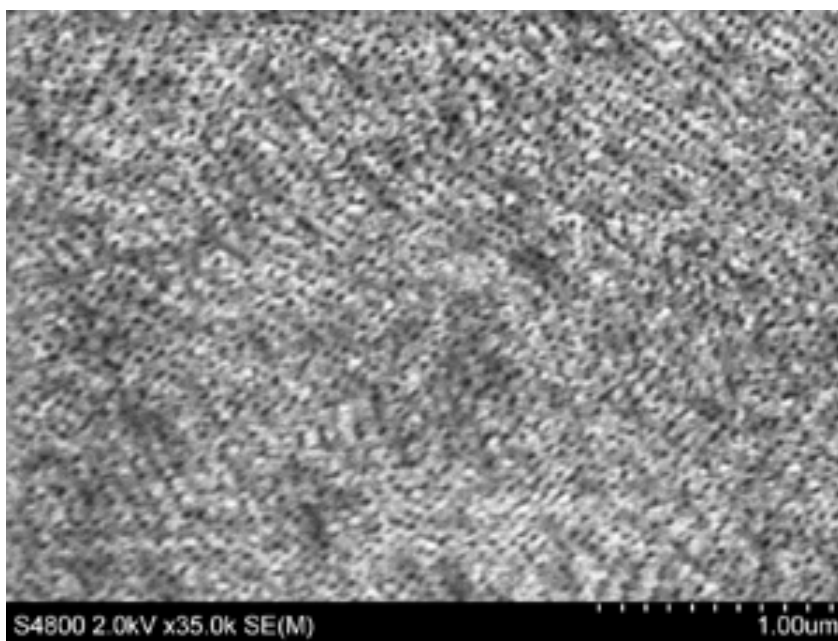
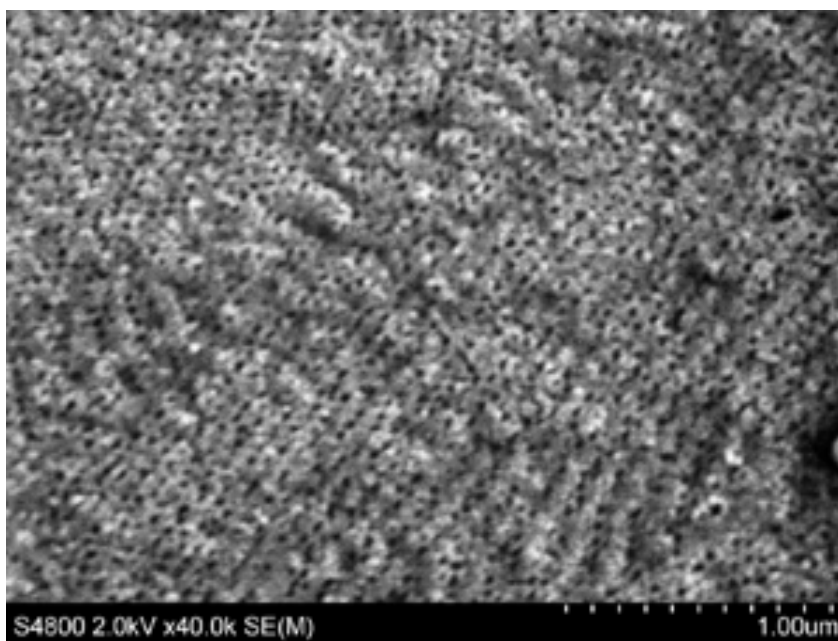


Figure 4.28 SEM micrographs of entry 20.

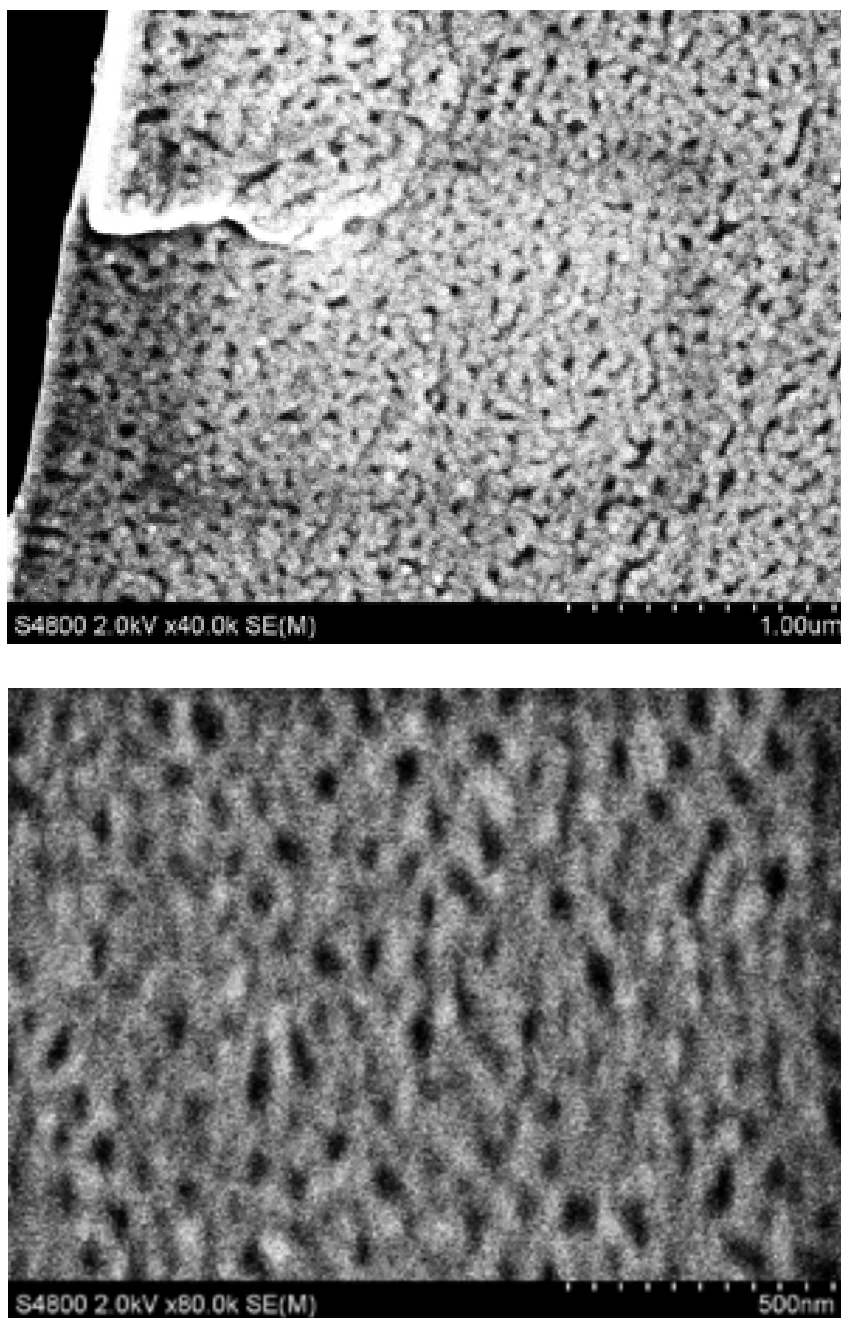


Figure 4.29 SEM micrographs of entry 21.

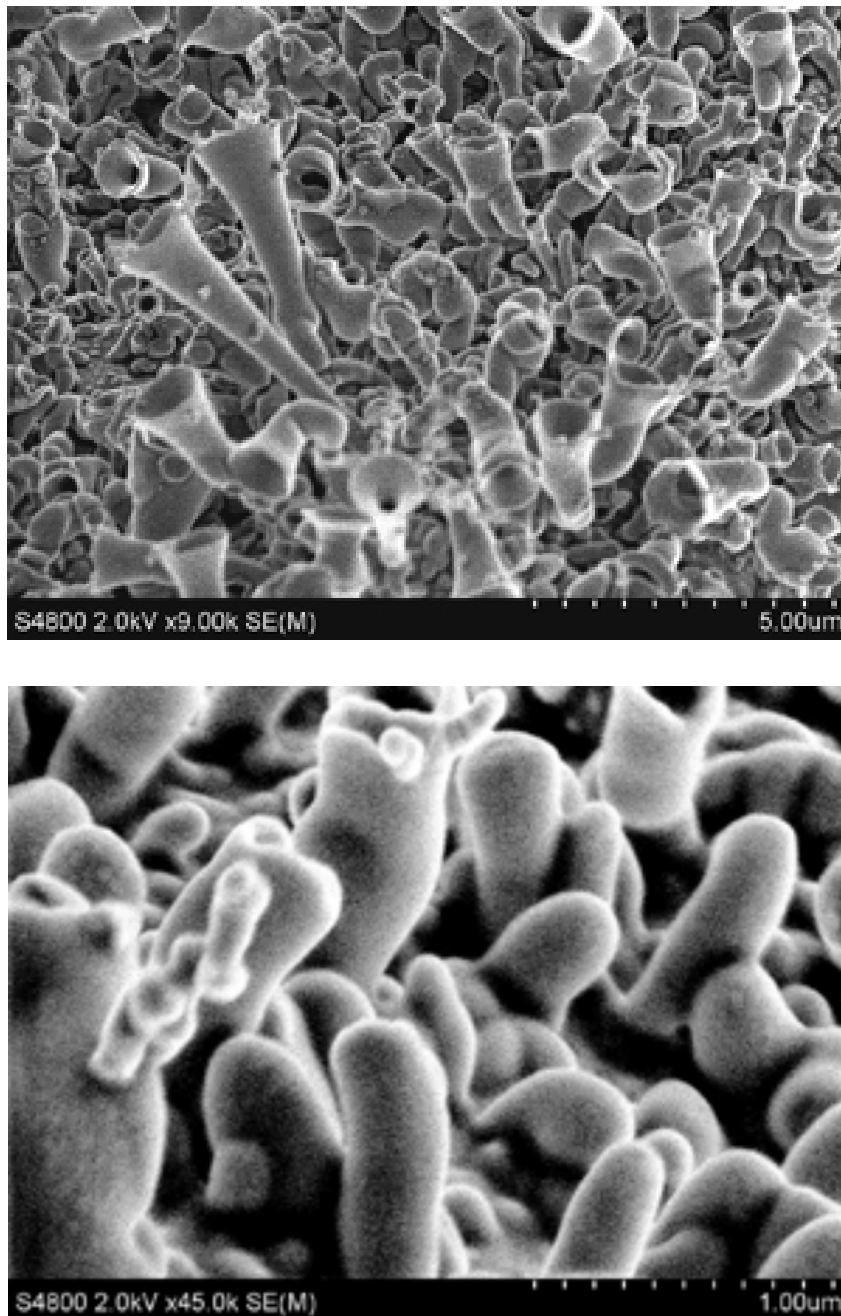


Figure 4.30 SEM micrographs of entry 22.

(Part of this work was accepted for publication in *polymer*, 2011.)

CHAPTER 5
FACILE SYNTHESIS OF THE GRUBBS FIRST GENERATION
METHYLIDENE CATALYST AND ITS REACTIVITY TOWARDS
STERICALLY HINDERED OXANORBORNES

Abstract

The Grubbs first generation catalyst was reacted with 1,7-octadiene to yield a ruthenium methylidene catalyst in 69% isolated yield. The reaction between this ruthenium methylidene catalyst and the commercially available Grubbs first and second generation catalysts with oxanorbornenes substituted with methyls at the bridgehead carbons was studied. Surprisingly, no reaction was observed even at high loadings of catalyst and oxanorbornene.

Introduction

The importance of the Grubbs catalysts in the synthesis of small molecules and polymers has made it one of the most studied catalysts in the last ten years.¹⁴⁷⁻¹⁵² These catalysts are very stable and active when substituted with a ruthenium benzylidene, but the ruthenium methylidene is significantly less stable (Figure 5.1). The methylidene is an intermediate in many ring closing and cross metathesis reactions which makes it an important molecule when considering how to improve the lifetime and activity of Grubbs catalysts.¹⁵³ Because of this importance, catalysts with a ruthenium methylidene have been synthesized and studied. The ruthenium methylidenes have been synthesized by exposing Grubbs catalysts to ethylene and, in the case of the Grubbs second generation catalyst, using heat to drive the reaction to completion.^{154, 155} Here, we report a facile synthesis of the ruthenium methylidene for the Grubbs first generation catalyst that does not require the use of a gas. Furthermore, we will describe how this catalyst reacts with oxanorbornenes that are substituted at the bridgehead carbons.

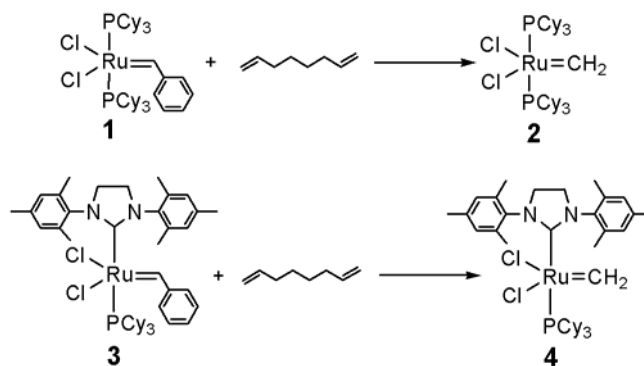


Figure 5.1 How the ruthenium methylidenes were synthesized.

Results and Discussion

When the Grubbs catalysts catalyze ring closing metathesis reactions with dienes, a ruthenium methylidene is formed if the dienes contain vinyl groups (Figure 5.1).¹⁵⁶⁻¹⁵⁸ This reaction was used to generate ruthenium methylidenes for the Grubbs first generation catalyst by reacting it with fifteen equivalents of 1,7-octadiene in methylene chloride. The catalyst was cleaned by removing methylene chloride, styrene, and cyclohexene under reduced pressure. The ruthenium methylidene was isolated in 69% yield and its ¹H and ¹³C NMR spectra matched the reported values.¹⁵⁵

The reaction between the Grubbs second generation catalyst and 1,7-octadiene was more complicated. This catalyst has a slow rate of initiation but fast rate of propagation, so a higher diene to catalyst loading was required to convert all of the catalyst to the ruthenium methylidene.^{154, 159} In addition, the ruthenium methylidene was reported to be unstable and decomposed in the solid state under N₂.¹⁵⁴ A reaction with a 100:1 molar ratio of 1,7-octadiene to Grubbs second generation catalyst yielded the ruthenium carbene at an approximate 80% crude yield after removal of the solvent in vacuo and redissolving in CDCl₃.

A clean sample of the Grubbs second generation catalyst with a ruthenium methylidene could not be isolated. It was generated as shown in Figure 5.1 and the solvent was removed, but when the solid ruthenium methylidene was washed with hexane under N₂, a gel formed that contained no evidence of product by ¹H NMR spectroscopy. Repeated efforts to purify the ruthenium methylidene catalyst failed.

The first and second generation catalysts were reacted with sterically hindered oxanorbornenes (Figure 5.2). Although the steric requirements around olefins for cross metathesis and ring closing metathesis reactions are well studied, these requirements for ring opening metathesis polymerization (ROMP) are less well understood.¹⁶⁰⁻¹⁶⁸ Norbornenes and oxanorbornenes are common monomers for ROMP because of their ease of synthesis by Diels-Alder reactions and rapid polymerization with Grubbs catalysts. For instance, monomer 5 from Figure 5.2 polymerizes with a first order rate constant of 0.84 L mol⁻¹ s⁻¹ with the Grubbs first generation catalyst.^{121, 122, 169, 170} The effect of endo and exo substituents on the rates of ROMP are well known, but no study had addressed substitutions at the bridgehead carbons (monomers 6 and 7 in Figure 5.2) prior to this work.

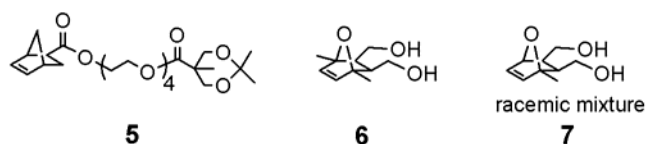


Figure 5.2 All of these molecules were isolated as the pure exo isomers.

To study the steric requirements for oxanorbornenes substituted at the bridgehead carbons, monomer 6 was reacted with the Grubbs first and second generation catalysts at monomer:catalyst loadings of 3:1 and high concentrations of catalyst (5.3×10^{-2} M). No

reaction occurred even after 2 h for either catalyst. When monomer 7 was reacted under similar conditions with catalysts 1 and 3, no reaction occurred. To eliminate any possibility of steric crowding between the benzylidene carbene and the methyl group on monomer 7, catalyst 2 was reacted with monomer 7. Even after 2 h at a monomer:catalyst loading of 3:1, no reaction was observed by ^1H NMR spectroscopy.

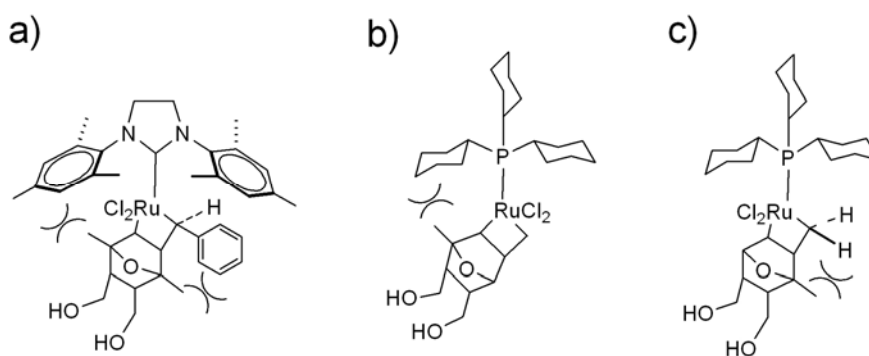


Figure 5.3 Steric effects of the methyl at the bridgehead position of oxanorbornes. a) Significant steric crowding exists between the Grubbs second generation catalyst and monomer 6 when it undergoes a metathesis reaction. b) and c) The reaction of monomer 7 and the Grubbs first generation methylidene catalyst has significant steric interactions in the transition state regardless of the orientation of molecule 7.

A possible explanation of these results is proposed based on the crystal structures of the Grubbs first and second generation catalysts.^{151, 171-174} An examination of these crystal structures does not indicate any potential steric interactions for the initial coordination of monomers 6 or 7 to ruthenium. In contrast, the metallocyclobutane intermediate would be expected cause significant steric interactions between the methyls and either the PCy_3 or imidazolium carbene ligand (Figure 5.3a and b). Somewhat

surprising to us was that monomer 7 did not react with the Grubbs first generation methylenide catalyst. Monomer 7 was synthesized as a racemic mixture and could form a metallocyclobutane with the methyl group pointed towards the PCy_3 or away from it (Figure 5.3b and c). A significant steric interaction may exist between the methyl group and the two hydrogens in Figure 5.3c that result in no reaction between molecules 7 and 2.

Conclusions

In summary, an efficient synthesis of the Grubbs first generation methylenide catalyst and its reactivity with oxanorbenes substituted at the bridgehead carbons was described. The lack of reaction between monomers 6 and 7 with the Grubbs catalysts 1, 2, and 3 demonstrated that a significant steric hindrance resulted when even one tertiary, bridgehead hydrogen was replaced with a methyl group in the monomer. These results were unexpected and are presented as a limitation for which monomers may react with the Grubbs catalysts.

Experimental Section

Synthesis and NMR Data

$\text{RuCl}_2(=\text{CH}_2)(\text{PCy}_3)_2$ (1)

A solution of Grubbs first generation catalyst (0.69 g, 0.84 mmol) in CH_2Cl_2 (20 mL) was stirred under an atmosphere of nitrogen at room temperature. After the addition of 1,7-octadiene (1.38 g, 12.5 mmol), the mixture was stirred for 2 h. The solvent was evaporated under vacuum, and the residue was washed with acetone (5 x 3 mL) and dried under vacuum for 4 h. The residue was redissolved in CH_2Cl_2 (10 mL) and the solvent was evaporated again under vacuum to yield a brown solid (0.43 g, 69%). ^{155}H NMR (CDCl_3): δ 1.51 (m, 60H), 2.48 (m, 6H), 18.92 (s, 2H). ^{13}C NMR (CDCl_3): δ 26.50 (s, *p*-

C of $\text{P}(\text{C}_6\text{H}_{11})_3$, 27.73 (*pseudo-t*, $J = 5.2$, *o*-C of $\text{P}(\text{C}_6\text{H}_{11})_3$), 29.16 (s, *m*-C of $\text{P}(\text{C}_6\text{H}_{11})_3$), 30.70 (*pseudo-t*, $J = 9.9$, *ipso*-C of $\text{P}(\text{C}_6\text{H}_{11})_3$), 293.84 (s, Ru=CH).

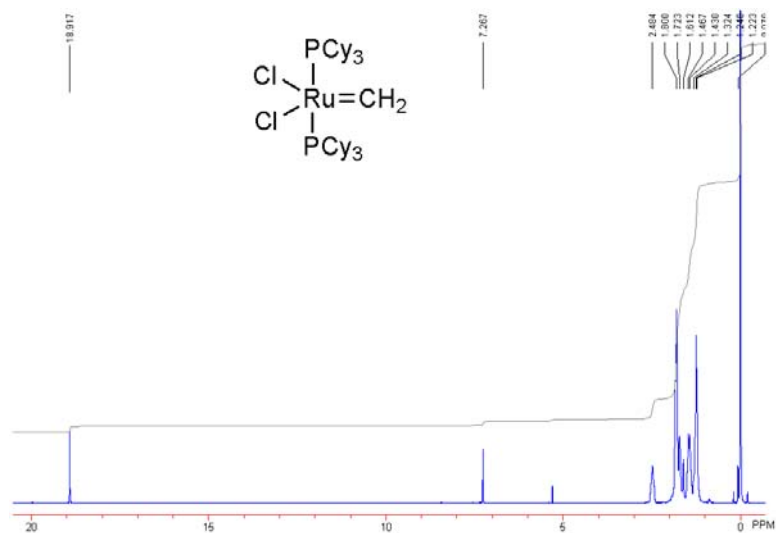


Figure 5.4 ^1H NMR spectrum of $\text{RuCl}_2(=\text{CH}_2)(\text{PCy}_3)_2$.

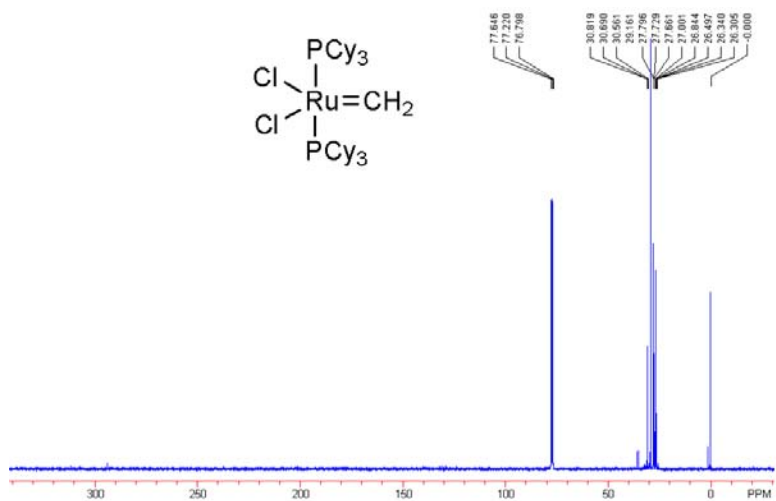


Figure 5.5 ^{13}C NMR spectrum of $\text{RuCl}_2(=\text{CH}_2)(\text{PCy}_3)_2$.

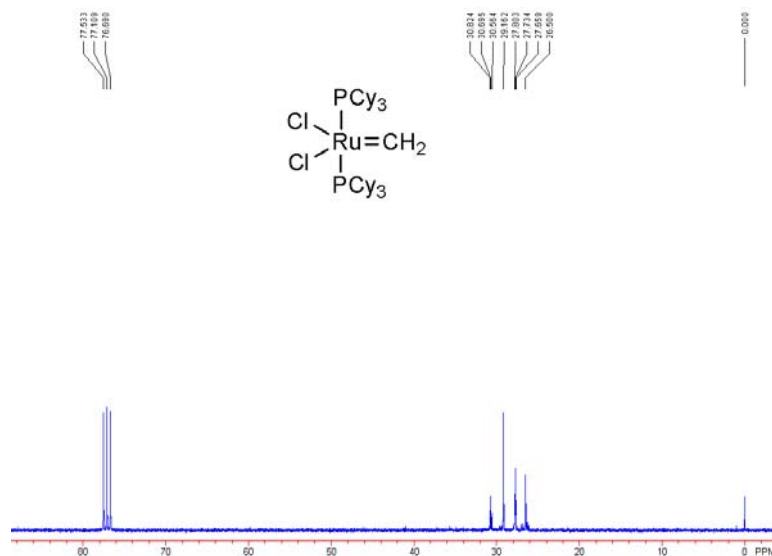


Figure 5.6 ^{13}C NMR spectrum of $\text{RuCl}_2(=\text{CH}_2)(\text{PCy}_3)_2$.

1,4-Dimethyl-7-oxabicyclo[2.2.1]heptene-2,3-dicarboxylic anhydride (A)

Maleic anhydride (5.1 g, 52.0 mmol) and 2,5-dimethylfuran (5.0 g, 52.0 mmol) were placed in a 100 mL of round bottom flask and 10 mL of anhydrous Et_2O was added. The mixture was stirred until the maleic anhydride completely dissolved. The flask was sealed and allowed to stand at room temperature for 5 days. The resulting crystals were filtered and washed with cold anhydrous Et_2O (3 x 10 mL) to yield a white solid (5.14 g, 51%).^{175, 176} This solid was the pure exo isomer. ^1H NMR (CDCl_3): δ 1.74 (s, 6H), 3.16 (s, 2H), 6.34 (s, 2H). ^{13}C NMR (CDCl_3): δ 15.65, 54.10, 88.90, 141.20, 168.67.

1-Methyl-7-oxabicyclo[2.2.1]heptene-2,3-dicarboxylic anhydride (B)

Maleic anhydride (2.00 g, 20.4 mmol) and 2-methylfuran (2.51 g, 30.6 mmol) were reacted according to the procedure used for compound A. The product was isolated

as a white solid (3.01 g, 82%). 176 ^1H NMR (CDCl_3): δ 1.78 (s, 3H), 3.04 (d, 1H, $J = 6.9$), 3.30 (d, 1H, $J = 6.9$), 5.33 (s, 1H), 6.35 (d, 1H, $J = 6.0$), 6.55 (m, 1H). ^{13}C NMR (CDCl_3): δ 15.50, 51.06, 51.94, 81.94, 89.64, 137.54, 140.77, 168.75, 170.23.

1,4-Dimethyl-7-oxabicyclo[2.2.1]heptene-2,3-dimethanol

(C)

Molecule A (1.72 g, 8.85 mmol) was added to a suspension of LiAlH_4 (0.84 g, 22.1 mmol) in dried THF (10 mL) at 0 °C under N_2 and stirred at room temperature for 24 h. The mixture was carefully quenched with water and 3 N HCl solution at 0 °C and extracted with CH_2Cl_2 (3 x 15 mL). The organic layer was dried over MgSO_4 , and evaporated. The product was cleaned by column chromatography using 80% EtOAc in hexanes to yield a white solid (0.52 g, 32%) ^1H NMR (CDCl_3): δ 1.52 (s, 6H), 2.08 (s, 2H), 3.52 (s, 2H), 3.91 (m, 4H), 6.17 (s, 2H). ^{13}C NMR (CDCl_3): δ 16.24, 46.35, 60.78, 86.67, 140.20.

1-Methyl-7-oxabicyclo[2.2.1]heptene-2,3-dimethanol (D)

Reduction of B (2.03 g, 11.3 mmol) was carried out with LiAlH_4 (1.11 g, 29.4 mmol) following the procedure used for compound C. The product was cleaned by column chromatography using EtOAc to yield a white solid (0.7 g, 35%). ^1H NMR (CDCl_3): δ 1.53 (s, 3H), 1.95 (m 1H), 2.09 (m, 1H), 3.72 (s, 2H), 3.85 (m, 4H), 4.58 (s, 1H), 6.18 (d, 1H, $J = 6.0$), 6.39 (m, 1H). ^{13}C NMR (CDCl_3): δ 16.00, 44.21, 44.69, 60.59, 63.30, 81.01, 87.10, 136.10, 139.94.

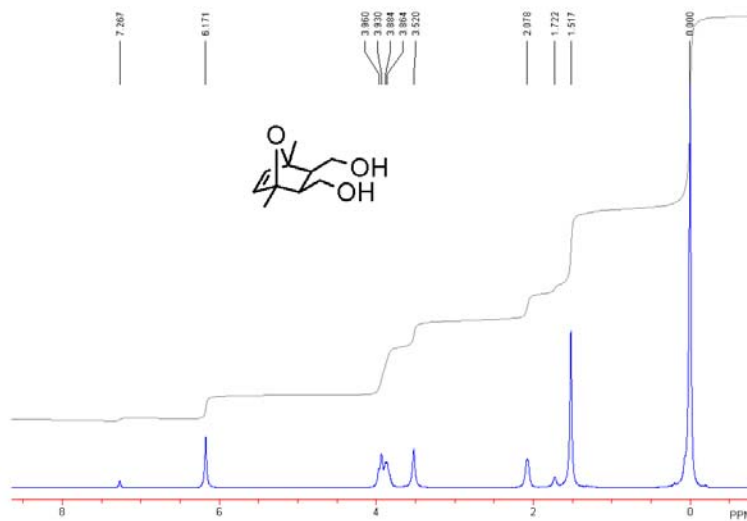


Figure 5.7 ^1H NMR spectrum of 1,4-Dimethyl-7-oxabicyclo[2.2.1]heptene-2,3-dimethanol.

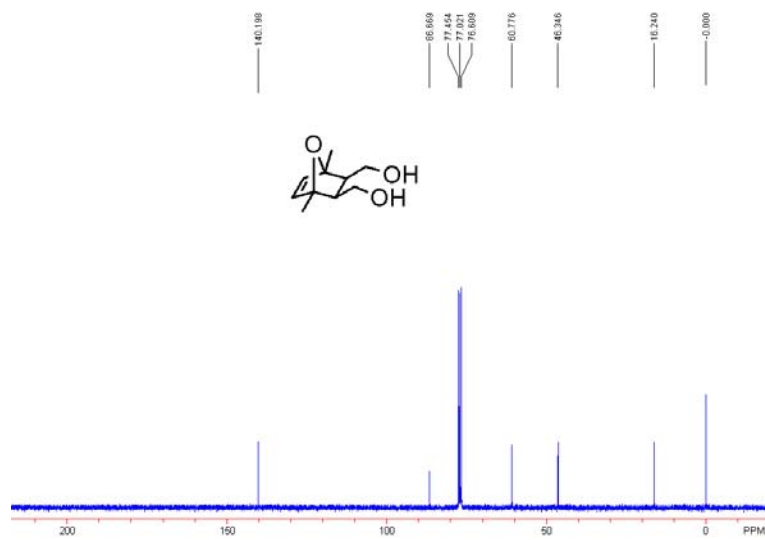


Figure 5.8 ^{13}C NMR spectrum of 1,4-Dimethyl-7-oxabicyclo[2.2.1]heptene-2,3-dimethanol.

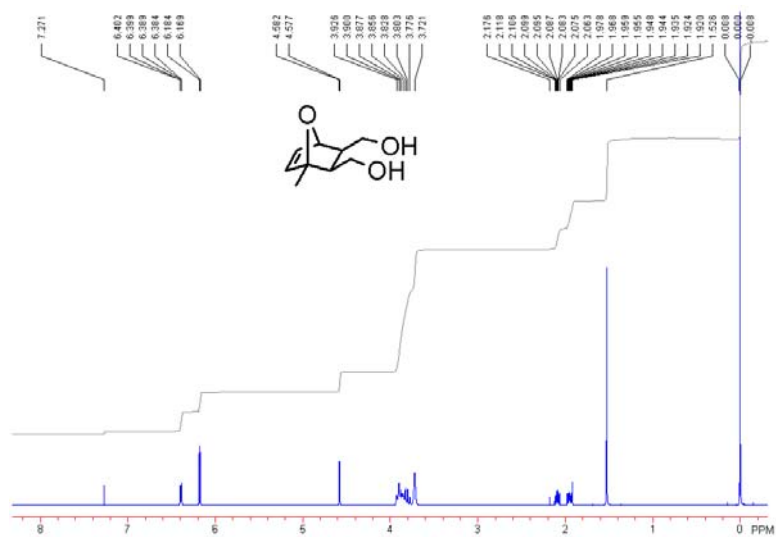


Figure 5.9 ^1H NMR spectrum of 1-Methyl-7-oxabicyclo[2.2.1]heptene-2,3-dimethanol.

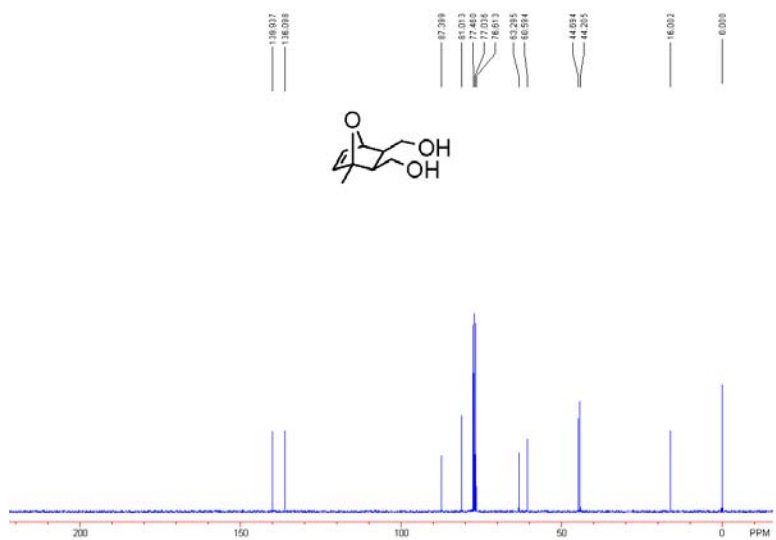


Figure 5.10 ^{13}C NMR spectrum of 1-Methyl-7-oxabicyclo[2.2.1]heptene-2,3-dimethanol.

CHAPTER 6

CONCLUSIONS AND RECOMMENDATIONS FOR FUTURE WORK

Conclusions

In this thesis, the main achievements of our research are syntheses of new biodegradable polymers called polysulfenamides that are composed of new functional groups (S-N and N-S-N bonds) along their backbones. Polysulfenamides provide a route to the synthesis of new biodegradable polymers based on S-N bond cleavage under acidic conditions. These polymers were well-defined and characterized, and they were the first biodegradable polymers based on these functional groups ever reported in the literature

A high conversion of transamination reactions was critical to the step-growth polymerization between sulfenamides and secondary diamines to yield polysulfenamides with S-N bonds. The polymerizations were completed at room temperature through the synthesis of dithiosuccinimides which possessed a good leaving group. Polysulfenamides were successfully synthesized with degrees of polymerization up to 97% through the transamination of dithiosuccinimides and secondary diamines. Microparticles were fabricated from polysulfenamides which were stable at physiological pH and degraded under acidic conditions. These microparticles were readily absorbed into JAWSII and HEK 293 cells and showed minimal toxicity with many potential applications in vaccine delivery and gene therapy. The surfaces of these microparticles were easily functionalized to express new functional groups through transamination reactions.

To synthesize a second new biodegradable polymer based on N-S-N bonds, an excellent sulfur-transfer reagent, bis(*N,N'*-dimethyl) sulfide was prepared. This molecule showed reasonable kinetics in a transamination reaction with a secondary amine in refluxing benzene and provided a method to prepare polymers with N-S-N bonds. These polymers are expected to possess a positive zeta value without functionalization of the

polymers and degrade more rapidly than polysulfenamides because the degradation products will consist of only free amines and SO gas.

The introduction of a new functional group (S-N or N-S-N bonds) in the synthesis of polymers will expand the types and properties of biomedical polymers and provide an easy method to functionalize microparticles. These polymers will provide new routes to design more complex and specific drug delivery matrices that will be required in medicine.

As for other achievements, we have developed the syntheses of three new sets of comb block copolymers with polymeric arms composed of poly(lactic acid), poly(butyl acrylate), and poly(styrene-*b*-vinylpyridine) using ring opening metathesis polymerization (ROMP), ring opening polymerization (ROP), and atom transfer radical polymerization (ATRP). The block copolymers were synthesized by the ROMP of oxanorbornene and norbornene using the Grubbs first generation catalyst. The olefins along the backbone were subsequently hydrogenated in a one-pot reaction to increase the stability of the polymers. The polymeric arms were grafted from the backbone polymers using ATRP or ROP. The challenging issue in grafting poly(vinylpyridine) onto comb polymers was overcome by using ATRP at a high dilution of the comb polymers with poly(styrene) arms. The synthesis of these polymers demonstrated that a range of comb block copolymers with expanded complexity and functional groups could be realized. The self-assembled morphologies in the solid state of comb tri- and tetrablock copolymers with poly(styrene) arms demonstrate some potential applications of these polymers.

In the context of the ROMP, the steric effect of oxanorbornene on the Grubbs catalysts was studied. The Grubbs first and second generation catalysts showed a lack of reactivity with oxanorbornene when one bridgehead-hydrogen was substituted with a methyl group. Even when Grubbs first generation methylenidene catalyst was synthesized and reacted with the methyl substituted oxanorbornene, there was no reaction. This result

implied a significant steric interaction between the methyl group and the two hydrogens of the metallocyclobutane intermediate. These results demonstrate that the oxanorbornenes substituted at the bridgehead position have limited reactivity with the Grubbs catalysts.

Recommendations for Future Work

In future work, optimization of the synthesis of polysulfenamides should be completed because there are possibilities to improve the yield of polymerization. In the first synthesis of polysulfenamides, the molecular weights of the polymers were below $10,000 \text{ g mol}^{-1}$ although the reaction of thiosuccinimides with secondary amines went to >97% conversion at reasonable concentrations at room temperature. Also, dithiosuccinimides were mainly reacted with secondary diamines for the polymerization because the reaction between disulfenamides and secondary diamines was hindered by slow kinetics of polymerization in refluxing aprotic solvents and lack of solubility of the polymer in protic solvents.

By improving some factors in polymerization, high molecular weight polysulfenamides can be synthesized. The reaction time of polymerization needs to be reexamined to find the best condition to obtain high molecular weight polymers because the polymerization time in the first synthesis was 24 hours although the kinetics of the polymerization showed >95% conversion within 50 min at room temperature. Some of the S-N bonds might be cleaved due to acidic protons originating from succinimide produced as a byproduct during the long polymerization time. Therefore, finding the optimal polymerization time is critical to obtaining high molecular weight polymers. Some bases such as triethylamine, pyridine, and potassium hydroxide can be applied together to neutralize the acidic protons from the succinimide, which might increase the molecular weight of the polymers.

The reactivity of disulfenamides with secondary diamines can be improved by replacing the leaving group, *N*-ethylmethylamine (boiling point of 36 °C) with dimethylamine which is easier to boil off because of its low boiling point of 7 °C as shown in Figure 6.1. In the synthesis of polymers with N-S-N bonds, dimethylamine proved an even better leaving group than *N*-ethylmethylamine, resulting in >97% conversion in refluxing benzene after 24 h and 97% conversion in CDCl₃ at 50 °C after 72 h. Therefore, the disulfenamide with dimethylamine will provide another novel route to synthesize polysulfenamides.

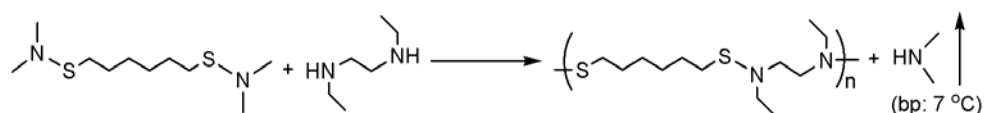


Figure 6.1 Polymerization of disulfenamide with dimethylamine as a leaving group.

Another recommendation for future work that needs to be pursued is the introduction of a functional group to the polysulfenamide backbones. Although the polysulfenamides are well-defined and biodegradable, their backbones are too simple to be functionalized for various applications in medicine. The modification of the backbone structures might be achieved by reacting dithiosuccinimides with *N,N'*-bis(2-hydroxyethyl)ethylenediamine as shown in Figure 6.2a. The alcohol groups along the backbone can be functionalized with a cyclooctyne derivative which exhibits Cu-free click chemistry with azide-modified biomolecules as shown in Figure 6.2a. This small modification of the backbone will allow the construction of bioconjugate systems with azide-modified biomolecules and polysulfenamides.¹⁷⁷

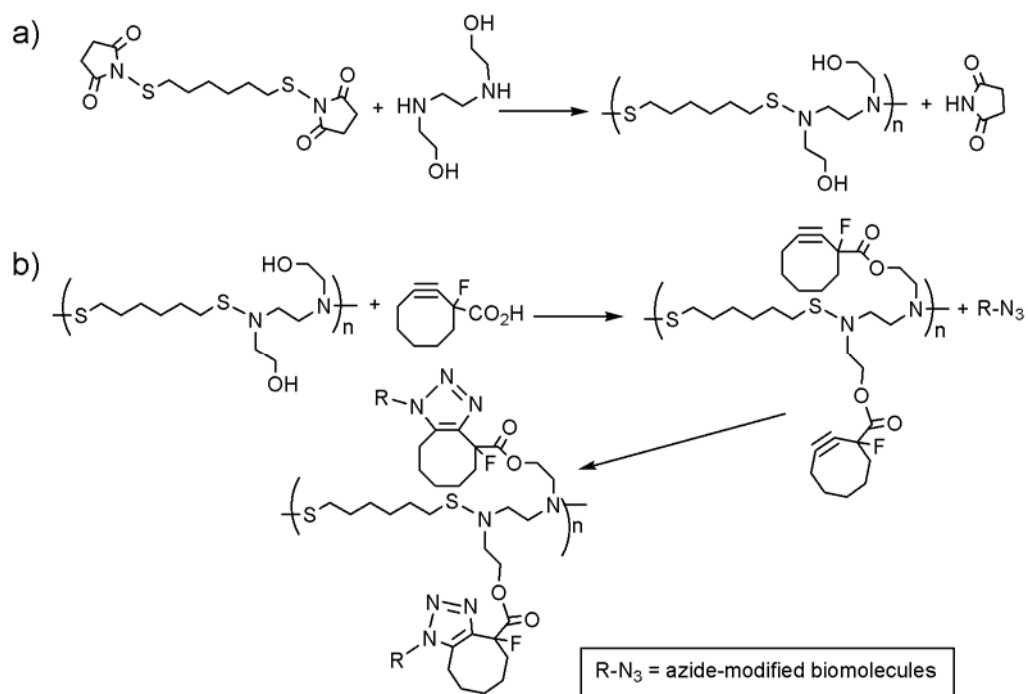
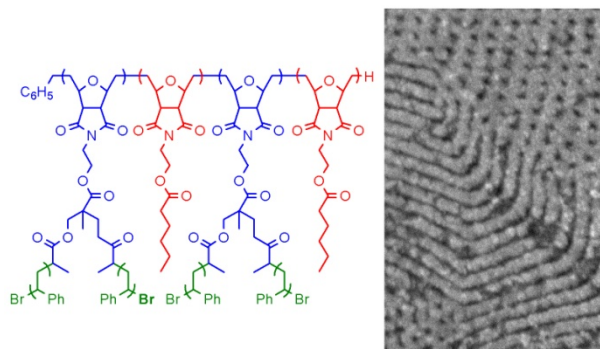


Figure 6.2 Functionalization of polysulfenamides. a) Synthesis of a polysulfenamide with an alcohol group along the backbone. b) Functionalization of a polysulfenamide with a cyclooctyne derivative using Cu-free click chemistry with azide-modified biomolecules.

APPENDIX
SYNTHESIS OF COMB TRI- AND TETRABLOCK COPOLYMERS
CATALYZED BY THE GRUBBS FIRST GENERATION CATALYST

Abstract

High molecular weight tri- and tetrablock copolymers were synthesized from the commercially available Grubbs first generation catalyst for the first time. These polymers had degrees of polymerization from 430 to 1100, molecular weights up to 419,000 g mol⁻¹, and narrow polydispersities. Oxanorbornene monomers were chosen due to their fast rates of polymerization and slow rates of cross metathesis. Polystyrene arms were grown from selected blocks by atom transfer radical polymerization to yield architecturally complex comb tri- and tetrablock copolymers. These polymers self-assembled in the solid state into ordered morphologies that were characterized by scanning electron microscopy.



Introduction

Ring opening metathesis polymerization (ROMP) is an important method to synthesize polymers that has recently found numerous applications in the synthesis of complex polymers.^{149, 160, 169, 178-183} Of the many metathesis catalysts reported in the literature, the Grubbs first, second, and third generation catalysts are the most widely used because of their wide functional group tolerance and high activities. The Grubbs first generation catalyst is the most common choice for ROMP, but its activity is much

lower than that of the second or third generation catalyst. Most examples of tri- or tetrablock copolymers synthesized with the Grubbs first generation catalyst have modest degrees of polymerization less than 100.¹⁸⁴⁻¹⁸⁸ Although, the second generation catalyst has a much higher activity than the first generation catalyst, it possesses a slow initiation step that leads to excessively poor control over molecular weight of the polymers.¹⁸⁹ This problem was addressed at some level by the addition of bromopyridine to the second generation catalyst to yield a third generation catalyst with a rate of initiation that increased by up to six orders of magnitude.^{190, 191} This catalyst has been reported to yield homo and block polymers with low PDIs and controlled molecular weights.

We and others are very interested in the development of block polymers for applications as diverse as photonic materials, catalysis, drug delivery, antimicrobial polymers, membranes, and microchip patterning.^{121, 130, 135, 178, 183, 192-197} ROMP provides an attractive route to block polymers, but it has remained underutilized compared to anionic and radical polymerizations. Two reasons for its underutilization are the lack of a wide range of commercially available strained cyclic olefins that are readily polymerized and the low activity of the Grubbs first generation catalyst. The latter problem was addressed at some level by the development of the Grubbs third generation catalyst that has a higher activity in ROMP, but it has only been used to synthesize a few examples of triblock copolymers with total degrees of polymerization between 140 and 460.^{190, 191, 198-201} In addition, the high cost of the third generation catalyst (\$322/g) compared to that of the first generation catalyst (\$72/g) limits its uses.

In this paper, we report the first synthesis of high molecular weight tri- and tetrablock copolymers by ROMP catalyzed via the Grubbs first generation catalyst.¹⁸⁸ Although tri- and tetrablock copolymers with degrees of polymerization up to 100 have been synthesized with the Grubbs first generation catalyst, the synthesis of these polymers with much higher degrees of polymerization is unknown. A possible reason for this limitation is that some monomers polymerize slowly such that cross metathesis

between the polymer chains limits the overall degree of polymerization. In this article, we will describe how a set of monomers polymerize rapidly such that tri- and tetrablock copolymers with high degrees of polymerization are possible. We define high degrees of polymerization as 1,000 units, which is an order of magnitude larger than reported by others for tri- and tetrablock copolymers synthesized with the Grubbs first generation catalyst.

This work builds on prior efforts by us to synthesize diblock copolymers with degrees of polymerization in excess of 1,000.¹²¹⁻¹²³ This work was successful and extended the degrees of polymerization to 2,000 units for diblock polymers synthesized via the Grubbs first generation catalyst. In this paper, we extend this work to include critical tri- and tetrablock copolymers and demonstrate that their degrees of polymerization can be exceed 1,000. The polymers reported in this work had degrees of polymerization up to 1,100 and molecular weights in excess of 400,000 g mol⁻¹. The monomers used in these studies were based on crystallizable exo-oxanorbornenes, and over a hundred grams were synthesized in two simple steps that required no chromatography or distillations.^{169, 202} These monomers were readily reacted to yield more complex molecules that displayed initiators for atom transfer radical polymerizations. These tri- and tetrablock copolymers were further used to synthesize comb block copolymers that assembled in the solid state into ordered arrays. This work demonstrated that the combination of appropriate monomers and the Grubbs first generation catalyst can be used to synthesize complex block copolymers.

Experimental Section

Materials

Chemicals were purchased from Aldrich or Acros and used as is unless otherwise stated. Methylene chloride was freeze-pump-thawed three times before filtration over

aluminum oxide in a glove box. CDCl_3 was freeze-pump-thawed three times before storage in a glove box.

Kinetic Experiments

For experiments with monomer to catalyst loading of 500 and 1,000 to one, monomer A (0.1 g, 330 μmol) was dissolved in 0.6 mL of CDCl_3 and added to an NMR tube. Grubbs catalyst (24.2 mg, 29 μmol) was dissolved in 17.9 mL of CDCl_3 . For a monomer to catalyst loading of 500 to one, 0.4 mL of the Grubbs catalyst solution was added to the NMR tube and ^1H NMR spectra were obtained approximately every minute. For a monomer to catalyst loading of 1,000 to one, 0.2 mL of catalyst solution was added to another NMR tube with the same amount of monomer and an additional 0.2 mL of methylene chloride. The polymerization rate of monomer B at a monomer to catalyst loading of 50 to one was investigated at a lower concentration. A solution of monomer B was prepared by dissolving 100 mg in 2.5 mL CDCl_3 , and 0.5 mL of solution was transferred to an NMR tube. Grubbs catalyst (21.7 mg, 26 μmol) was dissolved in 11.4 mL CDCl_3 . 0.5 mL of this catalyst solution was added to monomer B and ^1H NMR spectra were recorded every minute.

Size Exclusion Chromatography (SEC)

The polymers were characterized by SEC using chloroform (1 mL min^{-1}) as the mobile phase at 35 °C. Two Waters columns (two styragel HMW7 columns or a combination of HR4 and HR5E columns) were used in series. The columns were connected to a DAWN EOS 18 angle laser light scattering detector from Wyatt Corp., a Wyatt QELS detector to measure quasi-elastic light scattering, and a Wyatt Optilab DSP to measure changes in refractive index. These detectors were used to find the absolute molecular weights without the need for polymer standards.

Synthesis of ABA Triblock Copolymer by ROMP

Grubbs first generation catalyst (103 mg, 0.12 mmol) was dissolved in 4.8 mL of methylene chloride. Monomer A (2.0 g, 6.5 mmol) was dissolved in 7.5 mL of methylene chloride. Grubbs catalyst solution (0.5 mL, 10.7 mg, 13 μ mol) was added to monomer A. The polymerization proceeded for 30 min before monomer B (0.448 g, 1.3 mmol) dissolved in 4 mL of methylene chloride was added and stirred for an additional 25 min. A second batch of monomer A (2.0 g, 6.5 mmol) was dissolved in 10 mL methylene chloride, added to the polymerization, and stirred for 45 min. Silica gel (400 mg) and 8 equivalents of Grubbs catalyst were added, the reaction vessel was placed in a Parr reactor, it was pressurized with H₂ to 1100 psi, and the Parr reactor was placed in a 50 °C oil bath. After 18 h, the Parr reactor was cooled and the polymer was filtered through silica gel and precipitated into methanol twice.

Synthesis of CACA Tetra-block Copolymer by ROMP

A solution of Grubbs first generation catalyst (101.5 mg, 123 μ mol) dissolved in 3.15 mL of methylene chloride was prepared. 0.5 mL of the Grubbs catalyst solution (16.1 mg, 20 μ mol) was added to monomer C (0.233 g, 0.39 mmol) dissolved in 1.7 mL methylene chloride while stirring. The polymerization proceeded for 15 min before the addition of monomer A (1.2 g, 3.9 mmol) dissolved in 3 mL methylene chloride and stirred for an additional 25 min. Monomer C (0.116 g, 195 μ mol) dissolved in 0.3 mL methylene chloride was added and then stirred for 20 min before the addition of monomer A (1.2 g, 3.9 mmol) dissolved in 7 mL. After 40 min, silica gel (300 mg) and 5 equivalents of Grubbs catalyst (80.5 mg, 98 μ mol) were added. The reaction was placed inside a Parr reactor, pressurized with H₂ to 1000 psi, and placed in a 50 °C oil bath. After 18 h the Parr reactor was cooled, the polymer was filtered through silica gel, and it was twice precipitated into methanol.

Synthesis of Comb Polymers and Cleavage of Their Arms from the Backbone

The polystyrene arms were grafted onto the backbone polymers using dilute, copper catalyzed atom transfer radical polymerizations as described in previous publications.¹²¹⁻¹²³ In addition, the polystyrene arms were cleaved from the backbone polymers under basic conditions using KOH.

Self-assembly of Comb Block Copolymer Films

Block copolymer films were prepared as reported previously by casting films from polymer solutions of 10-30 mg mL⁻¹ in methylene chloride.^{121, 123} These films were vapor annealed with methylene chloride for three days. The films were frozen in liquid nitrogen and fractured to expose their interiors. The samples were stained with RuO₄ vapor prior to imaging by scanning electron microscopy (SEM) on a Hitachi 4800 at accelerating voltages between 1 to 5 kV.

Results and Discussion

Exo-oxanorbornenes were chosen for this study because they are readily synthesized and have high rates of polymerization (Figure A.1).^{123, 169, 202} The first step in their synthesis is the Diels-Alder reaction between furan and maleic anhydride. This reaction is very clean, and the product forms crystals of the exo-Diels-Alder adduct at room temperature. The anhydride is readily converted to a crystallizable imide in one step by reaction with ethanol amine. This synthesis provided simple access to over one hundred grams of clean product without requiring column chromatography or a distillation. The monomers used in this work were synthesized by simple reactions from this common intermediate.¹²¹

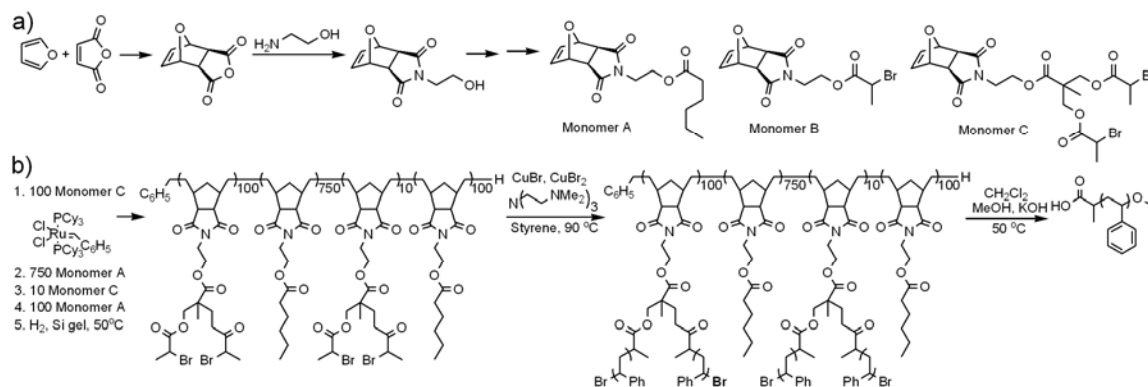


Figure A.1 Synthesis of comb tri- and tetra block copolymers. a) The simple, two-step synthesis of an oxanorbornene and the resulting monomers used in this study. b) The synthesis of comb block copolymers by ROMP and ATRP. In the final step, the arms were cleaved from the backbone polymer and characterized by SEC.

To polymerize these monomers by ROMP into tri- and tetrablock copolymers, their kinetics of polymerization were studied to learn when each monomer was completely consumed. This information was critical to the synthesis of block polymers because the sequential addition of monomers requires that each monomer be consumed prior to the addition of a new monomer. Three different monomer to catalyst ratios of 50, 500, and 1,000 to 1 were studied to obtain their kinetics of polymerization by ^1H NMR spectroscopy (Figure A.2). The rates of polymerization were very rapid; in fact, with initial monomer concentrations of 0.33 M polymerizations with a monomer to catalyst ratio of 1,000 to 1 reached >97% completion in 15 min and required only 12 min to reach >97% completion for a monomer to catalyst ratio of 500 to 1. This concentration was too high to gather meaningful data on the rates of polymerization at lower monomer to

catalyst ratios, so the initial monomer concentration was lowered to 0.058 M for a monomer to catalyst loading of 50 to 1. At this lower concentration, the kinetics of polymerization were easily measured and were close to the concentration of monomers in the synthesis of the tri- and tetrablock copolymers. Notably, even at this low concentration of monomer, the polymerization reached >97% completion in under 20 min.

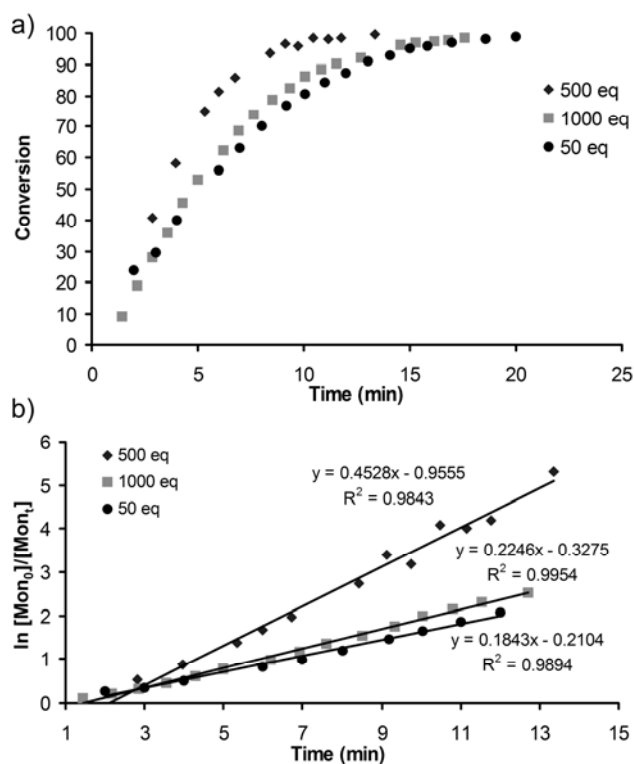


Figure A.2 Kinetics of ring opening metathesis polymerizations of monomer A and B. a) Plots of conversion versus time were measured by ^1H NMR spectroscopy for monomer B with a monomer to catalyst ratio of 50:1, and monomer A with monomer to catalyst ratios of 500:1 and 1000:1. The initial concentration of monomer was 0.058 M for the monomer to catalyst ratio of 50:1, and it was 0.33 M for monomer to catalyst ratios of 500:1 and 1000:1. b) The kinetics of the polymerizations were measured for the monomer to catalyst ratios of 50:1, 500:1, and 1000:1.

Although the polymerizations were rapid, cross metathesis was a potential limiting problem for these polymerizations. Cross metathesis between polymer chains would scramble them leading to an increase in the polydispersity and polymers with either none or two ruthenium carbenes on their ends. Although these undesired side reactions are typically slower than ROMP of strained olefins, they are well documented for the Grubbs first generation catalyst.^{160, 161} Prior work by us and others indicated that cross metathesis would be slow and have little noticeable effect on the polymer, and experiments were carried out to confirm these results.¹²¹⁻¹²³ In one experiment, 500 equivalents of monomer A were polymerized and the polymer was studied by SEC as a function of time. The molecular weight and PDI of the polymer did not vary with time for 4 h despite the presence of the active Ru catalyst on the end of the polymer.

To further probe the effect of cross metathesis on the polymers, 500 equivalents of monomer A were polymerized followed by the addition of 100 equivalents of 4-octene. The 4-octene would lower the molecular weight of the polymer by nearly two orders of magnitude and result in a broad polydispersity if cross metathesis was rapid. Even under these conditions, the values for Mn and PDI remained mostly constant over 4 hours (Figure A.3b). This work clearly demonstrated that cross metathesis was much slower than ROMP.

Based on these experiments, tri- and tetrablock copolymers were synthesized according to Figure A.1 and the results are shown in Table A.1. The times required for each polymerization were short and were based on the kinetic experiments completed earlier. Twice the necessary time was typically used to ensure that each reaction went to >97% completion.

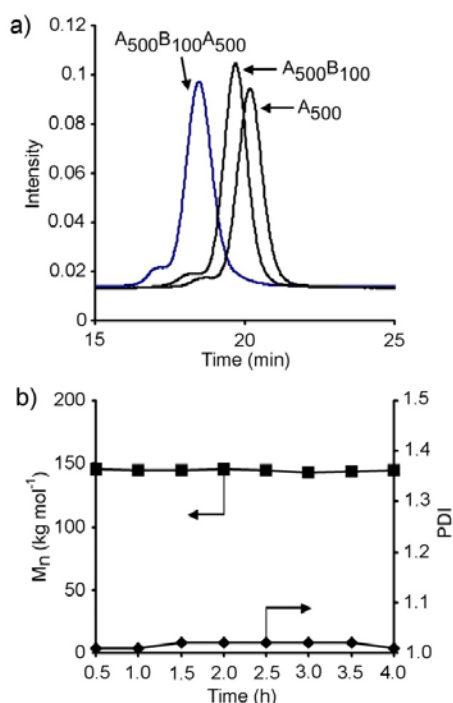


Figure A.3 Changes of SEC traces, M_n , and PDI of block polymers. a) SECs of three polymers to show the progression from a homopolymer to diblock polymer to triblock polymer. b) Monomer A (500 units) was initially polymerized to completion. Next, 100 equivalents of 4-octene were added to study the effect of cross metathesis on the polymer. The molecular weight and PDI of the polymer were consistent over four hours after the addition of 4-octene.

Table A.1 Characterization of multi-block backbones.

^a Backbone Polymer Composition	Predicted M_n (kg mol^{-1})	^b Measured M_n (kg mol^{-1})	PDI	^c Monomer concentration (mole L^{-1})	^c Polymerization time (min)
$A_{500}B_{100}A_{500}$	344	360	1.04	0.30:0.06:0.20	30:25:45
$B_{50}A_{1000}B_{50}$	344	398	1.25	0.30:0.59:0.032	51:70:90
$A_{500}C_{100}A_{500}$	369	389	1.15	0.81:0.13:0.26	30:20:40
$C_{50}A_{1000}C_{50}$	369	415	1.17	0.17:0.66:0.02	15:65:60
$C_{20}A_{200}C_{10}A_{200}$	142	138	1.35	0.18:0.75:0.04:0.31	15:25:20:40
$A_{200}C_{10}A_{750}C_{100}$	359	407	1.17	0.87:0.03:0.65:0.08	20:15:60:35
$A_{500}B_{100}A_{500}$	344	419	1.12	0.33:0.05:0.15	43:21:44
$A_{300}B_{100}A_{300}$	220	268	1.06	0.33:0.08:0.14	26:15:36
$A_{500}B_{100}A_{500}$	343	344	1.05	0.33:0.05:0.15	30:15:41

^aThe numbers in subscript refer to the degree of polymerization of each monomer.

^bMeasured M_n by SEC with light scattering and refractive index detectors. ^cThe monomer concentration and polymerization times for each block polymerization.

In Figure A.3, the SEC traces of a series of block polymers are shown to demonstrate the clean conversion of each polymer to the subsequent block copolymer. First, 500 equivalents of monomer A were polymerized to yield a homopolymer displaying the Grubbs catalyst at the end of each polymer chain. A small high molecular weight peak was seen in the SEC, and this peak was still present after 100 equivalents of B and another 500 equivalents of A were block polymerized onto the initial polymer. This peak was studied by Register et al. and was found to be due to the a cross metathesis reaction between two polymer chains that resulted in a small fraction of polymer with ruthenium carbenes on each end.^{203, 204} This peak has been observed by other groups including, most recently, the Grubbs group.²⁰⁴ Despite this peak, the measured molecular weights agreed with the predicted molecular weights and the polymers had low PDIs (typically below 1.25). No evidence of unreacted A₅₀₀ or A₅₀₀B₁₀₀ was observed in the SEC trace of the final triblock polymer, which demonstrated clean conversion of these polymerizations.

After completion of the polymerizations, the backbone was hydrogenated according to our previously described method outlined in the experimental section.¹²² Both silica gel and 5x to 10x equivalents of the Grubbs catalyst were added and the reaction vessel was pressurized with approximately 1,000 psi of H₂. The excess Grubbs catalyst was added to provide more Ru metal to act as a hydrogenation catalyst. The reactor was heated to 50 °C for 18 h to hydrogenate the backbone. Greater than >97% of the olefins along the backbone were hydrogenated as judged by the lack of olefin hydrogens in the ¹H NMR spectra. This method was robust and successful for all of the polymers in Table A.1. Thus, a blocky polymer was synthesized and the backbone was hydrogenated in one reactor without intervening cleaning steps.

The polymers were hydrogenated to increase their resistance to oxidation and to limit side reactions when styrene was polymerized from them via atom transfer radical

polymerization (ATRP). Monomers B and C exposed one or two ATRP initiators that were useful for the synthesis of polystyrene under modified, dilute ATRP conditions (Figure A.1 and Table A.2). The experimental aspects of these polymerizations were reported elsewhere, but it is noted that they were completed at low concentrations to yield comb polymers that were not cross-linked but readily characterized by SEC.¹²¹⁻¹²³ Comb polymers with low to moderate molecular weight arms were emphasized such that the comb polymers would assemble well in the solid state.

The comb polymers and arms were each characterized by SEC with refractive index and multiangle laser light scattering detectors to measure their molecular weights and PDIs. Because the arms were readily cleaved from the backbone polymers under basic conditions, it was simple to characterize the molecular weights of the arms independent of the backbone (Figure A.1). The PDIs of the arms were low and consistent with what was observed before for these polymerizations.^{184, 188} The molecular weights of the comb polymers were predicted from the composition of the backbone polymer and the molecular weights of the arms; these values matched the measured molecular weights with a reasonable degree of accuracy. The PDIs were low for the comb polymers which reflected the low PDIs for the backbone polymers and arms.

Although these comb polymers had molecular weights of several hundred thousand to two million grams per mole, they assembled in the solid state into well-ordered arrays. In prior work, we demonstrated that comb diblock copolymers assembled in the solid state into ordered arrays; here, we extend this result to include more complex comb tri- and tetrablock copolymers.¹²³ In Figure A.4 we show two representative examples of assembled polymers. In each of these examples, the polymer was dissolved in methylene chloride at approximately 10 mg/mL, the solvent was allowed to evaporate, and the resulting polymer was solvent annealed for three days by placing it under static vacuum with methylene chloride.

Table A.2 Characterization of multi-block comb polymers.

^a Comb block Polymer	^b Predicted Mn (kg mol ⁻¹)	^c Measured Mn (kg mol ⁻¹)	PDI	^d R _z (nm)	^e R _h (nm)	^f Arms Mn (g mol ⁻¹)
A ₅₀₀ B _{100:1430} A ₅₀₀	487	552	1.14	56.5	45.5	1,430
A ₅₀₀ B _{100:4630} A ₅₀₀	807	1,267	1.27	41.2	26.8	4,630
A ₅₀₀ B _{100:3950} A ₅₀₀	739	756	1.15	51.6	22.4	3,950
A ₅₀₀ B _{100:11400} A ₅₀₀	1,480	2,080	1.16	37.2	26.0	11,400
B _{50:5190} A ₁₀₀₀ B _{50:5190}	863	614	1.21	38.6	21.7	5,190
B _{50:8530} A ₁₀₀₀ B _{50:8530}	1,197	1,530	1.43	57.3	28.6	8,530
A ₅₀₀ C _{100:2740} A ₅₀₀	917	753	1.16	29.3	20.0	2,740
A ₅₀₀ C _{100:3370} A ₅₀₀	1,043	900	1.18	28.5	21.0	3,370
A ₅₀₀ C _{100:6810} A ₅₀₀	1,731	1,587	1.17	31.0	22.7	6,810
A ₅₀₀ C _{100:7280} A ₅₀₀	1,826	1,506	1.14	27.8	21.5	7,280
C _{50:1830} A ₁₀₀₀ C _{50:1830}	732	477	1.20	33.9	19.7	1,830
C _{50:4700} A ₁₀₀₀ C _{50:4700}	1,309	983	1.17	38.6	21.7	4,700
C _{50:6520} A ₁₀₀₀ C _{50:6520}	1,672	1,451	1.22	35.6	20.2	6,520
C _{50:4750} A ₁₀₀₀ C _{50:4750}	1,320	726	1.17	32.4	18.5	4,750
C _{20:4050} A ₂₀₀ C _{10:4050} A ₂₀₀	385	314	1.18	21.2	13.6	4,050
A ₂₀₀ C _{10:3280} A ₇₅₀ C _{100:3280}	1,080	820	1.13	30.0	19.1	3,280
A ₅₀₀ B _{100:3240} A ₅₀₀	656	655	1.03	22.3	17.6	3,240
A ₃₀₀ B _{100:8710} A ₃₀₀	1,033	1,298	1.10	24.1	16.6	8,710
A ₃₀₀ B _{100:5770} A ₃₀₀	762	785	1.07	19.6	14.8	5,770
A ₃₀₀ B _{100:13200} A ₃₀₀	1,189	1,177	1.13	29.7	19.5	13,200
A ₃₀₀ B _{100:3550} A ₃₀₀	595	526	1.04	17.5	13.8	3,550
A ₅₀₀ B _{100:4120} A ₅₀₀	688	617	1.06	20.1	16.8	4,120
A ₅₀₀ B _{100:2680} A ₅₀₀	625	496	1.07	23.2	16.7	2,680
A ₅₀₀ B _{100:7420} A ₅₀₀	1,198	1,023	1.06	24.8	17.9	7,420
A ₅₀₀ B _{100:1390} A ₅₀₀	448	354	1.08	29.0	24.1	1,390
A ₅₀₀ B _{100:12400} A ₅₀₀	1,906	1,580	1.13	28.6	19.7	12,400
A ₅₀₀ B _{100:3800} A ₅₀₀	750	581	1.08	24.4	16.8	3,800
A ₅₀₀ B _{100:4710} A ₅₀₀	875	614	1.08	20.7	16.5	4,710

^a) The numbers in subscript refer to the degree of polymerization of each block along the backbone and to the molecular weights of the polystyrene arms. ^b) The Mn is predicted based on the measured molecular weight of the backbone polymer, the composition of the backbone polymer, and the measured molecular weights of the arms. ^c) Measured using SEC with light scattering and refractive index detectors. ^d) Radius of gyration. ^e) Hydrodynamic radius. ^f) The arms were cleaved from the backbone according to Figure 1 and characterized by SEC.

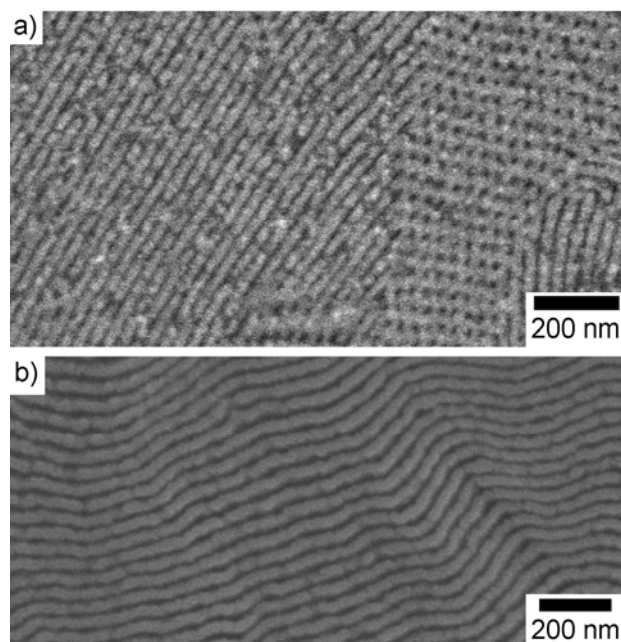


Figure A.4 SEM micrographs of morphologies of a) $A_{200}C_{10:3280}A_{750}C_{100:3280}$ and b) $A_{500}B_{100:1430}A_{500}$ that were assembled in the solid state.

SEM micrographs are shown of well-ordered cylindrical and lamellar morphologies that were assembled from two different polymers (Figure A.4). Polymer labeled $A_{200}C_{10:3280}A_{750}C_{100:3280}$ (the numbers in subscripts refer to the degree of polymerization of each monomer along the backbone polymer and the Mn of the polystyrene arms) assembled into the cylindrical morphology with a domain size of approximately 60 nm and polymer $A_{500}B_{100:1430}A_{500}$ assembled into a lamellar morphology with a domain size of approximately 52 nm. These results are particularly notable because the polymers had complex architectures and molecular weights of 820,000 and 552,000 g mol^{-1} ; yet, they assembled under standard conditions.

Conclusions

In summary, we report the first examples of high molecular weight triblock copolymers and the first tetrablock copolymers synthesized from the Grubbs first generation catalyst. This result is important because it extends the types and molecular weights of block copolymers that can be polymerized with this commercially available, important catalyst. Oxanorbornene monomers were chosen for this work because of their high rates of polymerization and ease of synthesis. These monomers are simple to fabricate in hundred-gram quantities and can be functionalized to display a variety of different groups. Architecturally complex comb tri- and tetrablock copolymers were synthesized and assembled in the solid state into ordered morphologies. The structure-property relationship of these polymers will be studied in future work.

(This work was published in *Macromol. Rapid Commun.* **2009**, *30*, 1392-1398.)

REFERENCES

1. Varghese, S.; Elisseeff, J., Hydrogels for musculoskeletal tissue engineering. *Adv. polym. sci.* **2006**, *203*, 95-144.
2. Di Lullo, G. A.; Sweeney, S. M.; Körkkö, J.; Ala-Kokko, L.; San Antonio, J. D., Mapping the ligand-binding sites and disease-associated mutations on the most abundant protein in the human, Type I Collagen. *J. Biol. Chem.* **2002**, *277*, 4223-4231.
3. Lee, C. H.; Singla, A.; Lee, Y., Biomedical applications of collagen. *Int. J. Pharm.* **2001**, *221*, 1-22.
4. Hayashi, T., Biodegradable polymers for biomedical uses. *Prog. Polym. Sci.* **1994**, *19*, 663-702.
5. Currie, L. J.; Sharpe, J. R.; Martin, R., The use of fibrin glue in skin grafts and tissue-engineered skin replacements: a review. *Plast. Reconstr. Surg.* **2001**, *108*, 1713-1726.
6. Tonnesen, H. H.; Kalsen, J., Alginate in drug delivery systems. *Drug Dev. Ind. Pharm.* **2002**, *28*, 621-630.
7. Fraser, J. R. E.; Laurent, T. C.; Laurent, U. B. G., Hyaluronan: its nature, distribution, functions and turnover. *J. Intern. Med.* **1997**, *242*, 27-33.
8. Campoccia, D.; Hunt, J. A.; Doherty, P. J.; Zhong, S. P.; Callegaro, L.; Benedetti, L.; Williams, D. F., Human neutrophil chemokinesis and polarization induced by hyaluronic acid derivatives. *Biomaterials* **1993**, *14*, 1135-1139.
9. Goldberg, V. M.; Buckwalter, J. A., Hyaluronans in the treatment of osteoarthritis of the knee: evidence for disease-modifying activity. *Osteoarthritis Cartilage* **2005**, *13*, 216-224.
10. Grigolo, B.; Roseti, L.; Fiorini, M.; Fini, M.; Giavaresi, G.; Nicoli Aldini, N.; Giardino, R.; Facchini, A., Transplantation of chondrocytes seeded on a hyaluronan derivative (Hyaff®-11) into cartilage defects in rabbits. *Biomaterials* **2001**, *22*, 2417-2424.
11. Chenite, A.; Chaput, C.; Wang, D.; Combes, C.; Buschmann, M. D.; Hoemann, C. D.; Leroux, J. C.; Atkinson, B. L.; Binette, F.; Selmani, A., Novel injectable neutral solutions of chitosan form biodegradable gels in situ. *Biomaterials* **2000**, *21*, 2155-2161.
12. Austin, P. R.; Brine, C. J.; Castle, J. E.; Zikakis, J. P., Chitin: new facets of research. *Science* **1981**, *212*, 49-753.
13. Taravel, M. N.; Domard, A., Relation between the physicochemical characteristics of collagen and its interactions with chitosan: I. *Biomaterials* **1993**, *14*, 930-938.
14. Hejazi, R.; Amiji, M., Chitosan-based gastrointestinal delivery systems. *J. Controlled Release* **2003**, *89*, 151-165.

15. Azad, A. K.; Sermsintham, N.; Chandkrachang, S.; Stevens, W. F., Chitosan membrane as a wound-healing dressing: characterization and clinical application. *J. Biomed. Mater. Res. Part B: Appl. Biomater.* **2004**, *69B*, 216-222.
16. Madihally, S. V.; Matthew, H. W. T., Porous chitosan scaffolds for tissue engineering. *Biomaterials* **1999**, *20*, 1133-1142.
17. Rimnac, C. M.; Kurtz, S. M., Ionizing radiation and orthopaedic prostheses. *Nucl. Instrum. Methods Phys. Res. Sect. B* **2005**, *236*, 30-37.
18. Kurtz, S. M.; Muratoglu, O. K.; Evans, M.; Edidin, A. A., Advances in the processing, sterilization, and crosslinking of ultra-high molecular weight polyethylene for total joint arthroplasty. *Biomaterials* **1999**, *20*, 1659-1688.
19. Edidin, A. A.; Kurtz, S. M., Influence of mechanical behavior on the wear of 4 clinically relevant polymeric biomaterials in a hip simulator. *J. Arthroplasty* **2000**, *15*, 321-331.
20. Langer, R., Polymer-controlled drug delivery systems. *Acc. Chem. Res.* **1993**, *26*, 537-542.
21. Pillai, O.; Panchagnula, R., Polymers in drug delivery. *Curr. Opin. Chem. Biol.* **2001**, *5*, 447-451.
22. Dunn, R. L.; Ottenbrite, R. M., *Polymeric drugs and drug delivery systems*. ed.; American Chemical Society: Washington D.C., 1990; Vol. p 11-23.
23. Griffith, L. G., Polymeric biomaterials. *Acta Mater.* **2000**, *48*, 263-277.
24. Cuchiara, M. P.; Allen, A. C. B.; Chen, T. M.; Miller, J. S.; West, J. L., Multilayer microfluidic PEGDA hydrogels. *Biomaterials* **2010**, *31*, 5491-5497.
25. Mintzer, M. A.; Simanek, E. E., Nonviral vectors for gene delivery. *Chem. Rev.* **2008**, *109*, 259-302.
26. Bonassar, L. J.; Vacanti, C. A., Tissue engineering: the first decade and beyond. *J. Cell. Biochem. Suppl.* **1998**, *72*, 297-303.
27. Woodfield, T. B. F.; Malda, J.; de Wijn, J.; Péters, F.; Riesle, J.; van Blitterswijk, C. A., Design of porous scaffolds for cartilage tissue engineering using a three-dimensional fiber-deposition technique. *Biomaterials* **2004**, *25*, 4149-4161.
28. Sachlos, E.; Czernuszka, J. T., Making tissue engineering scaffolds work. Review on the application of solid freeform fabrication technology to the production of tissue engineering scaffolds. *Eur. Cell. Mater.* **2003**, *5*, 29-40.
29. Peppas, N. A.; Bures, P.; Leobandung, W.; Ichikawa, H., Hydrogels in pharmaceutical formulations. *Eur. J. Pharm. Biopharm.* **2000**, *50*, 27-46.
30. West, J. L.; Hubbell, J. A., Photopolymerized hydrogel materials for drug delivery applications. *React. Polym.* **1995**, *25*, 139-147.

31. Nguyen, K. T.; West, J. L., Photopolymerizable hydrogels for tissue engineering applications. *Biomaterials* **2002**, *23*, 4307-4314.
32. Shung, A. K.; Behraves, E.; Jo, S.; Mikos, A. G., Crosslinking characteristics of and cell adhesion to an injectable poly(propylene fumarate-co-ethylene glycol) hydrogel using a water-soluble crosslinking system. *Tissue Eng.* **2003**, *9*, 243-254.
33. Elisseeff, J.; McIntosh, W.; Anseth, K.; Riley, S.; Ragan, P.; Langer, R., Photoencapsulation of chondrocytes in poly(ethylene oxide)-based semi-interpenetrating networks. *J. Biomed. Mater. Res.* **2000**, *51*, 164-171.
34. Elisseeff, J.; Anseth, K.; Sims, D.; McIntosh, W.; Randolph, M.; Langer, R., Transdermal photopolymerization for minimally invasive implantation. *Proc. Natl. Acad. Sci. USA* **1999**, *96*, 3104-3107.
35. Olson, H. E.; Rooney, G. E.; Gross, L.; Nesbitt, J. J.; Galvin, K. E.; Knight, A.; Chen, B.; Yaszemski, M. J.; Windebank, A. J., Neural stem cell- and schwann cell-loaded biodegradable polymer scaffolds support axonal regeneration in the transected spinal cord. *Tissue Eng. Part A* **2009**, *15*, 1797-1805.
36. Wang, S.; Yaszemski, M. J.; Knight, A. M.; Gruetzmacher, J. A.; Windebank, A. J.; Lu, L., Photo-crosslinked poly([epsilon]-caprolactone fumarate) networks for guided peripheral nerve regeneration: material properties and preliminary biological evaluations. *Acta Biomater.* **2009**, *5*, 1531-1542.
37. Thombre, A. G.; Appel, L. E.; Chidlaw, M. B.; Daugherty, P. D.; Dumont, F.; Evans, L. A. F.; Sutton, S. C., Osmotic drug delivery using swellable-core technology. *J. Controlled Release* **2004**, *94*, 75-89.
38. Kipper, M. J.; Shen, E.; Determan, A.; Narasimhan, B., Design of an injectable system based on bioerodible polyanhydride microspheres for sustained drug delivery. *Biomaterials* **2002**, *23*, 4405-4412.
39. Kumar, N.; Langer, R. S.; Domb, A. J., Polyanhydrides: an overview. *Adv. Drug Delivery Rev.* **2002**, *54*, 889-910.
40. Domb, A.; Amselem, S.; Shah, J.; Maniar, M., Polyanhydrides: synthesis and characterization. *Biopolymers I* **1993**, *107*, 93-141.
41. Domb, A. J.; Langer, R., Polyanhydrides. I. Preparation of high molecular weight polyanhydrides. *J. Polym. Sci., Part A: Polym. Chem.* **1987**, *25*, 3373-3386.
42. Domb, A. J.; Ron, E.; Langer, R., Poly(anhydrides). 2. One-step polymerization using phosgene or diphosgene as coupling agents. *Macromolecules* **1988**, *21*, 1925-1929.
43. Leong, K. W.; Simonte, V.; Langer, R., Synthesis of polyanhydrides: melt-polycondensation, dehydrochlorination, and dehydrative coupling. *Macromolecules* **1987**, *20*, 705-712.
44. Dang, W.; Daviau, T.; Ying, P.; Zhao, Y.; Nowotnik, D.; Clow, C. S.; Tyler, B.; Brem, H., Effects of GLIADEL® wafer initial molecular weight on the erosion of wafer and release of BCNU. *J. Controlled Release* **1996**, *42*, 83-92.

45. Park, M.; Weaver Jr, C.; Donahue, J.; Sampath, P., Intracavitary chemotherapy (Gliadel®) for recurrent esthesioneuroblastoma: case report and review of the literature. *J. Neuro-Oncol.* **2006**, *77*, 47-51.
46. Doiron, A.; Homan, K.; Emelianov, S.; Brannon-Peppas, L., Poly(lactic-co-glycolic) acid as a carrier for imaging contrast agents. *Pharm. Res.* **2009**, *26*, 674-682.
47. Chasin, M.; Langer, R., *Biodegradable polymers as drug delivery systems*. ed.; Marcel Dekker: New York, NY, 1990; Vol. 45, p 1-41.
48. Jenkins, M., *Biomedical polymers*. ed.; Woodhead Publishing and Maney Publishing: Boca Raton, FL, 2007; Vol. p 83-110.
49. Stridsberg, K.; Ryner, M.; Albertsson, A.-C., Controlled ring-opening polymerization: polymers with designed macromolecular architecture. *Adv. polym. Sci.* **2002**, *157*, 41-65.
50. Chasin, M.; Langer, R., *Biodegradable polymers as drug delivery systems*. ed.; Marcel Dekker: New York, NY, 1990; Vol. 45, p 71-120.
51. Kaihara, S.; Matsumura, S.; Mikos, A. G.; Fisher, J. P., Synthesis of poly(L-lactide) and polyglycolide by ring-opening polymerization. *Nat. Protocol.* **2007**, *2*, 2767-2771.
52. Bailey, W. J.; Ni, Z.; Wu, S.-R., Synthesis of poly-ε-caprolactone via a free radical mechanism. Free radical ring-opening polymerization of 2-methylene-1,3-dioxepane. *J. Polym. Sci., Polym. Chem. Ed.* **1982**, *20*, 3021-3030.
53. Garlotta, D., A literature review of poly(lactic acid). *J. Polym. Environ.* **2001**, *9*, 63-84.
54. Ignatius, A. A.; Claes, L. E., In vitro biocompatibility of bioresorbable polymers: poly(, -lactide) and poly(-lactide-co-glycolide). *Biomaterials* **1996**, *17*, 831-839.
55. Anderson, J. M.; Shive, M. S., Biodegradation and biocompatibility of PLA and PLGA microspheres. *Adv. Drug Delivery Rev.* **1997**, *28*, 5-24.
56. Mundargi, R. C.; Babu, V. R.; Rangaswamy, V.; Patel, P.; Aminabhavi, T. M., Nano/micro technologies for delivering macromolecular therapeutics using poly(d,l-lactide-co-glycolide) and its derivatives. *J. Controlled Release* **2008**, *125*, 193-209.
57. Green, J. J.; Langer, R.; Anderson, D. G., A combinatorial polymer library approach yields insight into nonviral gene delivery. *Acc. Chem. Res.* **2008**, *41*, 749-759.
58. Thomas, M.; Klibanov, A. M., Enhancing polyethylenimine's delivery of plasmid DNA into mammalian cells. *Proc. Natl. Acad. Sci. USA* **2002**, *99*, 14640-14645.
59. Cao, J.; Langer, R., Nanotechnology in drug delivery and tissue engineering: from discovery to applications. *Nano Lett.* **2010**, *10*, 3223-3230.

60. Green, J. J.; Langer, R.; Anderson, D. G., A combinatorial polymer library approach yields insight into nonviral gene delivery. *Acc. Chem. Res.* **2008**, *41*, 749-759.
61. Jabbari, E.; Lu, L.; Yaszemski, M. J., Synthesis and characterization of injectable and biodegradable composites for orthopedic applications. *Handbook of biodegradable polymeric materials and their applications* **2006**, *2*, 239-270.
62. Nguyen, D. N.; Green, J. J.; Chan, J. M.; Langer, R.; Anderson, D. G., Polymeric materials for gene delivery and DNA vaccination. *Adv. Mater.* **2009**, *21*, 847-867.
63. Peter, S. J.; Miller, M. J.; Yasko, A. W.; Yaszemski, M. J.; Mikos, A. G., Polymer concepts in tissue engineering. *J. Biomed. Mater. Res.* **1998**, *43*, 422-427.
64. Twaites, B.; de las Heras Alarcon, C.; Alexander, C., Synthetic polymers as drugs and therapeutics. *J. Mater. Chem.* **2005**, *15*, 441-445.
65. Anderson, D. G.; Nurdick, J. A.; Langer, R., Materials science: smart biomaterials. *Science* **2004**, *305*, 1923-1924.
66. Ciuffarin, E.; Gambarotta, S.; Isola, M.; Senatore, L., Chemistry of sulphenates in acidic media. *J. C. S. Perkin II* **1978**, 554-557.
67. Saito, G.; Swanson, J. A.; Lee, K.-D., Drug delivery strategy utilizing conjugation via reversible disulfide linkages: role and site of cellular reducing activities. *Adv. Drug Delivery Rev.* **2003**, *55*, 199-215.
68. Arima, H.; Motoyama, K., Recent findings concerning PAMAM dendrimer conjugates with cyclodextrins as carriers of DNA and RNA. *Sensors* **2009**, *9*, 6346-6361.
69. Meng, H. X., M.; Xia, T.; Zhao, Y.-L.; Tamaoi, F.; Stoddart, J. F.; Zink, J. I.; Nel, A. E., Autonomous in vitro anticancer drug release from mesoporous silican nanoparticles by pH-sensitive nanovalves. *J. Am. Chem. Soc.* **2010**, *132*, 12690-12697.
70. Mohanad, M.; Dixon, A. S.; Lim, C. S., Controlling subcellular delivery to optimize therapeutic effect. *Therapeutic Del.* **2010**, *1*, 169-193.
71. Oh, K. T.; Yin, H.; Lee, E. S.; Bae, Y. H., Polymeric nanovheicles for anticancer drugs with triggering release mechanisms. *J. Mater. Chem.* **2007**, *17*, 3987-4001.
72. Kroeze, R. J.; Helder, M. N.; Govaert, L. E.; Smit, T. H., Biodegradable polymers in bone tissue engineering. *Materials* **2009**, *2*, 833-856.
73. Kohane, D. S.; Langer, R., Biocompatibility and drug delivery systems. *Chem. Sci.* **2010**, *1*, 441-446.
74. Kwon, G. S.; Furgeson, D. Y., Biodegradable polymers for drug delivery systems. *Biomedical polymers* **2007**, 83-110.
75. Vert, M., Degradable and bioresorbable polymers in surgery and pharmacology: beliefs and facts. *J. Mater. Sci.: Mater. Med.* **2009**, *20*, 437-446.

76. Williams, C. K., Synthesis of functionalized biodegradable polyesters. *Chem. Soc. Rev.* **2007**, *36*, 1573-1580.
77. Capozzi, G.; Modena, G.; Pasquato, L., *The chemistry of sulphenic acids and their derivatives*. ed.; John Wiley & Sons: New York, 1990; Vol. p 819.
78. Craine, L.; Raban, M., The chemistry of sulfenamides. *Chem. Rev.* **1989**, *89*, 689-712.
79. Guarino, V. R.; Karunaratne, V.; Stella, V. J., Sulfenamides as prodrugs of NH-acidic compounds: a new prodrug option for the amide bond. *Bioorg. Med. Chem. Lett.* **2007**, *17*, 4910-4913.
80. Knapp, S.; Darout, E.; Amorelli, B., New glycomimetics: anomeric sulfonates, sulfenamides, and sulfonamides. *J. Org. Chem.* **2006**, *71*, 1380-1389.
81. Koval, I. V., Synthesis and applications of sulfenamides. *Russian Chem. Rev.* **1996**, *65*, 421-440.
82. Matsuo, J.-I.; Kawana, A.; Yamanaka, H.; Mukaiyama, T., Sulfenamide-catalyzed oxidation of primary and secondary alcohols with molecular bromine. *Chem. Lett.* **2003**, *32*, 182-183.
83. Hemenway, J. N.; Nti-Addae, K.; Guarino, V. R.; Stella, V. J., Preparation, characterization, and in vivo conversion of new water-soluble sulfenamide prodrugs of carbamazepine. *Bioorg. Med. Chem. Lett.* **2007**, *17*, 6629-6632.
84. Lopez, M.; Drilland, N.; Bornaghi, L. F.; Poulsen, S.-A., Synthesis of S-glycosyl primary sulfonamides. *J. Org. Chem.* **2009**, *74*, 2811-2816.
85. Owen, D. J.; Davis, C. B.; Hartnell, R. D.; Madge, P. D.; Thomson, R. J.; Chong, A. K. J.; Coppel, R. L.; von Itzstein, M., Synthesis and evaluation of galactofuranosyl N,N-dialkyl sulfenamides and sulfonamides as antimycobacterial agents. *Bioorg. Med. Chem. Lett.* **2007**, *17*, 2274-2277.
86. Elfinger, M.; Uezguen, S.; Rudolph, C., Nanocarriers for gene delivery -- polymer structure, targeting ligands, and controlled-release devices. *Curr. Nanoscience* **2008**, *4*, 322-353.
87. Gaucher, G.; Marchessault, R. H.; Leroux, J.-C., Polyester-based micelles and nanoparticles for the parenteral delivery of taxanes. *J. Controlled Release* **2010**, *143*, 2-12.
88. Lee, S. S.; Hughes, P.; Ross, A. D.; Robinson, M. R., Biodegradable implants for sustained drug release in the eye. *Pharm. Res.* **2010**, *27*, 2043-2053.
89. Malyala, P.; O'Hagan, D. T.; Singh, M., Enhancing the therapeutic efficacy of CpG oligonucleotides using biodegradable microparticles. *Adv. Drug Delivery Rev.* **2009**, *6*, 218-225.
90. Kice, J. L., Mechanisms and reactivity in reactions of organic oxyacids of sulfur and their anhydrides. *Adv. Phys. Org. Chem.* **1980**, *17*, 65-181.

91. Nagy, P.; Ashby, M. T., Reactive sulfur species: kinetics and mechanism of the hydrolysis of cysteine thiosulfinate ester. *Chem. Res. Toxicol.* **2007**, *20*, 1364-1372.
92. Freeman, F.; Kodera, Y., Garlic chemistry: stability of S-(2-propenyl) 2-propene-1-sulfinothioate (allicin) in blood, solvents, and simulated physiological fluids. *J. Agric. Food Chem.* **1995**, *43*, 2332-2338.
93. Nagy, P.; Ashby, M. T., Reactive sulfur species: kinetics and mechanism of the oxidation of cystine by hypochlorous acid to give *N,N'*-dichlorocystine. *Chem. Res. Toxicol.* **2005**, *18*, 919-923.
94. Kice, J. L.; Rogers, T. E., Mechanism of the alkaline hydrolysis of aryl thiosulfonates and thiosulfonates. *J. Am. Chem. Soc.* **1974**, *96*, 8009-8014.
95. Buncl, E.; Um, I.-H., The α -effect and its modulation by solvent. *Tetrahedron* **2004**, *60*, 7801-7825.
96. Anslyn, E. V.; Dougherty, D. A., *Modern physical organic chemistry*. ed.; University Science Books: Sausalito, California, 2006; Vol. p 1099.
97. Branchaud, B. P., Studies on the preparation and reactions of tritylsulfenimines. *J. Org. Chem.* **1983**, *48*, 3531-3538.
98. Henke, A.; Srogl, J., Thioimides: new reagents for effective synthesis of thioesters from carboxylic acids. *J. Org. Chem.* **2008**, *73*, 7783-7784.
99. Freeman, F.; Keindl, M. C., A facile synthesis of symmetrical alkanesulfonothioic *S*-alkyl esters (*S*-alkyl alkanethiosulfonates). *Synthesis* **1983**, 913-915.
100. Freeman, F.; Angeletakis, C. N., Carbon-13 nuclear magnetic resonance study of the conformations of disulfides and their oxide derivatives. *J. Org. Chem.* **1982**, *47*, 4194-4200.
101. Freeman, F.; Angeletakis, C. N.; Maricich, T. J., ^1H NMR and ^{13}C NMR spectra of disulfides, thiosulfonates and thiosulfonates. *Org. Magn. Reson.* **1982**, *17*, 53-58.
102. Harpp, D. N.; Gingras, M.; Aida, T.; Chan, T. H., Bis(tributyltin) sulfide: an effective and general sulfur-transfer reagent. *Synthesis* **1987**, *12*, 1122-1124.
103. Kapanda, C. N.; Muccioli, G. G.; Labar, G.; Poupaert, J. H.; Lambert, D. M., Bis(dialkylaminethiocarbonyl)disulfides as potent and selective monoglyceride lipase inhibitors. *J. Med. Chem.* **2009**, *52*, 7310-7314.
104. Sun, R.; Zhang, Y.; Chen, L.; Li, Y.; Li, Q.; Song, H.; Huang, R.; Bi, F.; Wang, Q., Design, synthesis, and insecticidal activities of new *N*-benzoyl-*N'*-phenyl-*N'*-sulfenylureas. *J. Agric. Food Chem.* **2009**, *57*, 3661-3668.
105. Alfred, S. F.; Al-Badri, Z. M.; Madkour, A. E.; Lienkamp, K.; Tew, G. N., Water soluble poly(ethylene oxide) functionalized norbornene polymers. *J. Polym. Sci., Part A: Polym. Chem.* **2008**, *46*, 2640-2648.
106. Bernaerts, K. V.; Fustin, C.-A.; Bomal-D'Haese, C.; Gohy, J.-F.; Martins, J. C.; Du Prez, F. E., Advanced polymer architectures with stimuli-responsive properties starting from inimers. *Macromolecules* **2008**, *41*, 2593-2606.

107. Chambon, P.; Fernyhough, C. M.; Im, K.; Chang, T.; Das, C.; Embery, J.; McLeish, T. C. B.; Read, D. J., Synthesis, temperature gradient interaction chromatography, and rheology of entangled styrene comb polymers. *Macromolecules* **2008**, *41*, 5869-5875.
108. Johnson, J. A.; Lu, Y. Y.; Burts, A. O.; Lim, Y.-H.; Finn, M. G.; Koberstein, J. T.; Turro, N. J.; Tirrell, D. A.; Grubbs, R. H., Core-clickable PEG-branch-azide bivalent-bottle-brush polymers by ROMP: grafting-through and clicking-to. *J. Am. Chem. Soc.* **2011**, *133*, 559-566.
109. Lanson, D.; Ariura, F.; Schappacher, M.; Borsali, R.; Deffieux, A., Comb copolymers with polystyrene and polyisoprene branches: effect of block topology on film morphology. *Macromolecules* **2009**, *42*, 3942-3950.
110. Lanson, D.; Schappacher, M.; Borsali, R.; Deffieux, A., Poly(styrene)comb-*b*-poly(ethylene oxide)comb copolymers: synthesis and AFM investigation of intra- and supramolecular organization as thin deposits. *Macromolecules* **2007**, *40*, 9503-9509.
111. Lee, J. H.; Driva, P.; Hadjichristidis, N.; Wright, P. J.; Rucker, S. P.; Lohse, D. J., Damping behavior of entangled comb polymers: experiment. *Macromolecules* **2009**, *42*, 1392-1399.
112. Nikopoulou, A.; Iatrou, H.; Lohse, D. J.; Hadjichristidis, N., Synthesis of exact comb polybutadienes with two and three branches. *J. Polym. Sci., Part A: Polym. Chem.* **2009**, *47*, 2597-2607.
113. Rekha, N.; Asha, S. K., Solvent-induced self-assembly in cardanol-based urethane methacrylate comb polymers. *J. Polym. Sci., Part A: Polym. Chem.* **2009**, *47*, 2996-3009.
114. Runge, M. B.; Yoo, J.; Bowden, N. B., Synthesis of comb tri- and tetrablock copolymers catalyzed by the Grubbs first generation catalyst. *Macromol. Rapid Commun.* **2009**, *30*, 1392-1398.
115. Schappacher, M.; Deffieux, A., Atomic force microscopy imaging and dilute solution properties of cyclic and linear polystyrene combs. *J. Am. Chem. Soc.* **2008**, *130*, 14684-14689.
116. Sun, R.; Wang, G.; Liu, C.; Huang, J., Preparation of comb-like copolymers with amphiphilic poly(ethylene oxide)-*b*-polystyrene graft chains by combination of "graft from" and "graft onto" strategies. *J. Polym. Sci., Part A: Polym. Chem.* **2009**, *47*, 1930-1938.
117. Weber, C.; Becer, C. R.; Hoogenboom, R.; Schubert, U. S., Lower critical solution temperature behavior of comb and graft shaped poly[oligo(2-ethyl-2-oxazoline)methacrylate]s. *Macromolecules* **2009**, *42*, 2965-2971.
118. Benhabbour, S. R.; Parrott, M. C.; Gratton, S. E. A.; Adronov, A., Synthesis and properties of carborane-containing dendronized polymers. *Macromolecules* **2007**, *40*, 5678-5688.

119. Canilho, N.; Kaseemi, E.; Schlueter, A. D.; Mezzenga, R., Comblike liquid-crystalline polymers from ionic complexation of dendronized polymers and lipids. *Macromolecules* **2007**, *40*, 2822-2830.
120. Jha, S.; Dutta, S.; Bowden, N. B., Synthesis of ultralarge molecular weight bottlebrush polymers using Grubbs' catalysts. *Macromolecules* **2004**, *37*, 4365-4374.
121. Runge, M. B.; Bowden, N. B., Synthesis of high molecular weight comb block copolymers and their assemble into ordered morphologies in the solid state. *J. Am. Chem. Soc.* **2007**, *129*, 10551-1060.
122. Runge, M. B.; Dutta, S.; Bowden, N. B., Synthesis of comb block copolymers by ROMP, ATRP and ROP and their assembly in the solid state. *Macromolecules* **2006**, *39*, 498-508.
123. Runge, M. B.; Lipscomb, C. E.; Ditzler, L. R.; Mahanthappa, M. K.; Tivanski, A. V.; Bowden, N. B., Investigation of the assembly of comb block copolymers in the solid state. *Macromolecules* **2008**, *41*, 7687-7694.
124. Samadi, F.; Wolf, B. A.; Guo, Y.; Zhang, A.; Schlueter, A. D., Branched versus linear polyelectrolytes: intrinsic viscosities of peripherically charged dendronized poly(methyl methacrylate)s and of their uncharged analogues. *Macromolecules* **2008**, *41*, 8173-8180.
125. Zhang, A.; Okrasa, L.; Pakula, T.; Schlueter, A. D., Homologous series of dendronized polymethacrylates with a methyleneoxycarbonyl spacer between the backbone and dendritic side chain: synthesis, characterization, and some bulk properties. *J. Am. Chem. Soc.* **2004**, *126*, 6658-6666.
126. Hillmyer, M. A., Polydisperse block copolymers: don't throw them away. *J. Polym. Sci. B: Polym. Sci.* **2005**, *45*, 3249-3251.
127. Epps III, T. H.; Bates, F. S., Effect of molecular weight on network formation in Linear ABC triblock copolymers. *Macromolecules* **2006**, *39*, 2676-2682.
128. Bondzic, S.; Polushkin, E.; Schouten, A. J.; Ikkala, O.; ten Brinke, G., The influence of grain size on the alignment of hexagonally ordered cylinders of self-assembled diblock copolymer-based supramolecules. *Polymer* **2007**, *48*, 4723-4732.
129. de Wit, J.; van Ekenstein, G. A.; Polushkin, E.; Kvashnina, K.; Bras, W.; Ikkala, O.; ten Brinke, G., Self-assembled poly(4-vinylpyridine)--surfactant systems using alkyl and alkoxy phenylazophenols. *Macromolecules* **2008**, *41*, 4200-4204.
130. Edrington, A. C.; Urbas, A. M.; DeRege, P.; Chem, C. X.; Swager, T. M.; Hadijchristidis, N.; Xenidou, M.; Fetters, L. J.; Joannopoulos, J. D.; Fink, Y.; Thomas, E. L., Polymer-based photonic crystals. *Adv. Mater.* **2001**, *13*, 421-425.
131. Kamp, M.; Happ, T.; Mahnkopf, S.; Forchel, A.; Anand, S.; Duan, G.-H., Photonic crystal based active optoelectronic devices. *Photonic Crystals* **2004**, 329-346.

132. Laiho, A.; Ras, R. H. A.; Valkama, S.; Ruokolainen, J.; Österbacka, R.; Ikkala, O., Control of self-assembly by charge-transfer complexation between C₆₀ fullerene and electron donating units of block copolymers. *Macromolecules* **2006**, *39*, 7648-7653.
133. Maldovan, M.; Thomas, E. L., Diamond-structured photonic crystals. *Nat. Mater.* **2004**, *3*, 593-600.
134. Mickiewicz, R. A.; Ntoukas, E.; Avgeropoulos, A.; Thomas, E. L., Phase behavior of binary blends of high molecular weight diblock copolymers with a low molecular weight triblock. *Macromolecules* **2008**, *41*, 5785-5792.
135. Urbas, A.; Sharp, R.; Fink, Y.; Thomas, E. L.; Xenidou, M.; Fetters, L. J., Tunable block copolymer/homopolymer photonic crystals. *Adv. Mater.* **2000**, *12*, 812-814.
136. Urbas, A. M.; Maldovan, M.; DeRege, P.; Thomas, E. L., Bicontinuous cubic block copolymer photonic crystals. *Adv. Mater.* **2002**, *14*, 1850-1853.
137. Valkama, S.; Nykänen, A.; Kosonen, H.; Ramani, R.; Tuomisto, F.; Engelhardt, P.; ten Brinke, G.; Ikkala, O.; Ruokolainen, J., Hierarchical porosity in self-assembled polymers: post-modification of block copolymer-phenolic resin complexes by pyrolysis allows the control of micro- and mesoporosity. *Adv. Funct. Mater.* **2007**, *17*, 183-190.
138. Yoon, J.; Lee, W.; Thomas, E. L., Self-assembly of block copolymers for photonic-bandgap materials. *MRS Bulletin* **2005**, *30*, 721-726.
139. Yoon, J.; Mathers, R. T.; Coates, G. W.; Thomas, E. L., Optically transparent and high molecular weight polyolefin block copolymers toward self-assembled photonic band gap materials. *Macromolecules* **2006**, *39*, 1913-1919.
140. Zhang, Q.; Gupta, S.; Emrick, T.; Russell, T. P., Surface-functionalized CdSe nanorods for assembly in diblock copolymer templates. *J. Am. Chem. Soc.* **2006**, *128*, 3898-3899.
141. Matyjaszewski, K.; Muller, A. H. E., *Controlled and living polymerizations: from mechanisms to applications* ed.; Wiley-YCH: Weinheim, Germany, 2009; Vol. p.
142. Johnson, J. A.; Lu, Y. Y.; Burts, A. O.; Xia, Y.; Durrell, A. C.; Tirrell, D. A.; Grubbs, R. H., Drug-loaded, bivalent-bottle-brush polymers by graft-through ROMP. *Macromolecules* **2010**, *43*, 10326-10335.
143. Xia, Y.; Olsen, B. D.; Kornfield, J. A.; Grubbs, R. H., Efficient synthesis of narrowly dispersed brush copolymers and study of their assemblies: the importance of side chain arrangement. *J. Am. Chem. Soc.* **2009**, *131*, 18525-18532.
144. Wang, Y.; Iwao, T.; Hansen, F. Y.; Peters, G. H.; Hassager, O., A theoretical study of the separation principle in size exclusion chromatography. *Macromolecules* **2010**, *43*, 1651-1659.
145. Calderara, F.; Riess, G., Characterization of polystyrene-block-poly(4-vinylpyridine) block copolymer micelles in toluene solution. *Macromol. Chem. Phys.* **1996**, *197*, 2115-2132.

146. Shen, H.; Zhang, L.; Eisenberg, A., Multiple pH-induced morphological changes in aggregates of polystyrene-block-poly(4-vinylpyridine) in DMF/H₂O mixtures. *J. Am. Chem. Soc.* **1999**, *121*, 2728-2740.
147. Aljarilla, A.; Lopez, J. C.; Plumet, J., Metathesis reactions of carbohydrates: recent highlights in cross-metathesis. *Eur. J. Org. Chem.* **2010**, *32*, 6123-6143.
148. Dias, E. L.; Nguyen, S. T.; Grubbs, R. H., Well-defined ruthenium olefin metathesis catalysts: mechanism and activity. *J. Am. Chem. Soc.* **2007**, *119*, 3887-3897.
149. Grubbs, R. H., *Handbook of Metathesis*. ed.; Wiley-VCH: Weinheim, Germany, 2003; Vol. 3, p.
150. Trnka, T. M.; Grubbs, R. H., The development of L₂X₂Ru=CHR olefin metathesis catalysts: an organometallic success story. *Acc. Chem. Res.* **2001**, *34*, 18-29.
151. van der Eide, E. F.; Piers, W. E., Mechanistic insights into the ruthenium-catalyzed diene ring-closing metathesis reaction. *Nat. Chemistry* **2010**, *2*, 571-576.
152. Vougioukalakis, G. C.; Grubbs, R. H., Ruthenium-based heterocyclic carbene-coordinated olefin metathesis catalysts. *Chem. Rev.* **2010**, *110*, 1746-1787.
153. Romero, P. E.; Peirs, W. E., Mechanistic studies on 14-electron ruthenacyclobutanes: degenerate exchange with free ethylene. *J. Am. Chem. Soc.* **2007**, *129*, 1698-1704.
154. Sanford, M. S.; Love, J. A.; Grubbs, R. H., Mechanism and activity of ruthenium olefin metathesis catalysts. *J. Am. Chem. Soc.* **2001**, *123*, 6543-6554.
155. Schwab, P.; Grubbs, R. H.; Ziller, J. W., Synthesis and applications of RuCl₂(=CHR')(PR₃)₂: the influence of the alkylidene moiety on metathesis activity. *J. Am. Chem. Soc.* **1996**, *118*, 100-110.
156. Conrad, J. C.; Fogg, D. E., Ruthenium-catalyzed ring-closing metathesis: recent advances, limitations, and opportunities. *Curr. Org. Chem.* **2006**, *10*, 185-202.
157. Grubbs, R. H.; Miller, S. J.; Fu, G. C., Ring-closing metathesis and related processes in organic synthesis. *Acc. Chem. Res.* **1995**, *28*, 446-452.
158. Thomas, R. M.; Grubbs, R. H., Nonproductive events in ring-closing metathesis using ruthenium catalysts. *J. Am. Chem. Soc.* **2010**, *132*, 8534-8535.
159. Correa, A.; Cavallo, L., The elusive mechanism of olefin metathesis promoted by (NHC)Ru-based catalysts: a trade between steric, electronic, and solvent effects. *J. Am. Chem. Soc.* **2006**, *128*, 13352-13353.
160. Bielawski, C. W.; Grubbs, R. H., Living ring-opening metathesis polymerization. *Prog. Polym. Sci.* **2007**, *32*, 1-29.
161. Chatterjee, A. K.; Choi, T.-L.; Sanders, D. P.; Grubbs, R. H., A general model for selectivity in olefin cross metathesis. *J. Am. Chem. Soc.* **2003**, *125*, 11360-11370.
162. Ilker, M. F.; Coughlin, E. B., Alternating copolymerizations of polar and nonpolar cyclic olefins by ring-opening metathesis polymerization. *Macromolecules* **2002**, *35*, 54-58.

163. Lane, D. R.; Beavers, C. M.; Olmstead, M. M.; Schore, N. E., Steric and electronic effects of carbene substitution in Grubbs First-generation catalysts. *Organometallics* **2009**, *28*, 6789-6797.
164. Lin, Y. A.; Chalker, J. M.; Davis, B. G., Olefin cross-metathesis on proteins: investigation of allylic chalcogen effects and guiding principles in metathesis partner selection. *J. Am. Chem. Soc.* **2010**, *132*, 16805-16811.
165. Rule, J. D.; Moore, J. S., ROMP reactivity of endo- and exo-dicyclopentadiene. *Macromolecules* **2002**, *35*, 7878-7882.
166. Song, A.; Lee, J. C.; Parker, K. A.; Sampson, N. S., Scope of the ring-opening metathesis polymerization (ROMP) reaction of 1-substituted cyclobutenes. *J. Am. Chem. Soc.* **2010**, *132*, 10513-10520.
167. Torker, S.; Muller, A.; Singrist, R.; Chen, P., Tuning the steric properties of a metathesis catalyst for copolymerization of norbornene and cyclooctene toward complete alternation. *Organometallics* **2010**, *29*, 2735-2751.
168. Vehlow, K.; Wang, D.; Buchmeiser, M. R.; Blechert, S., Alternating copolymerization using a Grubbs-type initiator with an unsymmetrical, chiral N-heterocyclic carbene ligand. *Ang. Chem. Int. Ed.* **2008**, *47*, 2615-2618.
169. Holland, M. G.; Griffith, V. E.; France, M. B.; Desjardins, S. G., Kinetics of the ring-opening metathesis polymerization of a 7-oxanorbornene derivative by Grubbs' catalyst. *J. Polym. Sci., Part A: Polym. Chem.* **2003**, *41*, 2125-2131.
170. Runge, M. B.; Dutta, S.; Bowden, N. B., Synthesis and self-assembly of bottlebrush block copolymers. *Polymer Preprints* **2005**, *92*, 5-6.
171. Anderson, D. R.; O'Leary, D. J.; Grubbs, R. H., Ruthenium-olefin complexes: effect of ligand variation upon geometry. *Chem. Eur. J.* **2008**, *14*, 7536-7544.
172. Leitao, E. M.; Dubberley, S. R.; Piers, W. E.; Wu, Q.; McDonald, R., Thermal decomposition modes for four-coordinate ruthenium phosphonium alkylidene olefin metathesis catalysts. *Chem. Eur. J.* **2008**, *14*, 11565-11572.
173. Naumov, S.; Buchmeiser, M. R., Comparative DFT study *J. Phys. Org. Chem.* **2008**, *21*, 963-970.
174. Rowley, C. N.; Van der Eide, E. F.; Piers, W. E.; Woo, T. K., DFT study of the isomerization and spectroscopic/structural properties of ruthenacyclobutane intermediates relevant to olefin metathesis. *Organometallics* **2008**, *27*, 6043-6045.
175. Chan, T.-L.; Mak, T. C. W.; Poon, C.-D.; Wong, H. N. C.; Jia, J. H.; Wang, L. L., A stable derivative of cyclooctatrienyne: synthesis and crystal structures of 1,4,7,10-tetramethyl-5,6-didehydrodibenzo[a,e]cyclooctene and 1,4,7,10-tetramethyldibenzo[a,e]cyclooctene. *Tetrahedron* **1986**, *42*, 655-661.
176. Dewar, M. J. S.; Pierini, A. B., Mechanism of the Diels-Alder reaction. Studies of the addition of maleic anhydride to furan and methylfurans. *J. Am. Chem. Soc.* **1984**, *106*, 203-208.

177. Schultz, M. K.; Parameswarappa, S. G.; Pigge, F. C., Synthesis of a DOTA–biotin conjugate for radionuclide chelation via Cu-Free click chemistry. *Org. Lett.* **2010**, *12*, 2398-2401.
178. Pollino, J. M.; Stubbs, L. P.; Weck, M., Living ROMP of exo-norbornene esters possessing PdII SCS pincer complexes or diaminopyridines. *Macromolecules* **2003**, *36*, 2230-2234.
179. Schrock, R. R., High oxidation state multiple metal-carbon bonds. *Chem. Rev.* **2002**, *102*, 145-179.
180. Schrock, R. R.; Gabert, A. J.; Singh, R.; Hock, A. S., Synthesis of high oxidation state bimetallic alkylidene complexes for controlled ROMP synthesis of triblock copolymers. *Organometallics* **2005**, *24*, 5058-5066.
181. Sill, K.; Emrick, T., Bis-dendritic polyethylene prepared by ring-opening metathesis polymerization in the presence of bis-dendritic chain transfer agents. *J. Polym. Sci., Part A: Polym. Chem.* **2005**, *43*, 5429-5439.
182. Singh, R.; Verploegen, E.; Hammond, P. T.; Schrock, R. R., Synthesis of ABA triblock copolymers via ring opening metathesis polymerization using a bimetallic initiator: influence of a flexible spacer in the side chain liquid crystalline block. *Macromolecules* **2006**, *39*, 8241-8249.
183. Smith, D.; Pentzer, E. B.; Nguyen, S. T., Bioactive and therapeutic ROMP polymers. *Polym. Rev.* **2007**, *47*, 419-459.
184. Burd, C.; Weck, M., Solvent influence on the orthogonality of noncovalently functionalized terpolymers. *J. Polym. Sci., Part A: Polym. Chem.* **2008**, *46*, 1936-1944.
185. Gibbs, J. M.; Park, S.-J.; Anderson, D. R.; Watson, K. J.; Mirkin, C. A.; Nguyen, S. T., Polymer–DNA hybrids as electrochemical probes for the detection of DNA. *J. Am. Chem. Soc.* **2005**, *127*, 1170-1178.
186. Miyamoto, Y.; Fujiki, M.; Nomura, K., Synthesis of homopolymers and multiblock copolymers by the living ring-opening metathesis polymerization of norbornenes containing acetyl-protected carbohydrates with well-defined ruthenium and molybdenum initiators. *J. Polym. Sci., Part A: Polym. Chem.* **2004**, *42*, 4248-4265.
187. South, C. R.; Leung, K. C. F.; Lanari, D.; Stoddart, J. F.; Weck, M., Noncovalent side-chain functionalization of terpolymers. *Macromolecules* **2006**, *39*, 3738-3744.
188. Weck, M.; Schwab, P.; Grubbs, R. H., Synthesis of ABA triblock copolymers of norbornenes and 7-oxanorbornenes via living ring-opening metathesis polymerization using well-defined, bimetallic ruthenium catalysts. *Macromolecules* **1996**, *29*, 1789-1793.
189. Bielawski, C. W.; Grubbs, R. H., Highly efficient ring-opening metathesis polymerization (ROMP) using new ruthenium catalysts containing N-heterocyclic carbene ligands. *Angew. Chem. Int. Ed.* **2000**, *39*, 2903-2906.

190. Choi, T.-L.; Grubbs, R. H., Controlled living ring-opening-metathesis polymerization by a fast-initiating ruthenium catalyst. *Angew. Chem. Int. Ed.* **2003**, *42*, 1743-1746.
191. Slugovc, C.; Riegler, S.; Hayn, G.; Saf, R.; Stelzer, F., Highly defined ABC triblock cooligomers and copolymers prepared by ROMP using an N-heterocyclic-carbene-substituted ruthenium benzylidene initiator. *Macromol. Rap. Comm.* **2003**, *24*, 435-439.
192. Alfred, S. F.; Lienkamp, K.; Madkour, A. E.; Tew, G. N., Water-soluble ROMP polymers from amine-functionalized norbornenes. *J. Polym. Sci. A: Polym. Chem.* **2008**, *46*, 6672-6676.
193. Deng, T.; Chen, C.; Honeker, C.; Thomas, E. L., Two-dimensional block copolymer photonic crystals. *Polymer* **2003**, *44*, 6549-6553
194. Higley, M. N.; Pollino, J. M.; Hollembeak, E.; Weck, M., A modular approach toward block copolymers. *Chem. Eur. J.* **2005**, *11*, 2946-2953.
195. Kim, H. C.; Jia, X.; Stafford, C. M.; Kim, D. H.; McCarthy, T. J.; Tuominen, M.; Hawker, C. J.; Russell, T. P., A route to nanoscopic SiO₂ posts via block copolymer templates. *Adv. Mater.* **2001**, *13*, 795-797.
196. Lienkamp, K.; Madkour, A. E.; Musante, A.; Nelson, C. F.; Nüsslein, K.; Tew, G. N., Antimicrobial polymers prepared by ROMP with unprecedented selectivity: a molecular construction kit approach. *J. Am. Chem. Soc.* **2008**, *130*, 9836-9843.
197. Ruiz, R.; Kang, H.; Detcheverry, F. A.; Dobisz, E.; Kercher, D. S.; Albrecht, T. R.; de Pablo, J. J.; Nealey, P. F., Density multiplication and improved lithography by directed block copolymer assembly. *Science* **2008**, *321*, 936-939.
198. Ishihara, Y.; Bazzi, H. S.; Toader, V.; Godin, F.; Sleiman, H. F., Molecule-responsive block copolymer micelles. *Chem. Eur. J.* **2007**, *13*, 4560-4570.
199. Love, J. A.; Sanford, M. S.; Day, M. W.; Grubbs, R. H., Synthesis, structure, and activity of enhanced initiators for olefin metathesis. *J. Am. Chem. Soc.* **2003**, *125*, 10103-10109.
200. Miki, K.; Kuramochi, Y.; Oride, K.; Inoue, S.; Harada, H.; Hiraoka, M.; Ohe, K., Ring-opening metathesis polymerization-based synthesis of ICG-containing amphiphilic triblock copolymers for in vivo tumor imaging. *Bioconjugate Chem.* **2009**, *20*, 511-517.
201. Riegler, S.; Demel, S.; Trimmel, G.; Slugovc, C.; Stelzer, F., Ring opening metathesis polymerisation initiated by RuCl₂(3-bromopyridine)₂(H₂IMes)(CHPh): scope and limitation in block copolymer synthesis. *J. Mol. Catal. A: Chem.* **2006**, *257*, 53-58.
202. France, M. B.; Alty, L. T.; Earl, T. M., Synthesis of a 7-oxanorbornene monomer: a two-step sequence preparation for the organic laboratory. *J. Chem. Educ.* **1999**, *76*, 659-null.
203. Lee, L.-B. W.; Register, R. A., Acyclic metathesis during ring-opening metathesis polymerization of cyclopentene. *Polymer* **2004**, *45*, 6479-6485.

204. Walker, R.; Conrad, R. M.; Grubbs, R. H., The living ROMP of trans-cyclooctene. *Macromolecules* **2009**, *42*, 599-605.